Supporting Information

Synthesis and reactivity of a $PC_{carbene}P$ cobalt(I) complex: The missing link in the cobalt PXP pincer series (X = B, C, N)

Simon Sung,[a] Qingyang Wang,[a] Tobias Krämer,[b] Rowan D. Young*[a]

[a] *Department of Chemistry, National University of Singapore, 3 Science Drive 3, Singapore 117543*

[b] *Department of Chemistry, Maynooth University, Maynooth Ireland*

**Corresponding Author*

Table of Contents

Experimental

General information

All syntheses were carried out in N_2 atmosphere using a glovebox or with standard Schlenk techniques. All reactions were performed in glassware that was oven-dried for at least 12 h. $[CoBr(PMe_3)_3]$,[1] $[Co(PMe_3)_4]$[2] **A**,[3] **A-H$_2$**,[4] $Na[BAr^F_4]$,[5] $Fc[BAr^F_4]$,[6] $[B(C_6F_5)_3]$[7] and $[H(OEt_2)][BAr^F_4]$[8] were prepared according to reported methods. Toluene, DCM, acetonitrile and hexanes were dried over activated alumina using a LC Technology Solutions Inc. SP-1 solvent purification system and then deoxygenated prior to use. CD_2Cl_2, C_6D_6, and fluorobenzene were stirred over CaH_2 at room temperature under a nitrogen atmosphere overnight prior to distillation under reduced pressure and storage over 4 Å molecular sieves. Toluene-d_8 was deoxygenated and stored over 4 Å molecular sieves before use. CD_3CN and acetone-d_6 were used as received from sealed ampoules. NMR spectra were recorded using Bruker AV500 and DRX500 spectrometers. All chemical shifts are quoted in parts per million (ppm) relative to $SiMe_4$ (^{1}H, ^{13}C) or H_3PO_4 (85%) (^{31}P). Magnetic moments were determined using Evan's method NMR with the necessary diamagnetic corrections subsequently applied using reported values.[9] Infrared spectra were recorded using an Agilent Cary 630 FTIR spectrometer. ESR spectra were recorded using a JEOL FA200 ESR Spectrometer (X-Band). *g*-values and *A*-values for ESR spectra were determined from simulated spectra generated using JEOL Isotropic and Anisotropic software. HRMS (ESI-TOF) spectra were obtained using an Agilent Technologies 6230 TOF LC/MS. Single crystal data were measured at low temperature (T = 100K) on a four circles goniometer Kappa geometry Bruker AXS D8 Venture equipped with a Photon 100 CMOS active pixel sensor detector using molybdenum monochromatized (λ = 0.71073 Å) or copper monochromatized (λ = 1.54178 Å) X-Ray radiation. Elemental analyses were obtained by the National University of Singapore's Chemical, Molecular and Materials Analysis Centre (CMMAC), however, where elemental analysis was not possible, purity of compounds was assessed with a combination of ^{1}H, ^{13}C and ^{31}P NMR spectroscopy.

Preparation of $[Co(PMe_3)_4][BAr^F_4]$[1]

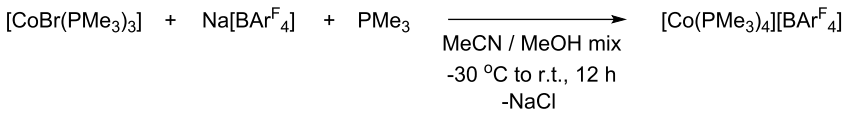

A solution of $[CoBr(PMe_3)_3]$ (675 mg, 1.84 mmol) and PMe_3 (191 µL, 1.84 mmol) in MeCN (30 mL) was treated dropwise with a solution of $Na[BAr^F_4]$ (1.634 g, 1.84 mmol) in MeOH (15 mL) at -30 °C. After complete addition, the mixture was allowed to warm slowly to room temperature and then stirred for 12 h. The reaction mixture was evaporated and then the product was extracted with Et_2O (2 x 20 mL). The extracts were concentrated to approx. 2 mL and then hexanes (15 mL) was added to precipitate the product. The green-blue solid was filtered, washed with hexanes (2 x 10 mL) and then dried under vacuum (2.169 g, 96 %).

HRMS (ESI-TOF) m/z: $[M]^+$ Calcd for $C_{12}H_{36}CoP_4$ 363.1094; Found 363.1094.

Magnetic moment (298 K): μ_{eff} = 3.20 µB (two unpaired electron, S = 1).

Preparation of complex 1

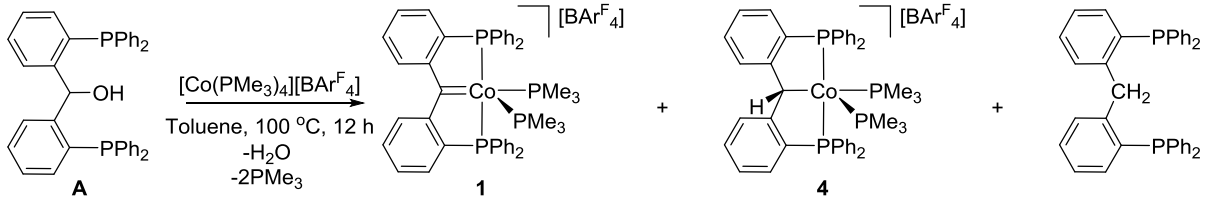

Toluene (50 mL) was added to a 100 mL Schlenk tube containing $[Co(PMe_3)_4][BAr^F_4]$ (1.840 g, 1.5 mmol) and Ligand **A** (0.829 g, 1.5 mmol) and then sealed. The mixture was heated at 100 °C for 12 h and then allowed to come to room temperature before filtering. The filtrate was concentrated under vacuum to approx. 10 mL, layered with hexanes (10 mL) and then left to crystallise at -20 °C. The resultant dark brown crystals of complex **1** were isolated by filtration, washed with cold toluene (3 x 10 mL) at 0 °C, and hexanes (3 x 10 mL) and then dried under high vacuum at 50 °C (1.134 g, 47%). Complex **4** was isolated after allowing the combined filtrate and washings to stand at room temperature and then filtering the resultant brown crystals (0.869 g, 36%). The reduced bisphosphine ligand $(Ph_2PC_6H_4)_2CH_2$ was isolated by evaporating the subsequent filtrate and subjecting the residue to column chromatography on silica gel in air (EtOAc : hexane, 1:1), collecting the first fraction (R_f = 0.90). After evaporating the fraction, $(Ph_2PC_6H_4)_2CH_2$ was obtained as a white solid (0.025 g, 3%).

Complex **1**:

^{1}H NMR (500 MHz, Acetone-d_6, 298 K) = δ_H 1.17 (d, *J* = 8.2 Hz, 18H, P*Me*$_3$), 7.27 (t, *J* = 7.7 Hz, 2H, Ar-*H*), 7.31 – 7.44 (m, 11H, Ar-*H*), 7.46 (t, *J* = 7.4 Hz, 7H, Ar-*H*), 7.57 (t, *J* = 7.3 Hz, 4H, Ar-*H*), 7.66 (s, 4H, [BAr$^F{}_4$] Ar-*H*), 7.78 (s, 8H, [BAr$^F{}_4$] Ar-*H*), 8.24 (t, *J* = 6.9 Hz, 2H, Ar-*H*), 8.52 (d, *J* = 7.8 Hz, 2H, Ar-*H*) ppm.

^{31}P{^{1}H} NMR (202 MHz, Acetone-d_6, 298 K) = δ_P 0.8 (s (br), 2P, *P*Me$_3$), 53.0 (s (br), 2P, PCP pincer *P*'s) ppm.

^{31}P{^{1}H} NMR (202 MHz, CD_2Cl_2, 198 K) = δ_P -9.2 (td, $^{2}J_{PP}$ = 58.5 (t), 22.3 (d) Hz, 1P, *P*Me$_3$), 15.0 (td, $^{2}J_{PP}$ = 31.0 (t), 25.6 (d) Hz, 1P, *P*Me$_3$), 54.7 (dd, $^{2}J_{PP}$ = 58.5 (d), 31.0 (d) Hz, 2P, PCP pincer *P*'s) ppm.

^{13}C{^{1}H} NMR (126 MHz, Acetone-d_6, 298 K) = δ_C 20.6 (dd, $^{1}J_{CP}$ = 24.0 Hz, $^{3}J_{CP}$ = 2.5 Hz), 118.2 – 118.5 (m, [BAr$^F{}_4$] *C*-H), 123.4 (dt, J_{CP} = 6.5 (d), J_{CP} = 6.2 (t) Hz), 125.3 (q, $^{1}J_{CF}$ = 272.2 Hz, [BAr$^F{}_4$] *C*F$_3$), 127.2 (s), 129.8 (t, J_{CP} = 4.7 Hz), 129.5 – 130.4 (m, [BAr$^F{}_4$] *C*-CF$_3$), 131.8 (s), 134.6 (t, J_{CP} = 5.7 Hz), 135.0 (d, *J* = 12.2 Hz), 135.2 (s), 135.3 (s), 135.5 (s, [BAr$^F{}_4$] *C*-H), 145.1 (tt, J_{CP} = 21.2 (t), 8.4 (t) Hz), 162.6 (q, $^{1}J_{CB}$ = 49.9 Hz, [BAr$^F{}_4$] *C*-B), 167.6 (tt, J_{CP} = 22.6 (t), 4.9 (t) Hz), 216.6 (ddt, $^{2}J_{CP}$ = 33.5 (d), 33.5 (d), 18.2 (t) Hz, Co=*C*) ppm.

HRMS (ESI-TOF) m/z: $[M]^+$ Calcd for $C_{43}H_{46}CoP_4$ 745.1876; Found 745.1890.

Found: C, 55.6; H, 3.9. Calc. for $C_{75}H_{58}BCoF_{24}P_4$: C, 56.0; H, 3.6%.

Complex **4**:

HRMS (ESI-TOF) m/z: $[M]^+$ Calcd for $C_{43}H_{47}CoP_4$ 746.1955; Found 746.1930.

Magnetic moment (298 K): μ_{eff} = 2.13 μB (one unpaired electron, *S* = 1/2).

Found: C, 56.4; H, 4.0. Calc. for $C_{75}H_{59}BCoF_{24}P_4$: C, 56.0; H, 3.7%.

Bisphosphine $(Ph_2PC_6H_4)_2CH_2$: data are in close agreement with those reported.[10]

^{1}H NMR (500 MHz, $CDCl_3$, 298 K) = δ_H 4.46 (t, $^{4}J_{HP}$ = 2.1 Hz, 2H, C*H*$_2$), 6.91 (tdd, *J* = 7.7 (t), 4.2 (d), 1.1 (d) Hz, 4H, Ar-*H*), 7.08 (td, *J* = 7.5 (t), 1.3 (d) Hz, 2H, Ar-*H*), 7.15 (td, *J* = 7.5 (t), 1.5 (d) Hz, 2H, Ar-*H*), 7.19 – 7.25 (m, 8H, Ar-*H*), 7.27 – 7.35 (m, 12H, Ar-*H*) ppm.

^{13}C{^{1}H} NMR (126 MHz, CD_2Cl_2, 298 K) = δ_C 38.5 (t, $^{3}J_{CP}$ = 23.2 Hz, *C*H$_2$), 126.5 (s), 128.5 – 128.6 (m), 128.8 (d, J_{CP} = 37.3 Hz), 130.2 (t, J_{CP} = 2.8 Hz), 133.5 (s), 134.1 (s), 134.1 (d, J_{CP} = 21.0 Hz), 136.5 (d, J_{CP} = 12.0 Hz), 136.9 (d, J_{CP} = 10.6 Hz), 145.4 (d, J_{CP} = 27.2 Hz) ppm.

^{31}P{^{1}H} NMR (202 MHz, $CDCl_3$, 298 K) = δ_P -14.1 (s, 2P, *P*Ph$_2$) ppm.

HRMS (ESI-TOF) m/z: $[M+H]^+$ Calcd for $C_{37}H_{30}P_2$ 537.1896; Found 537.1926.

***In situ* preparation of complex 2**

C_6D_6 (0.6 mL) was added to a mixture of complex **1** (8.0 mg, 0.005 mmol) and $B(C_6F_5)_3$ (5.1 mg, 0.005 mmol) in a J. Young valve NMR tube. After mixing at room temperature overnight, the deep red-pink coloured mixture containing complex **2** was analysed by NMR spectroscopy. Attempts to isolate the pure complex failed due to its instability out of solution and short-term stability in solution. Complex **1** could be reformed by addition of PMe_3 (2.6 µL, 0.025 mmol) to the mixture at room temperature, causing it to turn orange colour immediately and form a biphasic mixture. After removing the top layer by cannula, ^{31}P NMR analysis of the bottom oily layer in fluorobenzene solvent confirmed the identity of complex **1**.

Complex **2**:

Selected ^1H NMR data determined using 1D 1H, 1H DOSY and HMQC (500 MHz, C_6D_6, 298 K) = δ_H -0.68 (d, $^2J_{HP}$ = 7.6 Hz, 9H, P*Me*$_3$), 5.27 (t, *J* = 7.5 Hz, 2H, Ar-*H*), 6.85 – 6.90 (m, 2H, Ar-*H*), 7.19 – 7.26 (m, 10H, Ar-*H*), 7.32 (d, *J* = 7.0 Hz, 4H, Ar-*H*), 7.69 – 7.77 (m, 8H, Ar-*H*), 8.68 (t, *J* = 7.1 Hz, 2H, Ar-*H*) ppm.

Selected ^{13}C NMR data from HMQC and HMBC spectra (126 MHz, C_6D_6, 298 K) = δ_C 10.1 (P*Me*$_3$), 117.7 ([BAr^F_4] *C*-H), 121.6, 126.2, 132.0, 134.0, 134.6, 135.0 ([BAr^F_4] *C*-H), 136.5, 138.7, 139.0, 162.4 ([BAr^F_4] *C*-B), 178.1 (possibly Co=C) ppm.

$^{31}P\{^1H\}$ NMR (202 MHz, C_6D_6, 298 K) = δ_P -54.8 (s(br), 1P, *P*Me_3), 4.6 (s(br), 2P, PCP pincer *P*'s) ppm.

HRMS (ESI-TOF) m/z: $[M]^+$ Calcd for $C_{40}H_{37}CoP_3$ 669.1435; Found 669.1435.

***In situ* preparation of complex 2·MeCN**

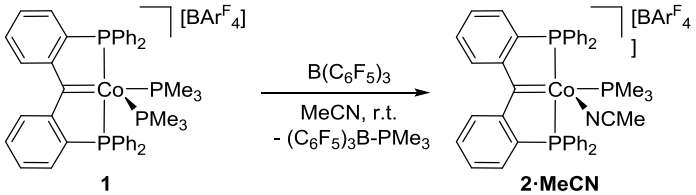

After allowing a solution of complex **1** (16.1 mg, 0.01 mmol) in MeCN (0.6 mL) in a J. Young valve NMR tube to stand at room temperature for 27 h, ^{31}P NMR spectroscopic analysis indicated that 17% of **1** had converted

to **2**·MeCN (see Figure S13). Alternatively, when a solution of complex **1** (16.1 mg, 0.01 mmol) in MeCN (0.6 mL) in a J. Young valve NMR tube was treated with $B(C_6F_5)_3$ (10.2 mg, 0.01 mmol) at room temperature, ^{11}B and ^{31}P NMR spectroscopic analysis indicated that complete conversion to **1** had occurred to **2**·MeCN within 90 min, with simultaneous formation of $Me_3P\text{-}B(C_6F_5)_3$ ($^{31}P\{^1H\}$ NMR δ_P = -1.4 (s(br)) ppm; ^{11}B NMR δ_B = -14.7 (d(br), $^1J_{BP}$ = 75 Hz) ppm;).

Complex [**2**·MeCN]:

$^{31}P\{^1H\}$ NMR (202 MHz, MeCN, 298 K) = δ_P 34.4 (s(br), 1P, *P*Me_3), 58.4 (s(br), 2P, PCP pincer *P's*) ppm.

HRMS (ESI-TOF) m/z: $[M\text{-MeCN}]^+$ Calcd for $C_{40}H_{37}CoP_3$ 669.1435; Found 669.1458.

Preparation of complex 3

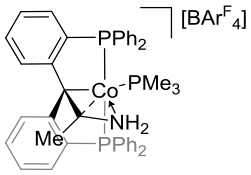

3

MeCN (2 mL) was added to a mixture of complex **1** (48.3 mg, 0.030 mmol) and NaH (2.6 mg, 0.066 mmol, 60% dispersion in mineral oil) in a 25 mL Schlenk tube and sealed. After stirring for 2 days at room temperature, the mixture was evaporated to dryness. The residue was extracted with toluene (3 x 5 mL) to give an orange solution. The solution was evaporated to dryness and the orange residue was then filtered through a short column of silica gel using DCM solvent, collecting the first orange fraction. The solution was evaporated to dryness again and then the residue was recrystallized by layering a concentrated toluene solution of the product with hexanes to give orange-brown crystals (25 mg, 52%).

^1H NMR (500 MHz, CD_2Cl_2, 298 K) = δ_H 0.93 (d, $^3J_{HP}$ = 13.0 Hz, 1H, N-*H*), 1.12 (d, $^2J_{HP}$ = 7.9 Hz, 9H, P*Me*$_3$), 2.07 (d, $^4J_{HP}$ = 7.1 Hz, 3H, N-C-C*H*$_3$), 2.77 (s(br), 1H, N-*H*), 6.58 (ddd, *J* = 10.9 (d), 8.3 (d), 1.1 (d) Hz, 2H, Ar-*H*), 6.69 (ddd, *J* = 9.6 (d), 8.3 (d), 1.2 (d) Hz, 2H, Ar-*H*), 6.83 (td, *J* = 7.9 (t), 2.2 (d) Hz, 2H, Ar-*H*), 6.86 – 6.98 (m, 4H, Ar-*H*), 7.08 – 7.15 (m, 3H, Ar-*H*), 7.19 – 7.27 (m, 2H, Ar-*H*), 7.31 – 7.49 (m, 8H, Ar-*H*), 7.49 – 7.60 (m, 8H, Ar-*H* and [BAr$^F_4$] Ar-*H*), 7.73 (s, 8H, [BAr$^F_4$] Ar-*H*), 7.95 – 8.03 (m, 2H, Ar-*H*) ppm.

$^{13}C\{^1H\}$ NMR (126 MHz, CD_2Cl_2, 298 K) = δ_C 20.6 (dd, $^2J_{CP}$ = 24.2 (d), $^4J_{CP}$ = 5.6 (d) Hz, P*Me*$_3$), 21.8 (s, N-C-*C*H$_3$), 77.3 (d, J_{CP} = 20.3 Hz), 82.6 (dd, J_{CP} = 10.9, 5.1 Hz), 117.9 (s, [BAr$^F_4$] *C*-H), 125.0 (q, $^1J_{CF}$ = 272.6

Hz, [BAr$^F_4$] *C*F$_3$), 126.7 (d, J_{CP} = 13.5 Hz), 128.2 (d, J_{CP} = 5.6 Hz), 128.9 – 129.0 (m), 129.0 – 129.2 (m), 128.8 – 129.7 (m, [BAr$^F_4$] *C*-CF$_3$), 129.4 (d, J_{CP} = 8.3 Hz), 130.4 (s), 130.5 (s), 130.8 (s), 131.4 (s), 131.5 (s), 131.9 (d, J_{CP} = 11.5 Hz), 132.1 (s), 132.6 (s), 133.7 (d, J_{CP} = 11.4 Hz), 134.5 (d, J_{CP} = 1.8 Hz), 135.2 (s, [BAr$^F_4$] *C*-H), 135.3 – 135.7 (m), 137.2 – 138.1 (m), 142.1 (d, J_{CP} = 45.6 Hz), 147.2 (d, J_{CP} = 43.8 Hz), 149.6 (d, J_{CP} = 28.7 Hz), 162.2 (q, $^1J_{CB}$ = 49.9 Hz, [BAr$^F_4$] *C*-B) ppm.

^{31}P{^{1}H} NMR (202 MHz, CD_2Cl_2, 298 K) = δ_P -8.1 (d, $^2J_{PP}$ = 64.3 Hz, 1P, *P*Me$_3$), 50.4 (d, $^2J_{PP}$ = 48.9 Hz, 1P, Pincer *P*), 65.5 (dd, $^2J_{PP}$ = 64.3 (d), 48.9 (d) Hz, 1P, Pincer *P*) ppm.

HRMS (ESI-TOF) m/z: [M]$^+$ Calcd for $C_{42}H_{42}CoNP_3$ 712.1857; Found 712.1863.

Direct preparation of complex 4 from complex 1

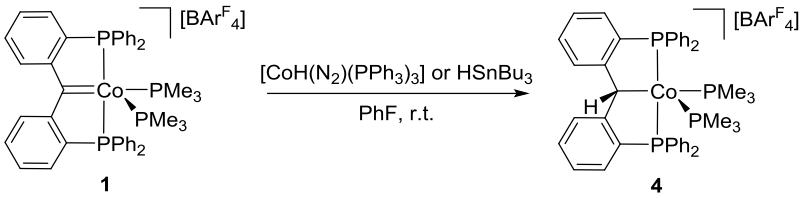

1 **4**

A solution of complex **1** (8.1 mg, 0.005 mmol) in fluorobenzene (0.6 mL) was treated with [CoH(N$_2$)(PPh$_3$)$_3$] (4.4 mg, 0.005 mmol) or HSnBu$_3$ (1.6 µL, 0.005 mmol). After 24 h at room temperature, the mixture was analysed by ESI-MS and EPR spectroscopy, which confirmed complete conversion of **1** and generation of complex **4**.

Preparation of complex 5

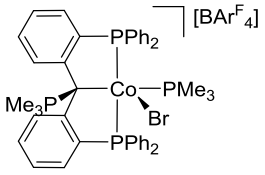

5

A solution of complex **1** (24.1 mg, 0.015 mmol) in fluorobenzene (0.6 mL) was treated with Br$_2$ (0.8 µL, 0.015 mmol) and mixed well. After allowing the solution to stand at room temperature for 24 h, the product was crystallised by layering with hexanes at room temperature to obtain the **1** as black crystals (15 mg, 60%).

HRMS (ESI-TOF) m/z: [M]$^+$ Calcd for $C_{43}H_{46}BrCoP_4$ 826.1048; Found 826.1046.

Magnetic moment (298 K): μ_{eff} = 3.63 µB (three unpaired electron, *S* = 3/2).

Found: C, 53.2; H, 3.7. Calc. for $C_{75}H_{58}BBrCoF_{24}P_4$: C, 53.3; H, 3.5%.

Preparation of complex 6

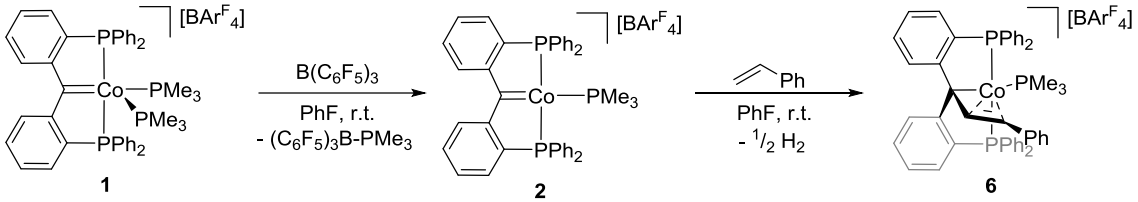

A solution of complex **1** (24.1 mg, 0.015 mmol) in fluorobenzene (1 mL) was treated with $B(C_6F_5)_3$ (15.4 mg, 0.030 mmol) and mixed well. After allowing the solution to stand at room temperature for 2 h, the deep pink solution was treated with styrene (1.7 µL, 0.015 mmol) and caused the solution to immediately turn orange. After 7 days at room temperature, the solution was filtered to remove the $(C_6F_5)_3B\text{-}PMe_3$ by-product. The filtrate was then layered with hexanes (8 mL) and stored at – 30 °C. The resultant dark brown solid **6** was isolated by filtration, washed with hexanes (2 x 3 mL) and then dried under vacuum (10 mg, 41%).

HRMS (ESI-TOF) m/z: $[M]^+$ Calcd for $C_{48}H_{44}CoP_3$ 772.1982; Found 772.1982.

Magnetic moment (298 K): μ_{eff} = 2.31 µB (one unpaired electron, S = 1/2).

Preparation of complex 7

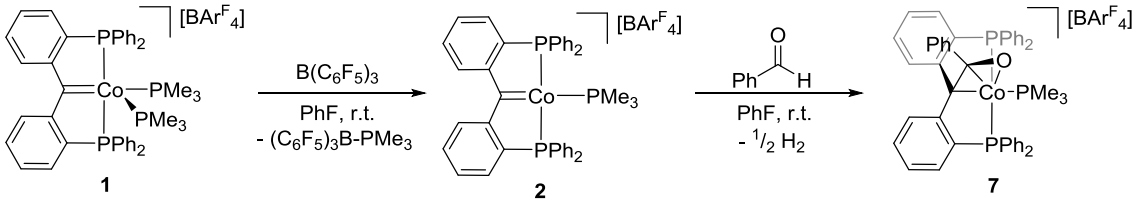

A solution of complex **1** (24.1 mg, 0.015 mmol) in fluorobenzene (1 mL) was treated with $B(C_6F_5)_3$ (15.4 mg, 0.030 mmol) and mixed well. After allowing the solution to stand at room temperature for 2 h, the deep pink solution was treated with benzaldehyde (1.6 µL, 0.015 mmol). After 7 days at room temperature, the solution was filtered to remove the $(C_6F_5)_3B\text{-}PMe_3$ by-product. The filtrate was then layered with hexanes (8 mL) and stored at – 30 °C. The resultant dark green solid **7** was isolated by filtration, washed with hexanes (2 x 3 mL) and then dried under vacuum (15 mg, 61%).

IR (nujol): 1021.3 cm^{-1} (v(C-O).

HRMS (ESI-TOF) m/z: $[M]^+$ Calcd for $C_{47}H_{42}CoOP_3$ 774.1775; Found 774.1801.

Magnetic moment (298 K): μ_{eff} = 2.41 μB (one unpaired electron, *S* = 1/2).

Found: C, 57.8; H, 3.6. Calc. for $C_{79}H_{54}BCoF_{24}OP_3$: C, 57.9; H, 3.3%.

Preparation of complex 8a

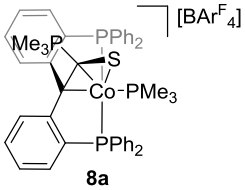

8a

A solution of complex **1** (48.3 mg, 0.03 mmol) and PMe_3 (4.1 μL, 0.04 mmol) in fluorobenzene (3 mL) was treated with carbon disulfide (3.0 μL, 0.05 mmol) and stirred at 55 °C for 16 h. The solution was then evaporated to dryness and filtered through a column of silica gel in air using EtOAc : DCM (1 : 1) solvent, collecting the dark red fraction (R_f = 0.50). The fraction was evaporated and then recrystallised by layering a concentration fluorobenzene solution with hexanes. The dark red solid was then dried under vacuum to give complex **8a** (45 mg, 91%).

^{1}H NMR (500 MHz, CD_2Cl_2, 298 K) = δ_H 1.16 (d, $^2J_{HP}$ = 8.0 Hz, 9H, P*Me*$_3$), 1.50 (d, $^2J_{HP}$ = 12.7 Hz, 9H, P*Me*$_3$), 6.33 – 6.43 (m, 2H, Ar-*H*), 6.79 (td, *J* = 8.2 (t), 2.2 (d) Hz, 2H, Ar-*H*), 6.84 (td, *J* = 7.8 (t), 0.8 (d) Hz, 1H, Ar-*H*), 6.87 – 6.97 (m, 4H, Ar-*H*), 7.00 (td, *J* = 7.7 (t), 0.8 (d) Hz, 1H), 7.07 – 7.24 (m, 8H, Ar-*H*), 7.31 – 7.40 (m, 2H, Ar-*H*), 7.48 (td, *J* = 7.5 (t), 1.5 (d) Hz, 2H, Ar-*H*), 7.53 – 7.59 (m, 6H, Ar-*H* and [BAr$^F_4$] Ar-*H*), 7.73 (s, 8H, [BAr$^F_4$] Ar-*H*), 7.87 – 7.94 (m, 3H, Ar-*H*), 8.10 (dd, *J* = 7.9 (d), 3.2 (d) Hz, 1H, Ar-*H*) ppm.

^{13}C{^{1}H} NMR (126 MHz, CD_2Cl_2, 298 K) = δ_C 12.7 (dd, $^1J_{CP}$ = 56.1 (d), $^2J_{CP}$ = 2.5 Hz, Co-P*Me*$_3$), 21.4 (ddd, $^1J_{CP}$ = 25.5 (d), $^4J_{CP}$ = 4.2, $^4J_{CP}$ = 1.8 Hz, C-P*Me*$_3$), 79.4 (d, J_{CP} = 65.3 Hz), 87.5 (ddd, J_{CP} = 29.1 (d), 7.0 (d), 1.8 (d) Hz), 117.9 (s, [BAr$^F_4$] *C*-H), 125.0 (q, $^1J_{CF}$ = 272.4 Hz, [BAr$^F_4$] *C*F$_3$), 126.7 (d, J_{CP} = 12.8 Hz), 128.3 (d, J_{CP} = 7.1 Hz), 128.7 (dd, J_{CP} = 9.6 (d), 4.0 (d) Hz), 129.0 (d, J_{CP} = 8.4 Hz), 129.3 (q, $^2J_{CF}$ = 31.5 Hz, [BAr$^F_4$] *C*-CF$_3$), 129.3 (s), 129.8 (s), 129.8 (d, J_{CP} = 2.5 Hz), 131.3 (s), 132.1 (s), 132.1 (s), 132.2 (d, J_{CP} = 2.9 Hz), 132.3 (d, J_{CP} = 2.2 Hz), 132.7 (d, J_{CP} = 8.2 Hz), 134.5 (d, J_{CP} = 13.2 Hz), 135.2 (s, [BAr$^F_4$] *C*-H), 135.9 (d, J_{CP} = 33.9 Hz), 139.3 (dd, J_{CP} = 42.5 (d), 6.4 (d) Hz), 141.1 (d, J_{CP} = 22.9 Hz), 144.4 (ddd, *J* = 48.7 (d), 13.4 (d), 5.1 (d) Hz), 152.5 (d, J_{CP} = 30.9 Hz), 153.7 (d, J_{CP} = 38.8 Hz), 162.1 (q, $^1J_{CB}$ = 49.8 Hz, [BAr$^F_4$] *C*-B) ppm.

$^{31}P\{^{1}H\}$ NMR (202 MHz, CD_2Cl_2, 298 K) = δ_P -13.4 (s(br), 1P, C-*P*Me_3), 23.8 (s, 1P, Co-*P*Me_3), 56.3 (s(br), 1P, PCP pincer *P*), 70.1 (s(br), 1P, PCP pincer *P*) ppm.

HRMS (ESI-TOF) m/z: $[M]^+$ Calcd for $C_{44}H_{46}CoP_4S$ 789.1597; Found 789.1597.

Preparation of complex 8b

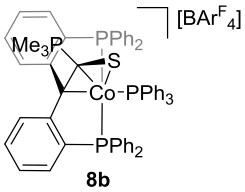

8b

A solution of complex **1** (32.2 mg, 0.02 mmol) and PPh_3 (5.8 mg, 0.022 mmol) in fluorobenzene (1 mL) was treated with carbon disulfide (2.9 µL, 0.048 mmol) and mixed at room temperature for 22 h. The solution was then evaporated to dryness and filtered through a column of silica gel in air using EtOAc : Hexane (1 : 1) solvent, collecting the dark purple fraction (R_f = 0.35). The dark purple fraction was evaporated and then recrystallised by layering a concentration fluorobenzene solution with hexanes. The dark purple solid was then dried under vacuum to give complex **8b** (19 mg, 52%).

^{1}H NMR (500 MHz, CD_2Cl_2, 298 K) = δ_H 1.14 (d, $^{2}J_{CP}$ = 7.9 Hz, 9H, P*Me*$_3$), 6.39 – 6.47 (m, 2H, Ar-*H*), 6.50 – 6.56 (m, 1H, Ar-*H*), 6.71 – 6.78 (m, 3H, Ar-*H*), 6.79 – 6.89 (m, 6H, Ar-*H*), 6.98 – 7.08 (m, 4H, Ar-*H*), 7.08 – 7.21 (m, 2H, Ar-*H*), 7.23 (td, *J* = 7.7 (t), 1.6 (d) Hz, 4H, Ar-*H*), 7.27 – 7.35 (m, 4H, Ar-*H*), 7.36 – 7.54 (m, 9H, Ar-*H*), 7.57 – 7.71 (m, 11H, Ar-*H* and BAr$^F_4$] Ar-*H*), 7.78 (s, 8H, BAr$^F_4$] Ar-*H*), 8.20 (dd, *J* = 7.8 (d), 2.5 (d) Hz, 1H, Ar-*H*) ppm.

$^{13}C\{^{1}H\}$ NMR (126 MHz, CD_2Cl_2, 298 K) = δ_C 22.2 (ddd, $^{1}J_{CP}$ = 24.7 (d), $^{4}J_{CP}$ = 4.8 (d), $^{4}J_{CP}$ = 1.7 (d) Hz, P*Me*$_3$), 91.9 (d, J_{CP} = 30.7 Hz), 117.9 (s, [BAr$^F_4$] *C*-H), 125.0 (q, $^{1}J_{CF}$ = 272.4 Hz, [BAr$^F_4$] *C*F$_3$), 127.4 (d, J_{CP} = 5.8 Hz), 128.0 (d, J_{CP} = 12.9 Hz), 128.4 (d, J_{CP} = 3.4 Hz), 128.5 (d, J_{CP} = 5.0 Hz), 128.8 (dd, J_{CP} = 33.4 (d), 8.8 (d) Hz), 129.0 – 129.1 (m), 128.8 – 129.8 (m, [BAr$^F_4$] *C*-CF$_3$), 129.6 (d, J_{CP} = 11.6 Hz), 130.4 (s), 130.6 (s), 131.4 (s), 131.5 (d, J_{CP} = 2.0 Hz), 131.7 (s), 132.1 (dd, J_{CP} = 9.7 (d), 7.3 (d) Hz), 133.0 (d, J_{CP} = 8.3 Hz), 133.0 (d, J_{CP} = 43.9 Hz), 133.9 (s), 134.8 (s), 135.2 (d, J_{CP} = 42.4 Hz), 135.2 (s, [BAr$^F_4$] *C*-H), 136.2 (d, J_{CP} = 37.9 Hz), 139.3 – 139.4 (m), 139.5 (dd, J_{CP} = 3.4 (d), 1.7 (d) Hz), 139.7 – 140.0 (m), 144.5 (d, J_{CP} = 51.9 Hz), 153.1 (d, J_{CP} = 31.4 Hz), 154.0 (d, J_{CP} = 40.4 Hz), 162.1 (q, $^{1}J_{CB}$ = 49.8 Hz, [BAr$^F_4$] *C*-B) ppm.

$^{31}P\{^{1}H\}$ NMR (202 MHz, CD_2Cl_2, 298 K) = δ_P -17.5 (t, 1P, $^{2}J_{PP}$ = 46.3 Hz, *P*Me_3), 23.3 (d, 1P, $^{3}J_{PP}$ = 9.3 Hz, *P*Ph_3), 59.95 (s(br), 1P, PCP pincer *P*), 68.3 (s(br), 1P, PCP pincer *P*) ppm.

HRMS (ESI-TOF) m/z: $[M]^+$ Calcd for $C_{59}H_{52}CoP_4S$ 975.2067; Found 975.2067.

Found: C, 59.3; H, 3.3. Calc. for $C_{91}H_{64}BCoF_{24}P_4S$: C, 59.4; H, 3.5%.

Preparation of complex 9

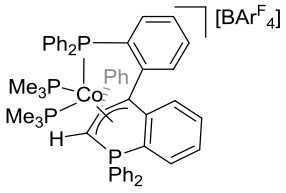

9

A solution of complex **1** (32.2 mg, 0.02 mmol) in fluorobenzene (1 mL) was treated with phenylacetylene (2.2 µL, 0.02 mmol) and mixed at room temperature for 9 h. The solution was then layered with hexanes (8 mL) and allowed to crystallise at room temperature. Red crystals of complex **9** were isolated by filtration and then washed with hexanes (2 x 5 mL) and then dried under vacuum (30 mg, 88%).

^{1}H NMR (500 MHz, Acetone-d_6, 298 K) = δ_H 0.55 (d, $^{2}J_{HP}$ = 6.0 Hz, 9H, P*Me*$_3$), 1.25 (d, $^{2}J_{HP}$ = 7.2 Hz, 9H, P*Me*$_3$), 3.15 (d, $^{2}J_{HP}$ = 13.7 Hz, 1H, allyl C-*H*), 6.50 (d, *J* = 8.0 Hz, 2H, Ar-*H*), 6.64 (t, *J* = 7.7 Hz, 2H, Ar-*H*), 6.97 (dt, *J* = 23.1 (d), 7.4 (t) Hz, 2H, Ar-*H*), 7.14 (t, *J* = 7.8 Hz, 2H, Ar-*H*), 7.26 (t, *J* = 8.8 Hz, 3H, Ar-*H*), 7.32 – 7.40 (m, 4H, Ar-*H*), 7.42 – 7.61 (m, 11H, Ar-*H*), 7.63 – 7.72 (m, 5H, Ar-*H* and [BAr^F_4] Ar-*H*), 7.77 – 7.86 (m, 11H, Ar-*H* and [BAr^F_4] Ar-*H*), 7.88 – 7.95 (m, 1H, Ar-*H*), 8.35 (dd, *J* = 11.3 (d), 7.9 (d) Hz, 2H, Ar-*H*) ppm.

$^{13}C\{^{1}H\}$ NMR (126 MHz, Acetone-d_6, 298 K) = δ_C 13.1 – 14.0 (m, allyl *C*-H), 20.0 (d, $^{1}J_{CP}$ = 18.2 Hz), 20.2 (dt, $^{1}J_{CP}$ = 21.4 (d), $^{2}J_{CP}$ = 3.5 Hz), 65.8 (dd, J_{CP} = 22.6, 9.2 Hz), 77.8 (s(br)), 109.1 (d, J_{CP} = 92.3 Hz), 118.4 (p, *J* = 3.9 Hz, [BAr^F_4] *C*-H), 124.2 (d, J_{CP} = 12.2 Hz), 125.4 (q, $^{1}J_{CF}$ = 272.9 Hz, [BAr^F_4] *C*F_3), 125.4 (s), 128.2 (s), 128.6 (s), 129.0 (d, J_{CP} = 9.4 Hz), 129.1 (d, J_{CP} = 5.7 Hz), 129.8 (d, J_{CP} = 8.5 Hz), 130.0 (t, J_{CP} = 12.9 Hz), 129.5 – 130.6 (m, [BAr^F_4] *C*-CF_3), 131.0 (d, J_{CP} = 34.6 Hz), 131.6 – 131.7 (m), 131.8 (s), 132.5 (d, J_{CP} = 5.5 Hz), 133.2 (d, J_{CP} = 10.1 Hz), 133.4 (d, J_{CP} = 2.6 Hz), 134.0 (t, J_{CP} = 10.6 Hz), 134.2 (d, J_{CP} = 19.1 Hz), 135.1 (d, J_{CP} = 2.8 Hz), 135.4 (d, J_{CP} = 8.7 Hz), 135.5 (s, [BAr^F_4] *C*-H), 136.7 (ddd, J_{CP} = 79.0 (d), 34.2 (d), 5.5 (d) Hz), 143.0 (dd, J_{CP} = 44.5 (d), 7.9 (d) Hz), 145.2 (s), 155.8 (dd, J_{CP} = 32.6 (d), 2.8 (d) Hz), 156.5 (td, J_{CP} = 8.0 (t), 4.5 (d) Hz), 162.6 (q, $^{1}J_{CB}$ = 49.8 Hz, [BAr^F_4] *C*-B) ppm.

$^{31}P\{^{1}H\}$ NMR (202 MHz, Acetone-d_6, 298 K) = δ_P -13.8 (s(br), 1P, P*Me*$_3$), -1.1 (s(br), 1P, P*Me*$_3$), 4.2 (d, $^{3}J_{PP}$ = 47.7 Hz, 1P, phosphonium *P*Ph$_2$), 61.3 (s(br), 1P, Pincer Co-*P*Ph$_2$) ppm.

HRMS (ESI-TOF) m/z: $[M]^+$ Calcd for $C_{51}H_{52}CoP_4$ 847.2346; Found 847.2348.

Found: C, 58.2; H, 4.3. Calc. for $C_{83}H_{64}BCoF_{24}P_4$: C, 58.3; H, 3.8%.

Preparation of complex 10

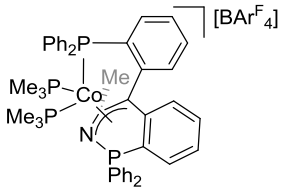

10

A solution of complex **1** (32.2 mg, 0.02 mmol) in MeCN (1 mL) was stirred at 80 °C for 20 h. The magenta coloured solution was then evaporated to dryness and then dissolved in toluene (20 mL). The toluene solution was then evaporated under vacuum under a red residue remained. This described co-evaporation with toluene was repeated three more times to ensure complete removal of MeCN. The remaining residue was then filtered through a pad of silica gel using toluene solvent, collecting the red fraction. The solution was concentrated under vacuum to approx. 0.5 mL and then hexanes (5 mL) were added and then the mixture was triturated until a red solid of product **10** was present. The solid was filtered, washed with hexanes (2 x 5 mL) and dried under vacuum (23 mg, 70%).

^{1}H NMR (500 MHz, C_6D_6, 298 K) = δ_H 0.23 (d, $^{2}J_{HP}$ = 5.3 Hz, 9H, P*Me*$_3$), 0.82 (d, $^{2}J_{HP}$ = 7.5 Hz, 9H, P*Me*$_3$), 1.42 (dd, $^{4}J_{HP}$ = 8.3 (d), $^{4}J_{HP}$ = 3.5 (d) Hz, 3H, NC*Me*), 6.54 (t, *J* = 7.8 Hz, 1H, Ar-*H*), 6.72 – 7.13 (m, 20H, Ar-*H*), 7.19 – 7.27 (m, 2H, Ar-*H*), 7.36 – 7.47 (m, 3H, Ar-*H*), 7.49 – 7.59 (m, 2H, Ar-*H*), 7.66 (s, 4H, [BAr$^F_4$] Ar-*H*), 8.42 (s, 8H, [BAr$^F_4$] Ar-*H*) ppm.

$^{13}C\{^{1}H\}$ NMR (126 MHz, C_6D_6, 298 K) = δ_C 18.2 – 18.6 (m, 2 x P*Me*$_3$), 24.5 (s, NC*Me*), 65.9 – 66.8 (m), 91.1 – 91.7 (m), 108.5 (dd, J_{CP} = 87.1, 4.6 Hz), 118.2 (s, [BAr$^F_4$] *C*-H), 123.7 (d, J_{CP} = 10.2 Hz), 125.3 (q, $^{1}J_{CF}$ = 272.6 Hz, [BAr$^F_4$] *C*F$_3$), 128.8 – 128.9 (m), 128.9 – 129.2 (m), 129.3 (d, J_{CP} = 12.1 Hz), 130.0 (q, $^{2}J_{CF}$ =31.6 Hz, BAr$^F_4$] *C*-CF$_3$), 130.5 (s), 130.6 (d, J_{CP} = 6.1 Hz), 131.1 (d, J_{CP} = 22.6 Hz), 131.7 (d, J_{CP} = 10.0 Hz), 132.2 (t, J_{CP} = 9.3 Hz), 132.6 (d, J_{CP} = 10.9 Hz), 133.0 (s), 133.3 (d, J_{CP} = 2.4 Hz), 133.7 (s), 133.8 – 134.0 (m),

134.1 (d, J_{CP} = 2.5 Hz), 134.7 (s), 135.5 (s, [BAr$^F_4$] *C*-H), 139.8 (dd, J_{CP} = 48.8 (d), 7.5 (d) Hz), 152.3 (d, J_{CP} = 29.9 Hz), 154.4 (s(br)), 162.8 (q, $^1J_{CB}$ = 49.8 Hz, [BAr$^F_4$] *C*-B) ppm.

$^{31}P\{^1H\}$ NMR (202 MHz, C_6D_6, 298 K) = δ_P -19.0 (ddd, $^2J_{PP}$ = 37.3 (d), $^2J_{PP}$ = 37.3 (d), $^3J_{PP}$ = 36.5 (d) Hz, 1P, P*Me*$_3$), -4.2 (dd, $^2J_{PP}$ = 37.3, $^2J_{PP}$ = 37.3 Hz, 1P, P*Me*$_3$), 17.6 (d, $^3J_{PP}$ = 36.5 Hz, 1P, phosphonium PPh_2), 60.8 (dd, $^2J_{PP}$ = 37.3, $^2J_{PP}$ = 37.3 Hz, 1P, Pincer Co-*P*Ph_2) ppm.

HRMS (ESI-TOF) m/z: $[M]^+$ Calcd for $C_{45}H_{49}CoNP_4$ 786.2142; Found 786.2146.

Preparation of complex III

Method A

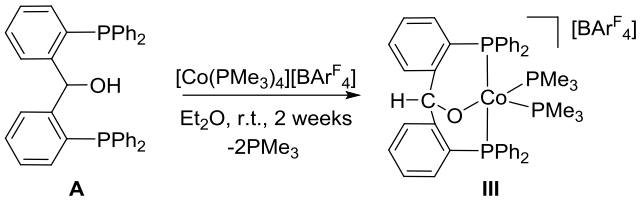

Et_2O (50 mL) was added to a mixture of [Co(PMe_3)$_4$][BAr$^F_4$] (122.6 mg, 0.1 mmol) and Ligand **A** (55.3 mg, 0.1 mmol) and then stirred at room temperature for two weeks in sealed Schlenk tube. ^{31}P NMR analysis of the reaction mixture indicated that complete conversion of ligand **A** had occurred. ESI-MS analysis indicated that complex **III** was the predominant species formed.

Method B

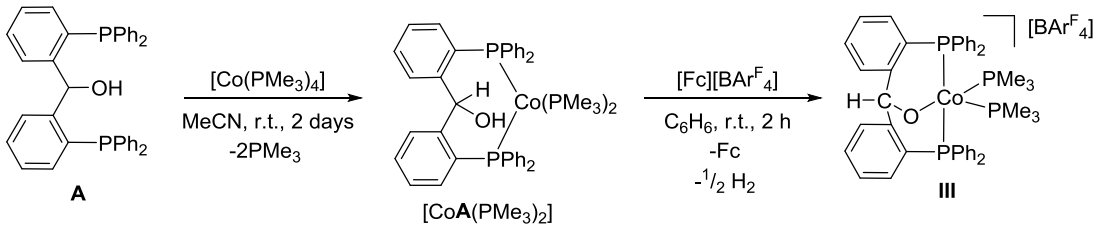

MeCN (10 mL) was added to a mixture of [Co(PMe_3)$_4$] (181.6 mg, 0.5 mmol) and Ligand **A** (276.3 mg, 0.5 mmol) and then stirred at room temperature for two days in sealed Schlenk tube. The precipitate was filtered, washed with MeCN (3 x 5 mL) and hexanes (3 x 10 mL) and then dried under vacuum to give the proposed [Co**A**(PMe_3)$_2$] complex as a brown solid (187 mg, 49%). This isolated species was not characterised in detail but is presumably the ligand exchange product between **A** and two PMe_3 ligands, as Li *et al* reported an analogous product when the similar bisphosphine ligand $(Ph_2PC_6H_4)_2CH_2$ and [Co(PMe_3)$_4$] were reacted.[11]

III was formed when [Co**A**(PMe_3)$_2$] (76.7 mg, 0.1 mmol) and [Fc][BAr^F_4] (104.9 mg, 0.1 mmol) were stirred in C_6H_6 (5 mL) for 2 h at room temperature. The dark green precipitate was filtered, washed with C_6H_6 (3 x 5 mL) and hexanes (3 x 10 mL) and then dried under vacuum to give pure complex **III** (127 mg, 78% relative to the amount of [Co**A**(PMe_3)$_2$] used).

HRMS (ESI-TOF) m/z: $[M]^+$ Calcd for $C_{43}H_{47}CoOP_4$ 762.1904; Found 762.1903.

Magnetic moment (298 K): μ_{eff} = 2.10 μB (one unpaired electron, S = 1/2).

Found: C, 55.2; H, 4.2. Calc. for $C_{75}H_{59}BCoF_{24}OP_4$: C, 55.4; H, 3.7%.

Preparation of complex V

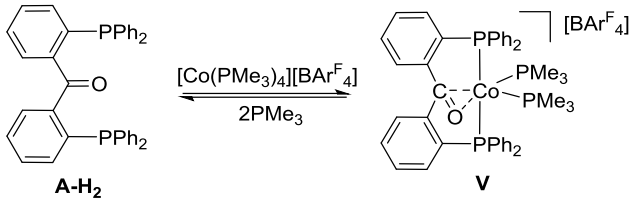

Toluene (10 mL) was added to a mixture of [Co(PMe_3)$_4$][BAr^F_4] (98.1 mg, 0.08 mmol) and Ligand **A-H$_2$** (44.0 mg, 0.08 mmol) and then stirred at room temperature. After 5 min, the reaction solution was evaporated under vacuum until a residue remained. Toluene (10 mL) was re-added to the reaction mixture, stirred for 5 min at room temperature and then evaporated again. This described co-evaporation with toluene was repeated two more times to ensure complete removal of PMe_3 by-product, driving the equilibrium towards complex **V**. The final red coloured residue was recrystallised by layering a concentrated fluorobenzene (2 mL) solution with hexanes (12 mL) and leaving at -20 °C. The dark red coloured crystallised complex **V** was isolated by filtration and then dried under vacuum (90 mg, 70%).

^{1}H NMR (500 MHz, C_6D_6, 298 K) = δ_H 0.46 (s, 9H, P*Me*$_3$), 0.83 (d, $^2J_{HP}$ = 6.9 Hz, 9H, P*Me*$_3$), 6.52 – 6.88 (m, 8H, Ar-*H*), 6.95 (t, *J* = 6.9 Hz, 4H, Ar-*H*), 7.01 – 7.10 (m, 4H, Ar-*H*), 7.10 – 7.14 (m, 2H, Ar-*H*), 7.30 (s(br), 8H, Ar-*H*), 7.66 (s, 4H, [BAr^F_4] Ar-*H*), 7.90 (d, *J* = 7.3 Hz, 2H, Ar-*H*), 8.41 (s, 8H, [BAr^F_4] Ar-*H*) ppm.

^{1}H NMR (500 MHz, Toluene-d_8, 253 K) = δ_H 0.35 (d, $^2J_{HP}$ = 7.7 Hz, 9H, P*Me*$_3$), 0.74 (d, $^2J_{HP}$ = 7.8 Hz, 9H, P*Me*$_3$), 6.61 – 6.77 (m, 8H, Ar-*H*), 6.86 (t, *J* = 7.4 Hz, 5H, Ar-*H*), 6.98 – 7.02 (m, 5H, Ar-*H*), 7.17 – 7.32 (m, 8H, Ar-*H*), 7.59 (s, 4H, [BAr^F_4] Ar-*H*), 7.82 (d, *J* = 7.7 Hz, 2H, Ar-*H*), 8.45 (s, 8H, [BAr^F_4] Ar-*H*) ppm.

$^{13}C\{^{1}H\}$ NMR (126 MHz, C_6D_6, 298 K) = δ_C 19.3 (d, $^{1}J_{CP}$ = 22.7 Hz, P*Me*$_3$), 21.2 (d, $^{1}J_{CP}$ = 21.8 Hz, P*Me*$_3$), 98.8 (d, $^{2}J_{CP}$ = 11.1 Hz, *C*=O), 118.1 (s, [BAr$^{F}_4$] *C*-H), 125.3 (q, $^{1}J_{CF}$ = 272.6 Hz, [BAr$^{F}_4$] *C*F$_3$), 126.8 (s), 127.6 (s), 128.7 (s), 129.9 (q, $^{2}J_{CP}$ = 31.7 Hz, BAr$^{F}_4$] *C*-CF$_3$), 131.0 (s), 131.1 (s), 132.0 – 132.4 (m), 132.4 (s), 134.5, 135.2 (d, J_{CP} = 138.2 Hz), 135.5 (s, [BAr$^{F}_4$] *C*-H), 150.4 – 150.8 (m), 162.8 (q, $^{1}J_{CB}$ = 49.8 Hz, [BAr$^{F}_4$] *C*-B) ppm.

$^{31}P\{^{1}H\}$ NMR (202 MHz, C_6D_6, 298 K) = δ_P -26.1 (s(br)), -11.8 (s(br), 1P, *P*Me$_3$), 22.7 (s(br), 2P, Pincer P's) ppm.

$^{31}P\{^{1}H\}$ NMR (202 MHz, Toluene-d$_8$, 253 K) = δ_P -30.8 (td, $^{2}J_{PP}$ = 83.9 (t), 48.5 (d) Hz, 1P, *P*Me$_3$), -16.6 (dt, $^{2}J_{PP}$ = 49.6 (d), 48.5 (t) Hz, 1P, *P*Me$_3$), 17.9 (dd, *J* = 83.9 (d), 49.6 (d) Hz, 2P, Pincer P's) ppm.

HRMS (ESI-TOF) m/z: $[M]^+$ Calcd for $C_{43}H_{46}CoOP_4$ 761.1826; Found 761.1823.

Found: C, 55.7; H, 3.1. Calc. for $C_{75}H_{58}BCoF_{24}OP_4$: C, 55.4; H, 3.6%.

Preparation of compound A^{Me}

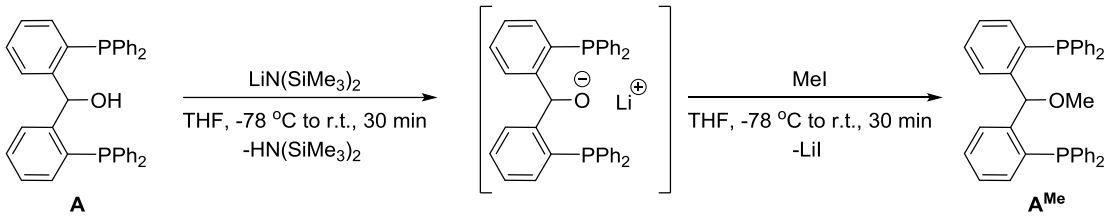

A solution of compound **A** (165.8 mg, 0.3 mmol) in THF (10 mL) was treated dropwise with a solution of LiN(SiMe$_3$)$_2$ (50.2 mg, 0.3 mmol) in THF (10 mL) at -78 °C. After complete addition, the solution was allowed to come to room temperature and stirred for 30 min. The reaction mixture was cooled to -78 °C, treated with MeI (18.7 mg, 0.3 mmol) and then slowly raised to room temperature. After stirring overnight, the reaction mixture was evaporated to dryness and then purified by column chromatography on silica gel in air using EtOAc:hexanes (1:9) (31 mg, 18%).

^{1}H NMR (500 MHz, $CDCl_3$, 298 K) = δ_H 3.00 (s, 3H, O*Me*), 6.93 (t, $^{4}J_{HP}$ = 6.8 Hz, 1H, C(OH)(*H*)), 6.97 – 7.07 (m, 2H, Ar-*H*), 7.08 – 7.17 (m, 6H, Ar-*H*), 7.17 – 7.25 (m, 10H, Ar-*H*), 7.28 – 7.41 (m, 10H, Ar-*H*) ppm.

6.8 (t, *J* = 7.4 Hz, 2H, Ar-*H*), 7.3 – 7.4 (m, 2H, Ar-*H*), 7.4 – 7.6 (m, 12H, PPh$_2$ H's), 7.8 – 8.0 (m, 8H, PPh$_2$ H's), 8.2 (d, *J* = 7.6 Hz, 2H, Ar-*H*), 8.3 – 8.3 (m, 2H, Ar-*H*) ppm.

$^{13}C\{^1H\}$ NMR (126 MHz, $CDCl_3$, 298 K) = δ_C 56.5 (s, *Me*) 80.9 (t, $^3J_{CP}$ = 23.5 Hz, *C*(OH)(H)), 127.8 (s), 128.0 (t, J_{CP} = 3.4 Hz), 128.3 (dt, J_{CP} = 16.2 (d), 3.4 (t) Hz), 128.4 (d, J_{CP} = 17.8 Hz), 128.9 (s), 133.8 – 134.1 (m), 134.8 (s), 137.3 – 137.6 (m), 145.4 – 145.9 (m) ppm.

$^{31}P\{^1H\}$ NMR (202 MHz, $CDCl_3$, 298 K) = δ_P 16.0 (s, 2P, PCP pincer *P*'s) ppm.

HRMS (ESI-TOF) m/z: $[M+H]^+$ Calcd for $C_{38}H_{33}OP_2$ 567.2001; Found 567.2001.

Preparation of compound A^{TIPS}

A **A^{TIPS}**

A solution of compound **A** (55.3 mg, 0.1 mmol), $SiCl(^iPr)_3$ (32.1 µL, 0.15 mmol) and imidazole (20.4 mg, 0.3 mmol) in DMF (0.3 mL) was heated at 110 °C for 2 days. The mixture was diluted with Et_2O (4 mL) and washed with water (3 x 1 mL). The organic layer was evaporated and then purified by column chromatography on silica gel in air using EtOAc:hexanes (1:9) (14 mg, 21%).

^1H NMR (500 MHz, $CDCl_3$, 298 K) = δ_H 0.71 – 0.90 (m, 21H, *^iPr* groups), 6.94 – 7.05 (m, 6H, Ar-*H*), 7.05 – 7.18 (m, 8H, Ar-*H*), 7.18 – 7.26 (m, 5H, Ar-*H*), 7.26 – 7.33 (m, 6H, Ar-*H*), 7.40 (t, *J* = 5.1 Hz, 1H, Ar-*H*), 7.92 (d, *J* = 7.2 Hz, 2H, Ar-*H*) ppm.

$^{13}C\{^1H\}$ NMR (126 MHz, $CDCl_3$, 298 K) = δ_C 13.2 (s, SiC*H*), 18.3 (s, *C*H_3), 74.2 (t, $^3J_{CP}$ = 19.7 Hz, *C*(H)(OSi(^{i}Pr)$_3$), 127.4 (d, J_{CP} = 66.0 Hz), 128.0 (t, J_{CP} = 2.9 Hz), 128.3 (t, J_{CP} = 3.2 Hz), 129.0 (s), 129.3 (t, J_{CP} = 5.9 Hz), 133.6 (dt, J_{CP} = 91.7, 10.1 Hz), 134.1 (dd, *J* = 8.8, 7.1 Hz), 135.8 (s), 138.4 (ddd, J_{CP} = 45.1 (d), 6.6)(d), 5.4 (d) Hz), 150.3 – 150.7 (m).

$^{31}P\{^1H\}$ NMR (202 MHz, $CDCl_3$, 298 K) = δ_P 18.2 (s, 2P, PCP pincer *P*'s) ppm.

HRMS (ESI-TOF) m/z: $[M+H]^+$ Calcd for $C_{46}H_{51}OP_2Si$ 709.3179; Found 709.3168.

Reaction between complex 1 and H_2

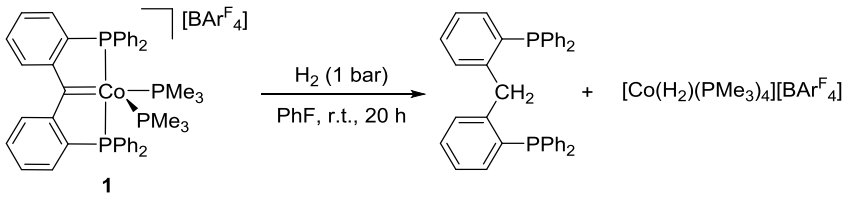

A solution of complex **1** (16.1mg, 0.01 mmol) in fluorobenzene (0.6 mL) was placed under an atmosphere of H_2 (1 bar) in a J. Young valve NMR tube and mixed at room temperature for 20 h. NMR spectroscopic and ESI-MS analyses indicated that the reduced bisphosphine ligand $(Ph_2PC_6H_4)_2CH_2$ and $[Co(H_2)(PMe_3)_4][BAr^F_4]$ had formed.

When this reaction was performed in MeCN (0.6 mL) instead, using the same quantity of **1**, a high-resolution $[M\text{-}H]^+$ fragment at *m*/*z* 576.2008 corresponding to MeCN being incorporated into the reduced ligand was observed in the ESI-MS mass spectrum of the crude reaction mixture after 4 days at r.t., in addition to $(Ph_2PC_6H_4)_2CH_2$ and $[Co(H_2)(PMe_3)_4][BAr^F_4]$.

Preparation of $[Co(H_2)(PMe_3)_4][BAr^F_4]$[12]

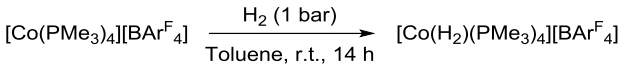

$[Co(H_2)(PMe_3)_4][BAr^F_4]$ was prepared to obtain analytical data of an authentic sample for comparison with the data obtained in the reaction between complex **1** and H_2. A solution of $[Co(PMe_3)_4][BAr^F_4]$ (36.9 mg, 0.03 mmol) in toluene (1 mL) was placed under an atmosphere of H_2 (1 bar) in a J. Young valve NMR tube and mixed at room temperature for 14 h. The pale blue crystalline solid was isolated by decanting away the supernatant. The pale blue product solid was washed with C_6H_6 (2 x 1 mL) and then dried under vacuum (25 mg, 68 %).

^{1}H NMR (500 MHz, CD_3CN, 298 K) = δ_H -14.96 (s(br), 2H, Co-H), 1.40 (d, $^2J_{HP}$ = 4.7 Hz, 18H, P*Me*$_3$), 1.46 (s, 18H, P*Me*$_3$), 7.68 (s, 4H, [BAr$^F_4$] Ar-*H*), 7.71 (s, 8H, [BAr$^F_4$] Ar-*H*) ppm.

^{13}C{^{1}H} NMR (126 MHz, zCD_3CN, 298 K) = δ_C 22.4 (t, *J* = 14.7 Hz, P*Me*$_3$), 25.8 (t, *J* = 16.2 Hz, P*Me*$_3$), 118.4 – 118.8 (m, [BAr$^F_4$] *C*-H), 125.4 (q, $^1J_{CF}$ = 272.1 Hz, [BAr$^F_4$] *C*F$_3$), 129.9 (q, $^2J_{CP}$ = 31.7 Hz, BAr$^F_4$] *C*-CF$_3$), 135.6 (s, [BAr$^F_4$] *C*-H), 162.6 (q, $^1J_{CB}$ = 49.8 Hz, [BAr$^F_4$] *C*-B) ppm.

^{31}P{^{1}H} NMR (202 MHz, CD_3CN, 298 K) = δ_P 2.4 (s(br), 2P, *P*Me$_3$), 6.9 (s(br), 2P, *P*Me$_3$) ppm.

IR (nujol): 1956.9 cm^{-1} (v(Co-H).

HRMS (ESI-TOF) m/z: $[M]^+$ Calcd for $C_{12}H_{38}CoP_4$ 365.1250; Found 365.1261.

Reaction between complex 1 and $[H(OEt_2)_2][BAr^F_4]$

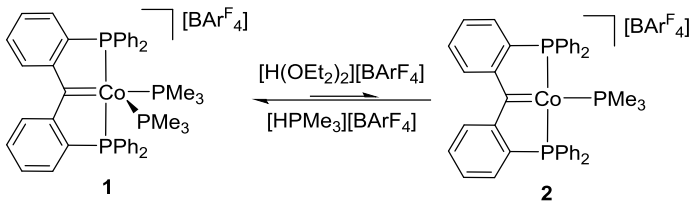

Fluorobenzene (0.6 mL) was added to a mixture of complex **1** (16.1 mg, 0.01 mmol) and $[H(OEt_2)_2][BAr^F_4]$ (10.1 mg, 0.01 mmol) in a J. Young valve NMR tube and mixed thoroughly at room temperature. After 1 h, the reaction solution was then analysed by ^{31}P NMR spectroscopy and indicated 22% conversion of **1** to give **2** and $[HPMe_3][BAr^F_4]$ had occurred.

Characterisation of $[HPMe_3][BAr^F_4]$[13] for comparative purposes

A solution of $[H(OEt_2)_2][BAr^F_4]$ (20.2mg, 0.02 mmol) in C_6D_6 (0.6 mL) in a J. Young valve NMR tube was treated with PMe_3 (2.0 µL, 0.02 mmol) and thoroughly mixed at room temperature. The upper layer was then decanted away from the colourless lower layer. ^{31}P NMR analysis of the lower layer in fluorobenzene solvent confirmed the formation of $[HPMe_3][BAr^F_4]$ in the reaction between complex **1** and $[H(OEt_2)_2][BAr^F_4]$, when the two spectra are compared.

$^{31}P\{^1H\}$ NMR (202 MHz, CD_2Cl_2, 298 K) = δ_P -3.6 (s, 1P, Phosphonium H*P*Me_3) ppm.

Attempted reaction between complex 1 and HCl

A solution of complex **1** (16.1mg, 0.01 mmol) in fluorobenzene (0.6 mL) in a J. Young valve NMR tube was treated with HCl in Et_2O (5.0 µL, 0.01 mmol, 2 M) at room temperature, sealed and then thoroughly mixed. After either allowing the solution to stand at room temperature for 2 days or heating at 80 °C for 3 h, ^{31}P NMR spectroscopic analysis indicated that complex **1** did not react.

Reaction between complex 1 and HBr

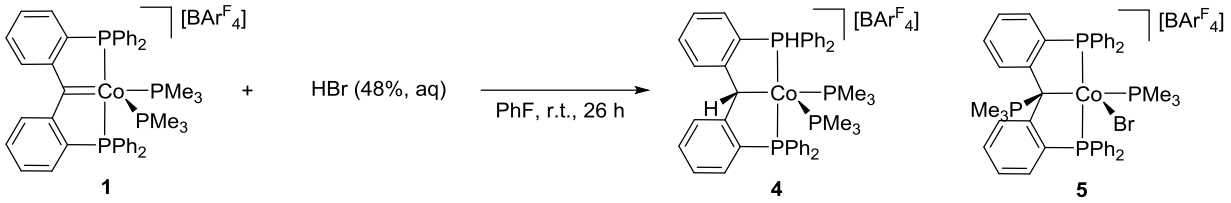

A solution of complex **1** (16.1mg, 0.01 mmol) in fluorobenzene (0.6 mL) in a J. Young valve NMR tube was treated with HBr (1.1 µL, 0.01 mmol, 48% aqueous) at room temperature, sealed and then thoroughly mixed. After allowing the solution to stand at room temperature for 26 h, the ^{31}P NMR spectrum of the reaction mixture did not contain any signals and the predominant ions observed by high-resolution ESI-MS spectrum corresponded to complexes **4** and **5**.

Attempted reaction between complex 1 and Et_3SiH

A solution of complex **1** (16.1mg, 0.010 mmol) in fluorobenzene (0.6 mL) in a J. Young valve NMR tube was treated with Et_3SiH (2.4 µL, 0.015 mmol) at room temperature, sealed and then thoroughly mixed. After heating at 80 °C for 23 h, ^{31}P NMR spectroscopic analysis indicated that complex **1** did not react.

Attempted reactions between $[Co(PMe_3)_4][BAr^F_4]$ and compounds A^{Me} or A^{TIPS}

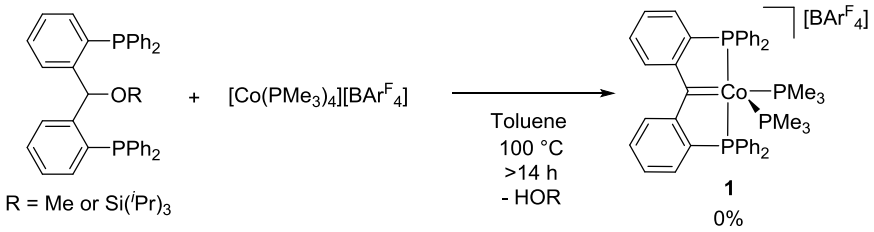

Toluene (0.6 mL) was added to a mixture of $[Co(PMe_3)_4][BAr^F_4]$ (12.3 mg, 0.01 mmol) and Ligand $\mathbf{A^{Me}}$ or $\mathbf{A^{TIPS}}$ (5.7 mg or 7.1 mg respectively, 0.01 mmol) in a J. Young valve NMR tube and then heated at 100 °C for at least 14 h. ^{31}P NMR spectroscopy and ESI-MS analyses of the reaction solution indicated that no reaction had occurred when either ligand was used.

Heating intermediate III to form complex 1

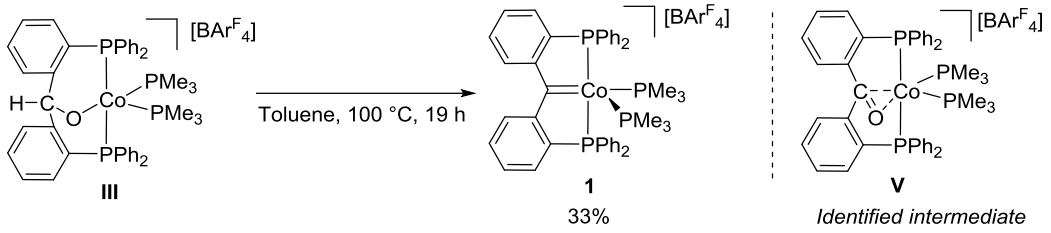

A mixture of complex **III** (16.2 mg, 0.01 mmol) in toluene (0.6 mL) in a J. Young valve NMR tube was heated at 100 °C and monitored by ^{31}P NMR spectroscopy. Within 1 h of heating, complex **V** was identified in the ^{31}P NMR spectrum and therefore is a proposed reaction intermediate. After 19 h of heating, complex **V** was found to be completely consumed. The reaction solution was evaporated, PPh_3 (2.6 mg, 0.01 mmol) was added as an internal standard, and then fluorobenzene (0.6 mL) was added to dissolve the mixture. From the ^{31}P NMR spectrum, the amount of complex **1** was determined to be 33%.

Reaction between complex V and H_2

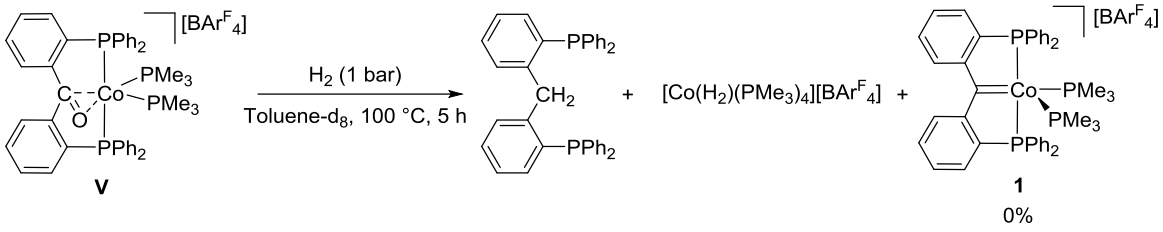

A solution of complex **V** (16.2 mg, 0.01 mmol) in toluene-d_8 (0.6 mL) was placed under an atmosphere of H_2 (1 bar) in a J. Young valve NMR tube and heated at 100 °C. After 5 h, NMR spectroscopic analyses showed that complex **1** was not present and that the predominant species present were the reduced bisphosphine ligand $(Ph_2PC_6H_4)_2CH_2$ and $[Co(H_2)(PMe_3)_4][BAr^F_4]$.

Assigning the identity of complex III

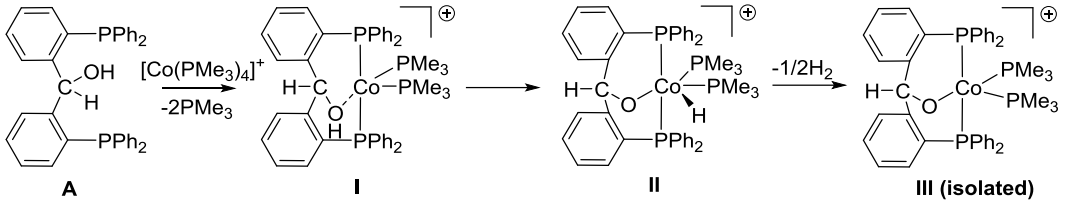

The identity of the resultant compound when ligand **A** reacted with $[Co(PMe_3)_4][BAr^F{}_4]$ at room temperature (see details in Experimental section) was assigned as Co(II) complex **III**, rather than Co(I) complex **I** or Co(III) complex **II**. The following support this assignment:

1. The high resolution ESI-MS data agree with the theoretical *m*/*z* and isotope pattern of **III** rather than **I** or **II**, which both have one more H atom in their formulae
2. The IR spectrum of the compound did not contain a characteristic metal-hydride stretching band (*ν*(M-H)) near 2000 cm^{-1} or hydroxy O-H stretching band (see Figure S89), which does not agree with it being Co(I) complex **I** or Co(III) complex **II**
3. Evans method NMR and EPR spectroscopy confirmed the compound was paramagnetic and had one unpaired electron in a low-spin configuration (*S* = 1/2), which agrees with the DFT calculated *S* = 1/2 state of low-spin configuration for **II** (*c.f. S* = 3/2 for high-spin configuration for **II,** *S* = 0 for **I** and **III**);
4. Co-O and Co-P bond distances are most similar those observed in the DFT calculated structure of **III** (Figure S98).

NMR Spectra of complex 1

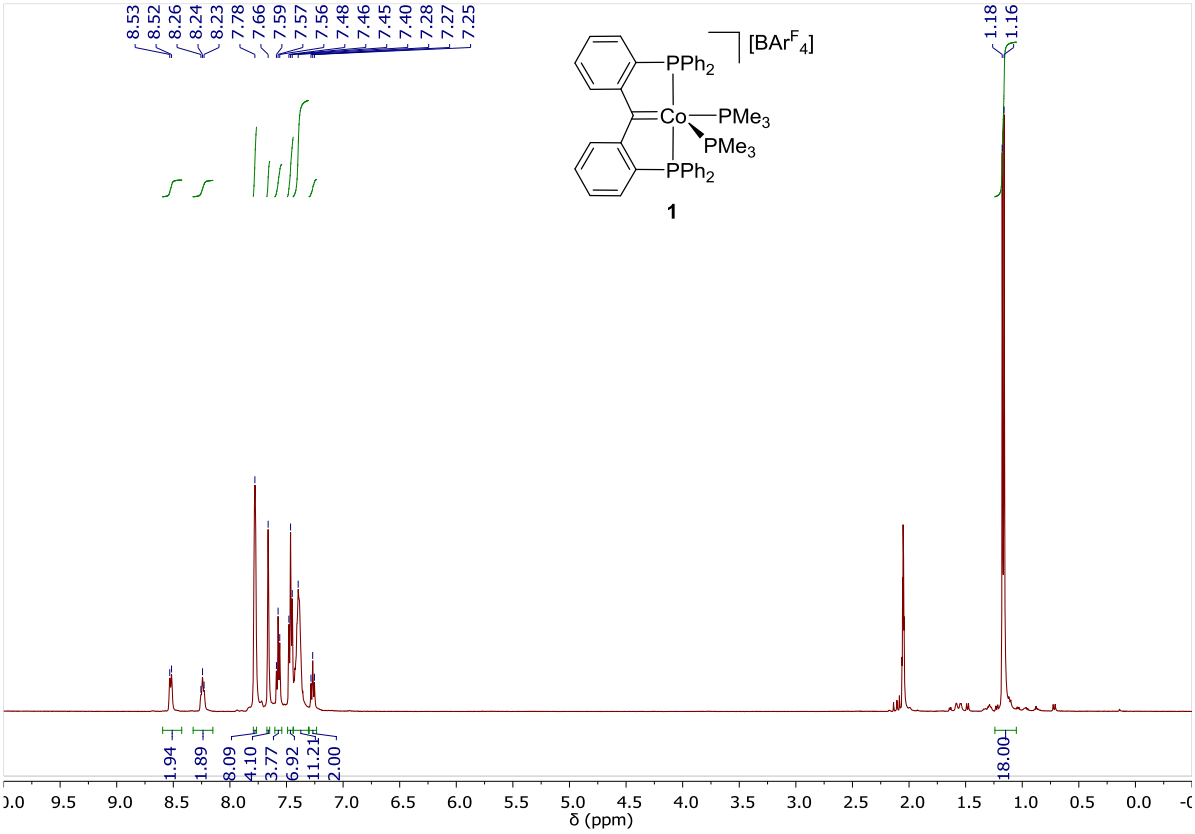

Figure S1 ^{1}H NMR of complex **1** in Acetone-d$_6$ at 298 K.

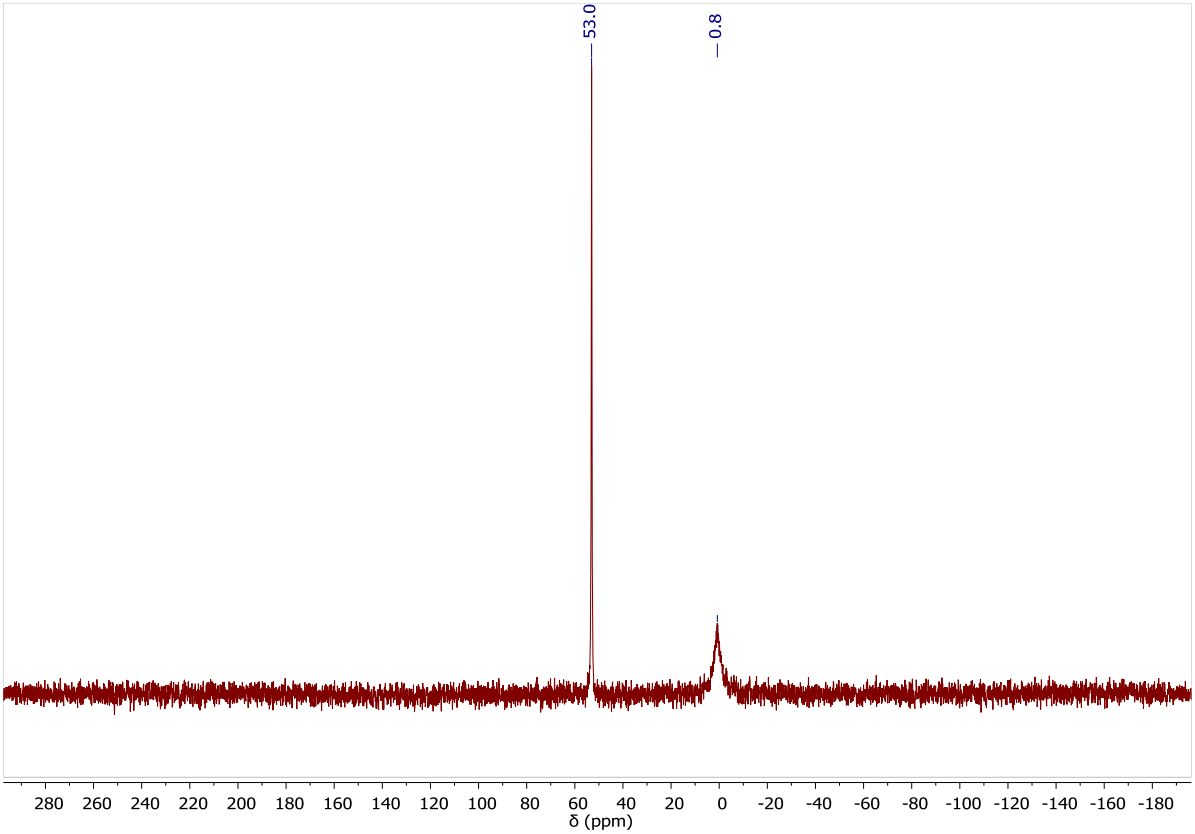

Figure S2 ^{31}P{^{1}H} NMR of complex **1** in Acetone-d$_6$ at 298 K.

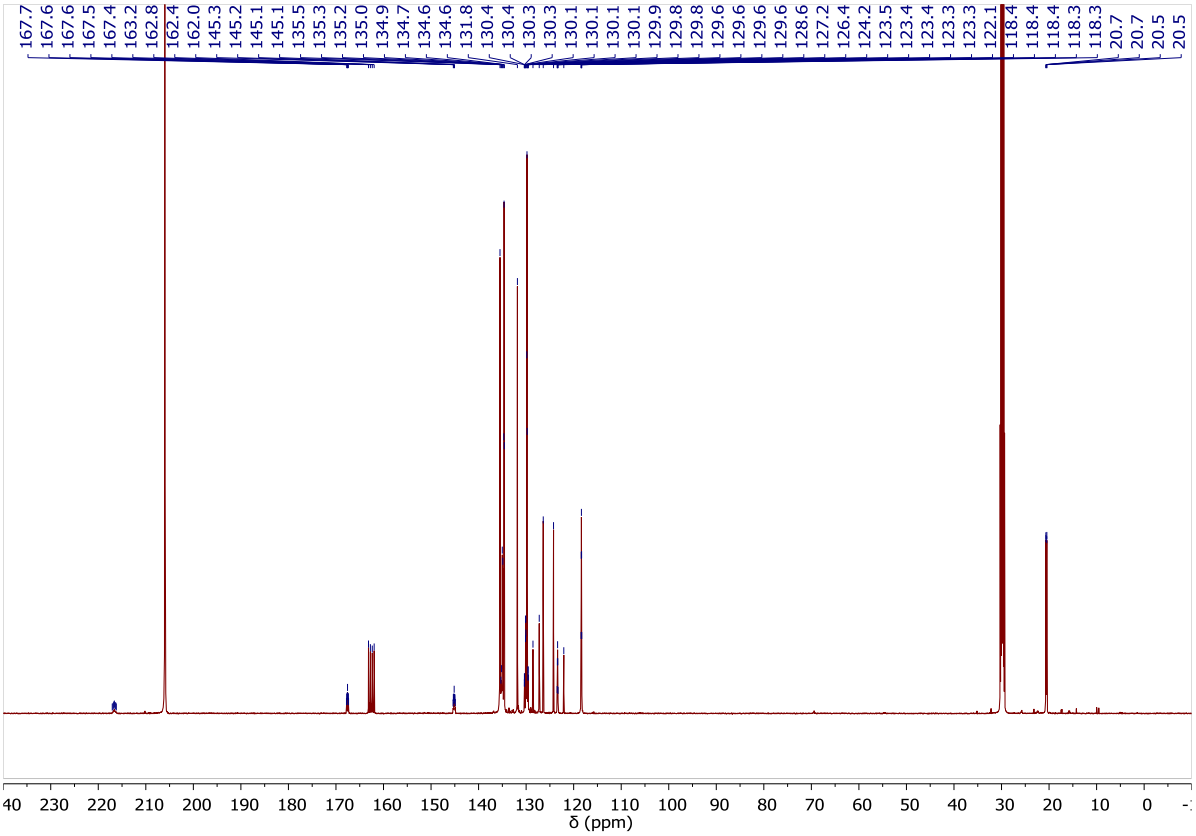

Figure S3 $^{13}C\{1H\}$ NMR of complex **1** in Acetone-d_6 at 298 K. Inset shows zoomed in spectrum of the Co=C resonance.

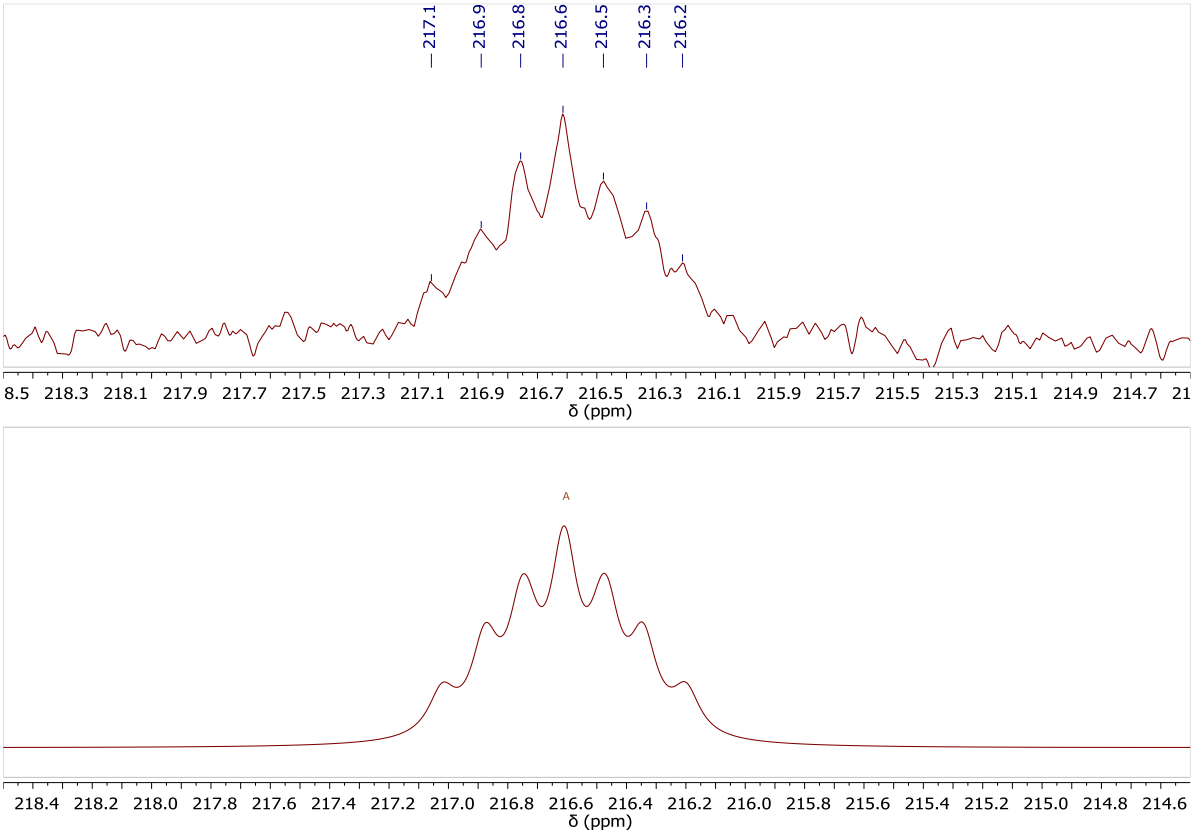

Figure S4 Experimental (top) and simulated (bottom) $^{13}C\{1H\}$ NMR spectra of the Co=C resonance of complex **1** in Acetone-d_6 at 298 K. Simulated resonance was produced using the experimentally determined *J* coupling constants in Mestrelab Research S.L. MestReNova.

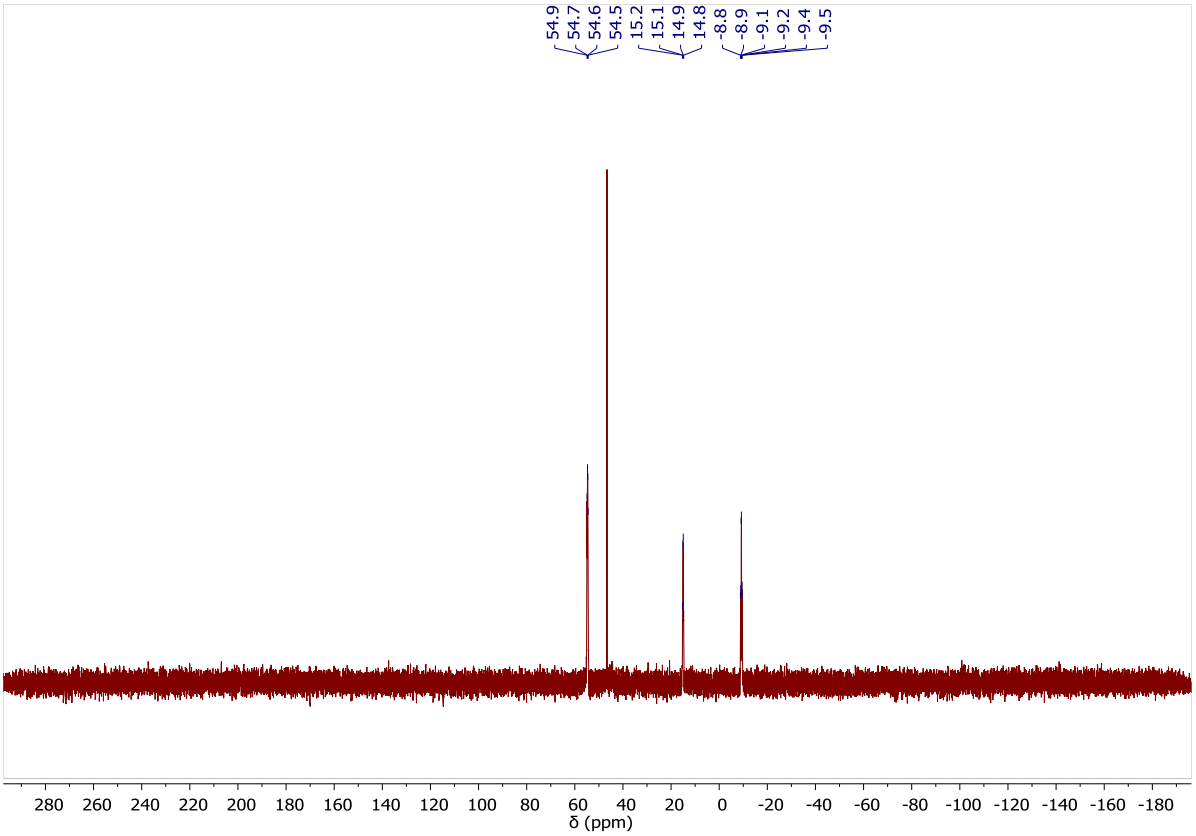

Figure S5 $^{31}P\{^{1}H\}$ NMR of complex **1** in CD_2Cl_2 at 198 K. Unknown peak at 46.6 ppm.

NMR Spectra of complex 2

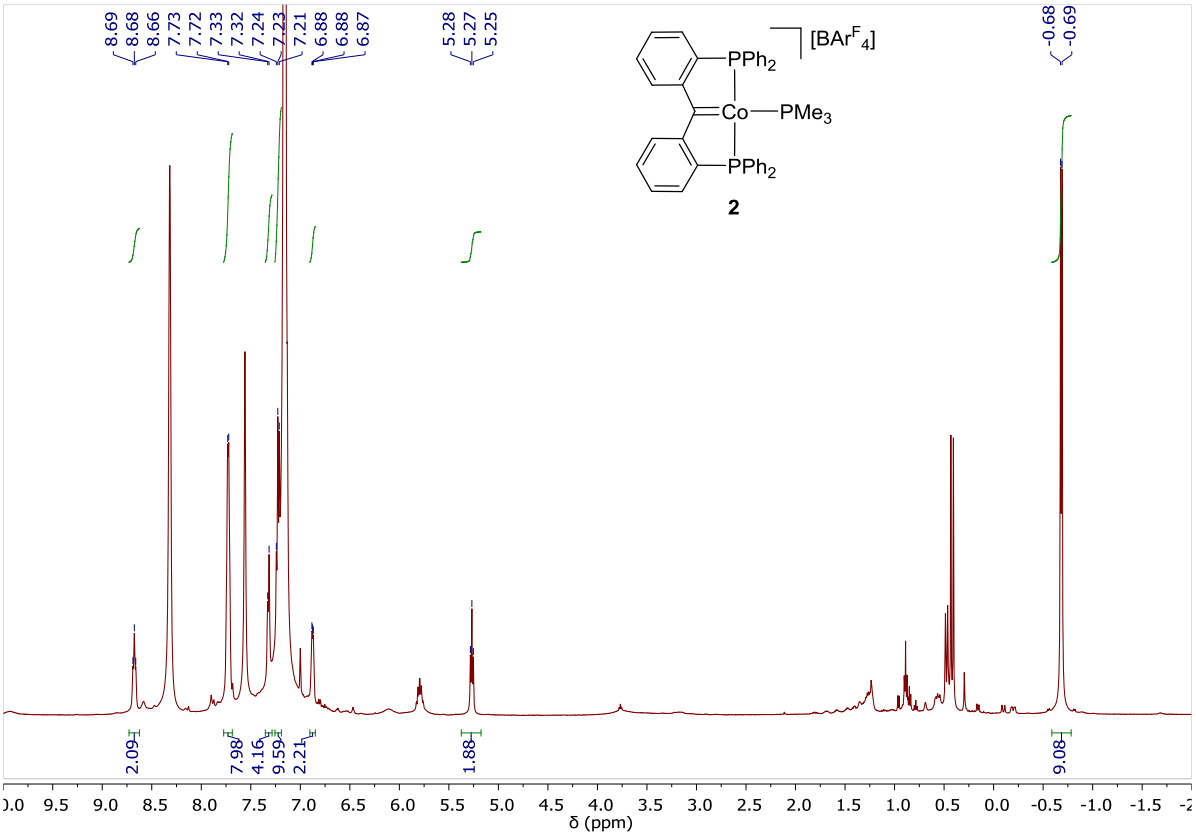

Figure S6 ^{1}H NMR of the reaction solution to form complex **2** in C_6D_6 at 298 K, highlighting the identified peaks.

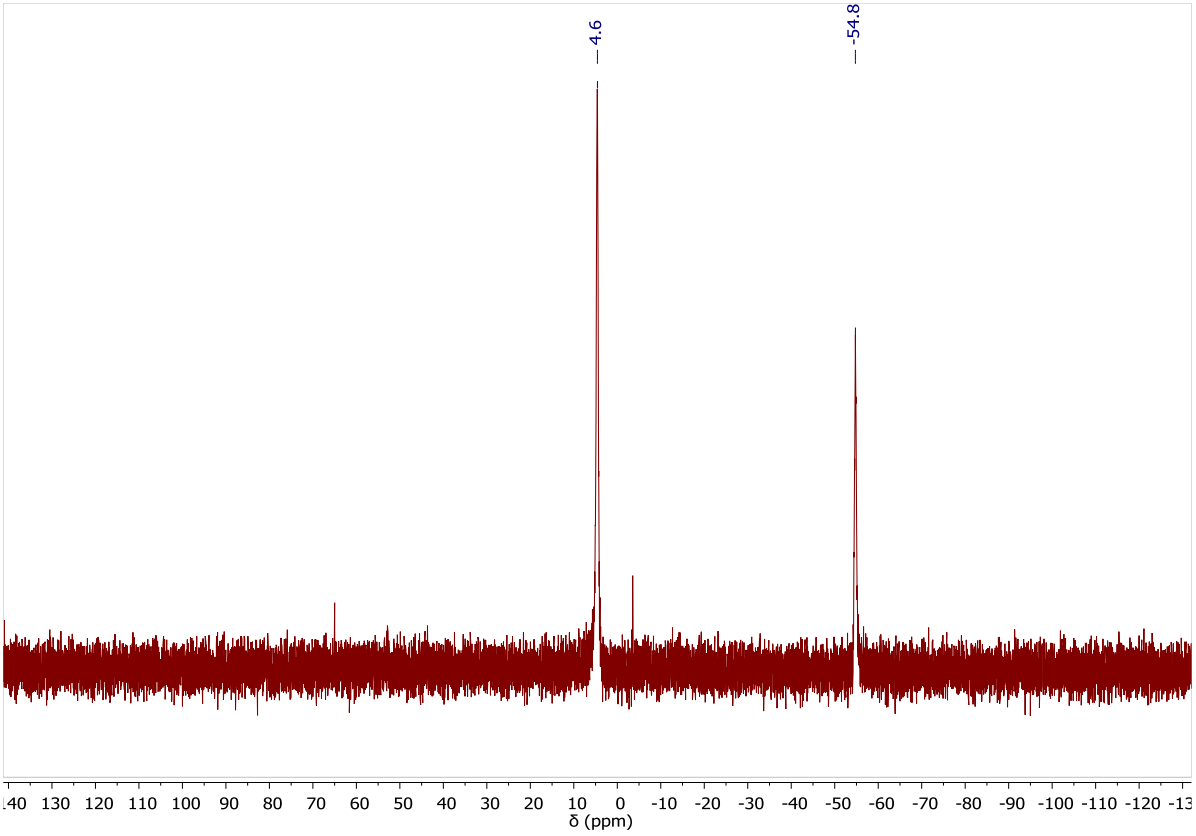

Figure S7 ^{31}P{^{1}H} NMR of the reaction solution to form complex **2** in C_6D_6 at 298 K.

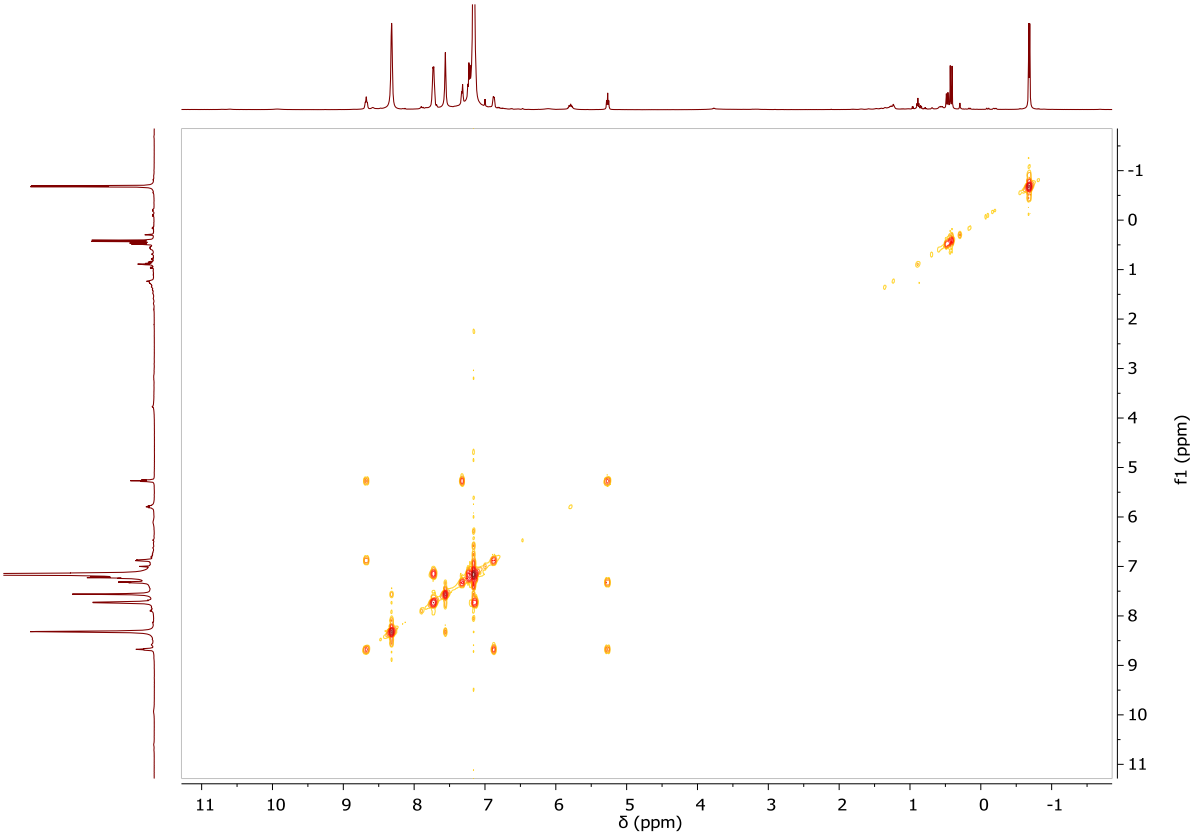

Figure S8 ^{1}H-^{1}H COSY NMR of the reaction solution to form complex **2** in C_6D_6 at 298 K.

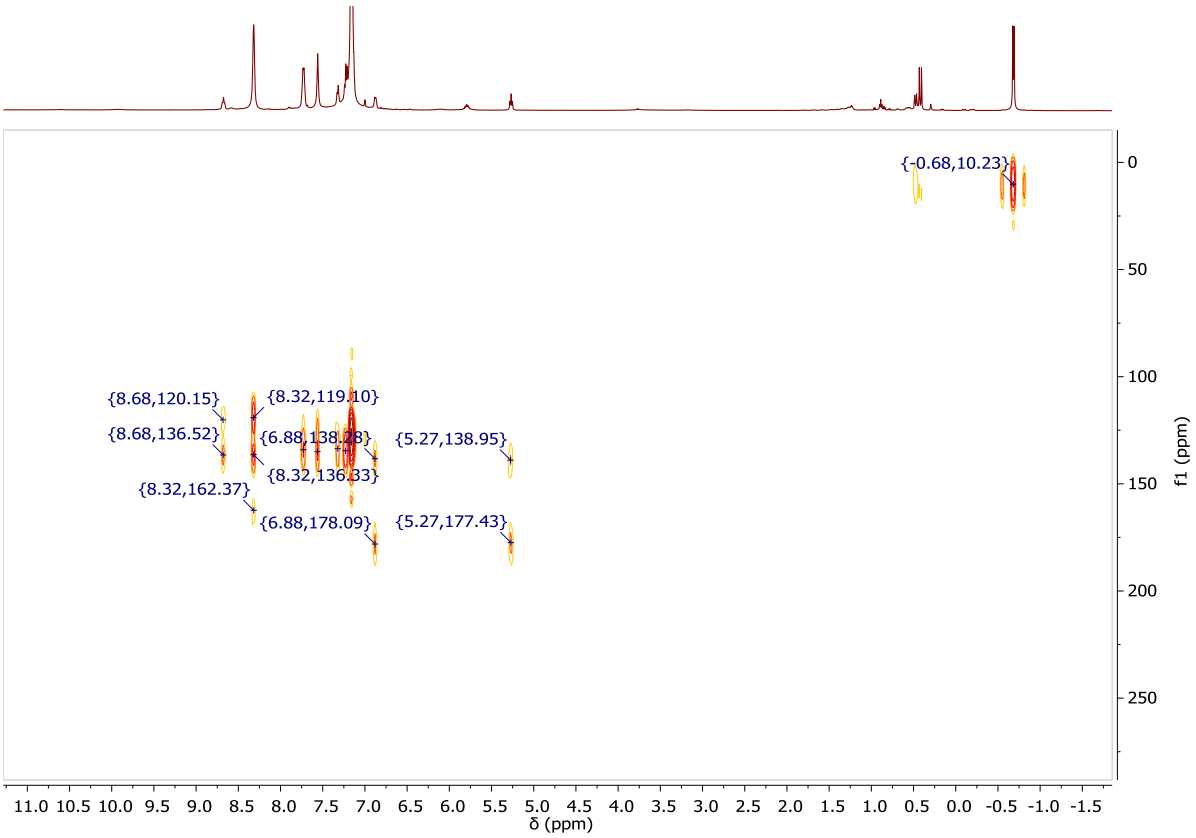

Figure S9 ^{1}H-^{13}C HMBC NMR of the reaction solution to form complex **2** in C_6D_6 at 298 K.

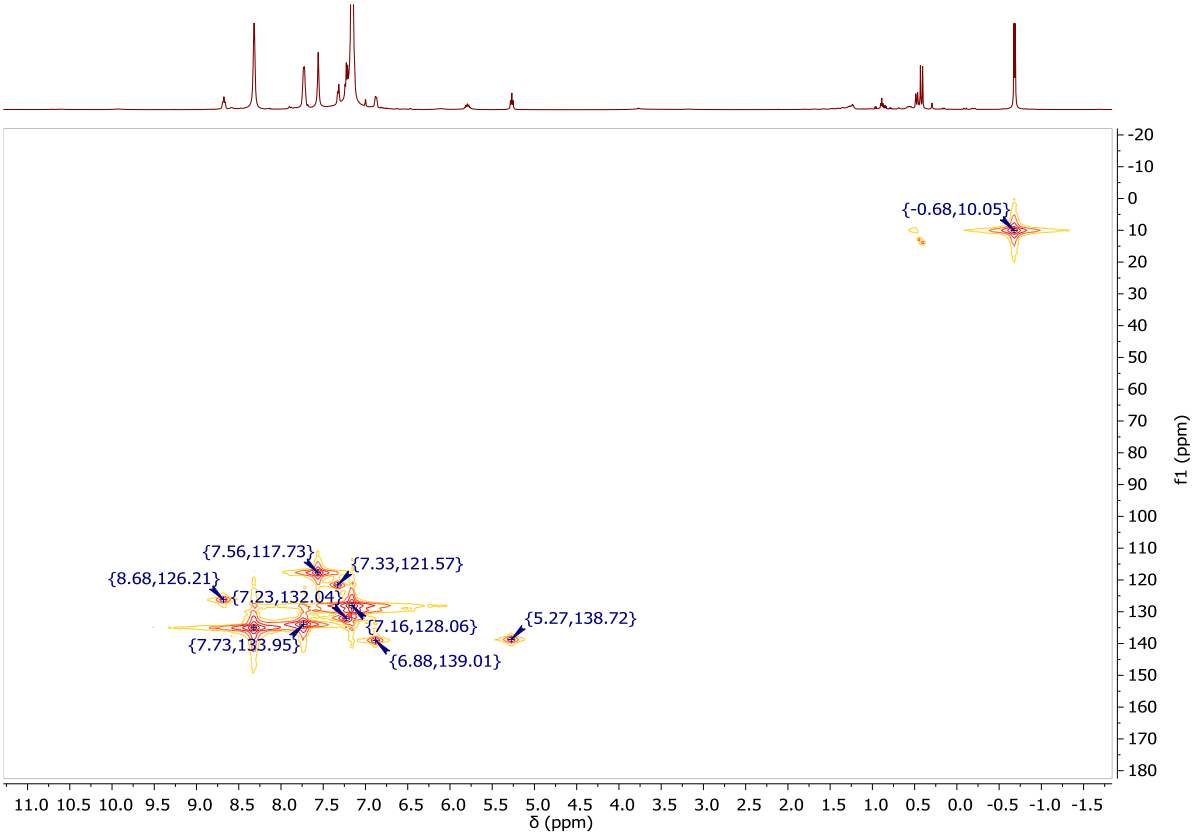

Figure S10 ^{1}H-^{13}C HMQC NMR of the reaction solution to form complex **2** in C_6D_6 at 298 K.

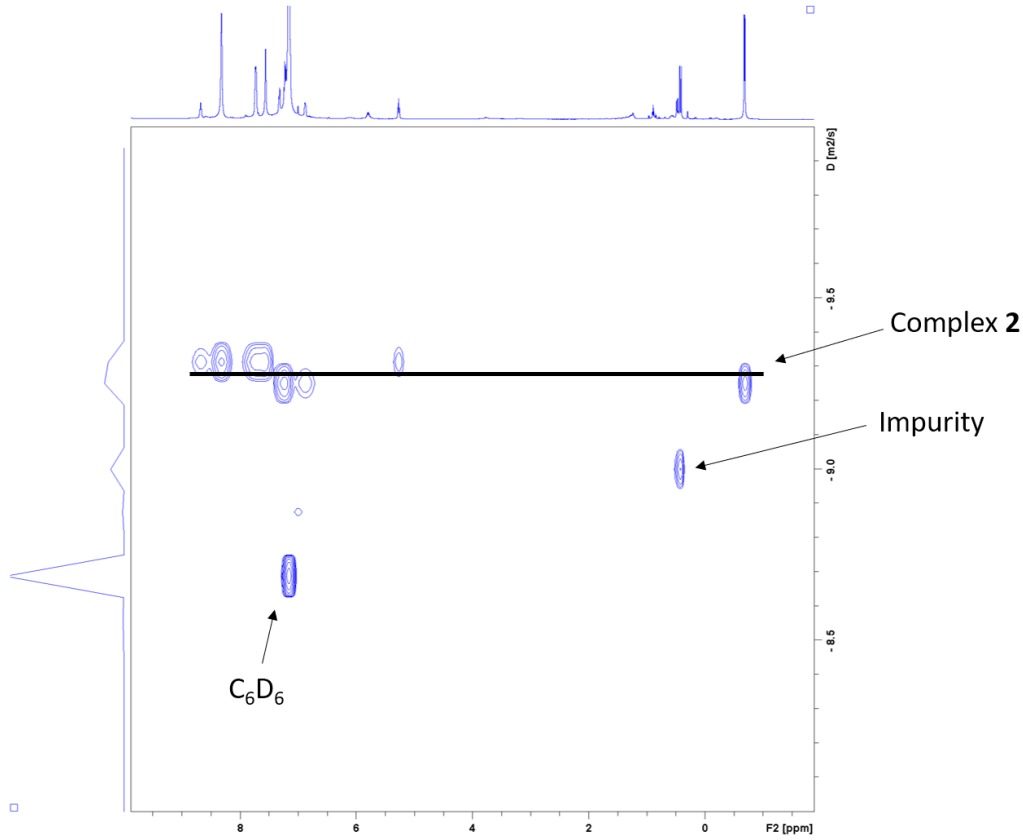

Figure S11 ^{1}H DOSY NMR of the reaction solution to form complex **2** in C_6D_6 at 298 K identifying which resonances in the ^{1}H NMR spectrum are part of complex **2**.

NMR Spectra of complex 2·MeCN

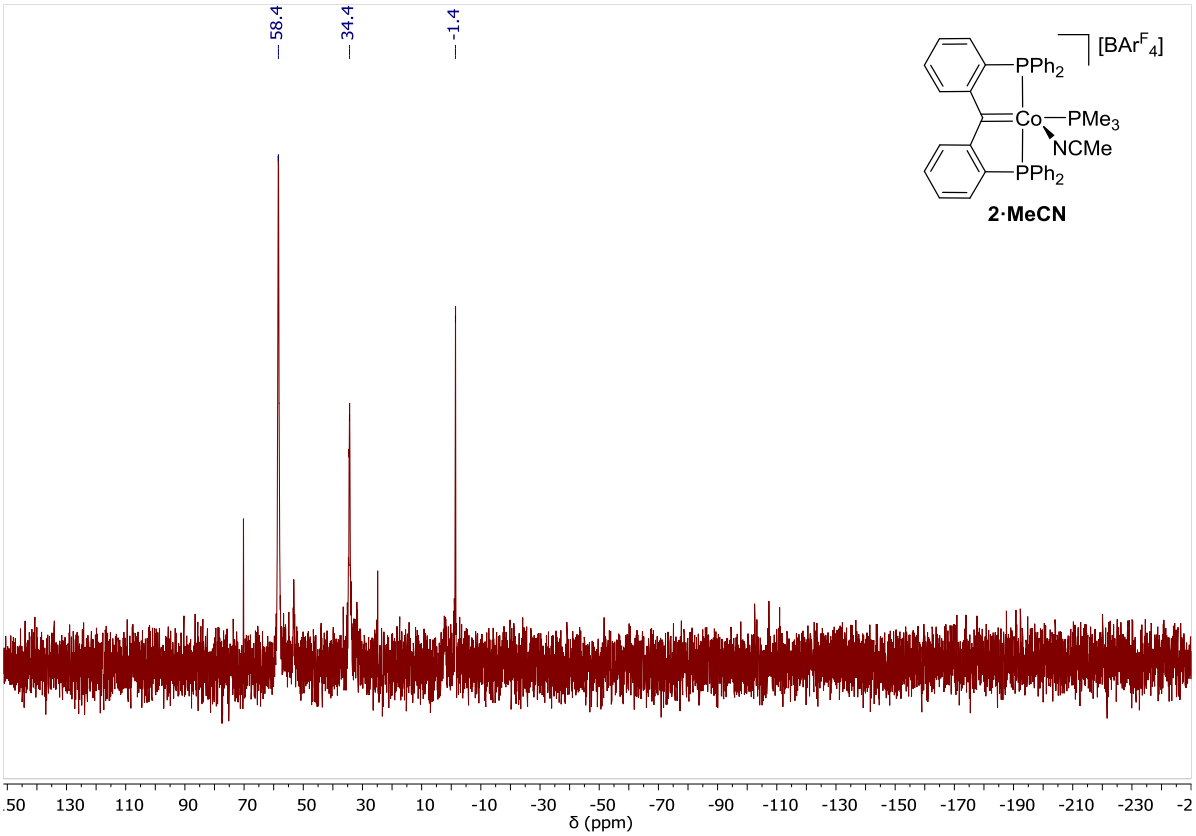

Figure S12 ^{31}P NMR of the reaction solution to form complex **2**·MeCN using $B(C_6F_5)_3$ in MeCN at 298 K, showing identified peaks for the complex and Me_3P-$B(C_6F_5)_3$.

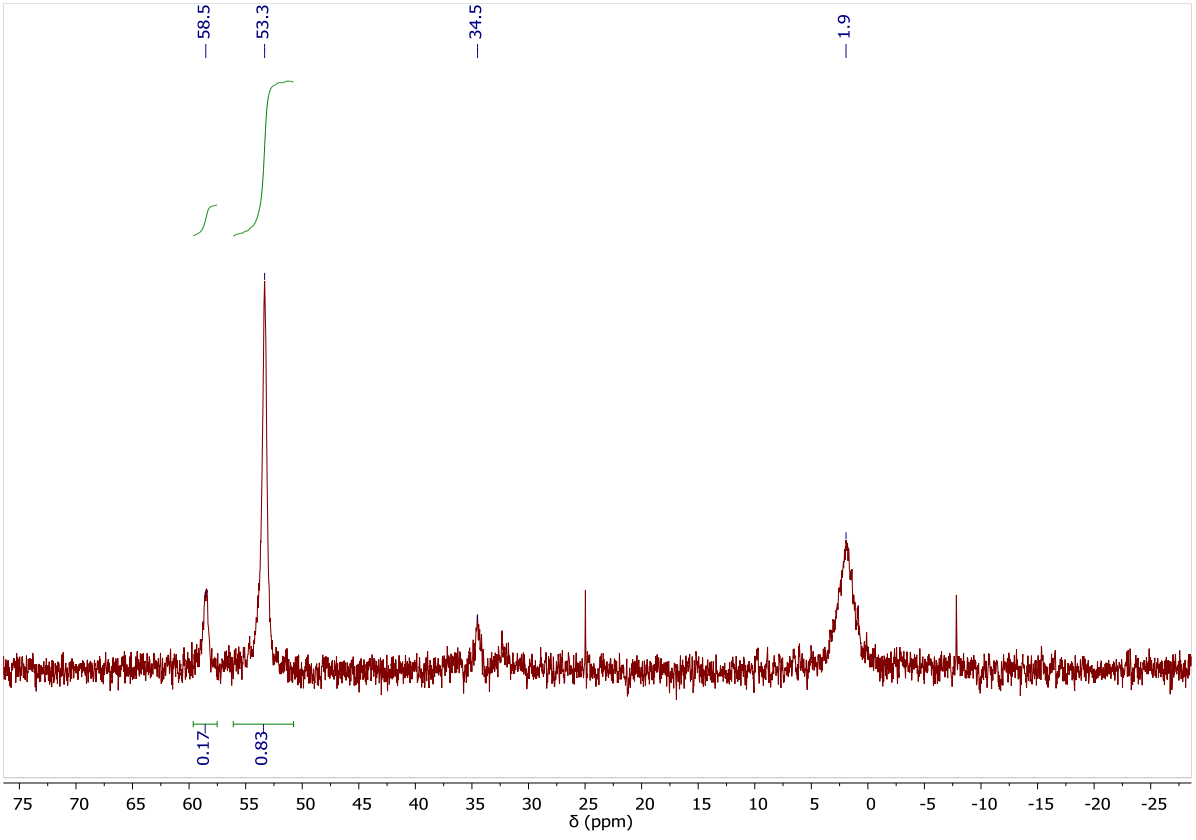

Figure S13 ^{31}P NMR of the reaction solution to form complex **2**·MeCN without $B(C_6F_5)_3$ in MeCN at 298 K, highlighting the 17% yield of formed **2**·MeCN relative to **1**.

NMR Spectra of complex 3

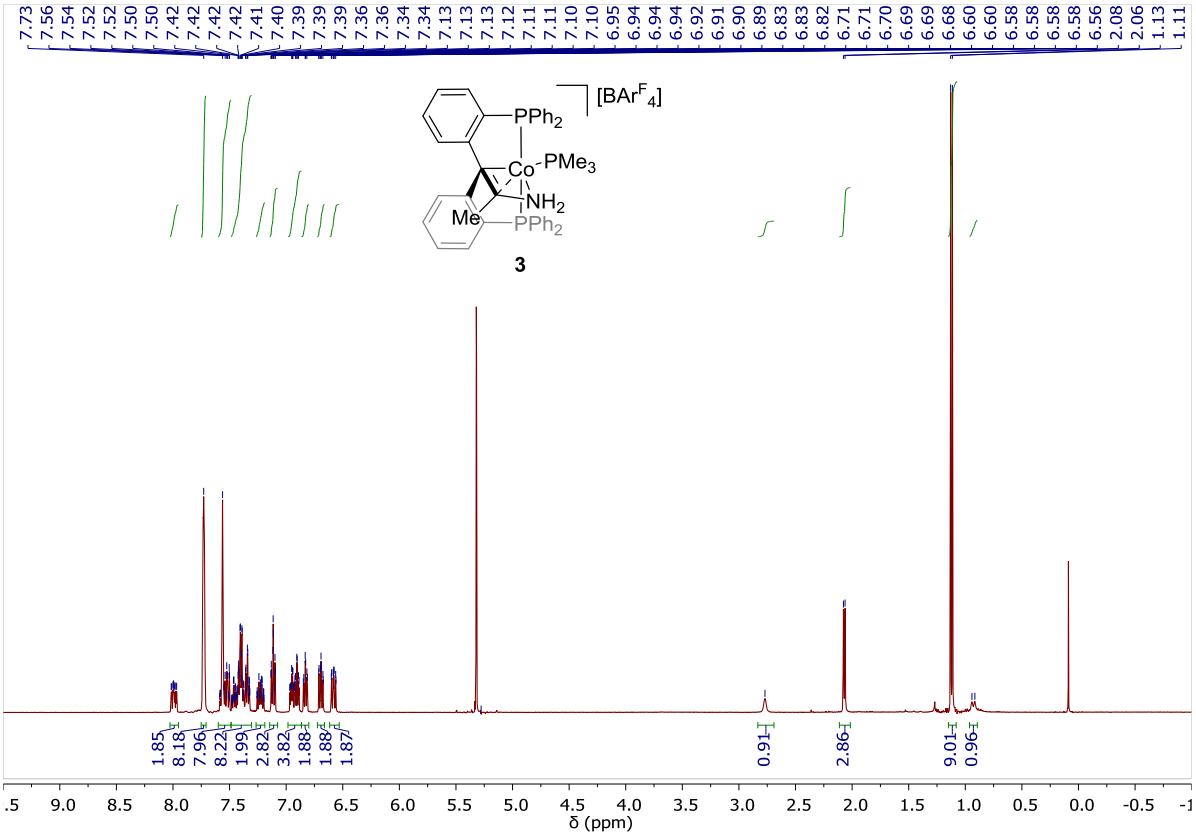

Figure S14 ^{1}H NMR of complex **3** in CD_2Cl_2 at 298 K.

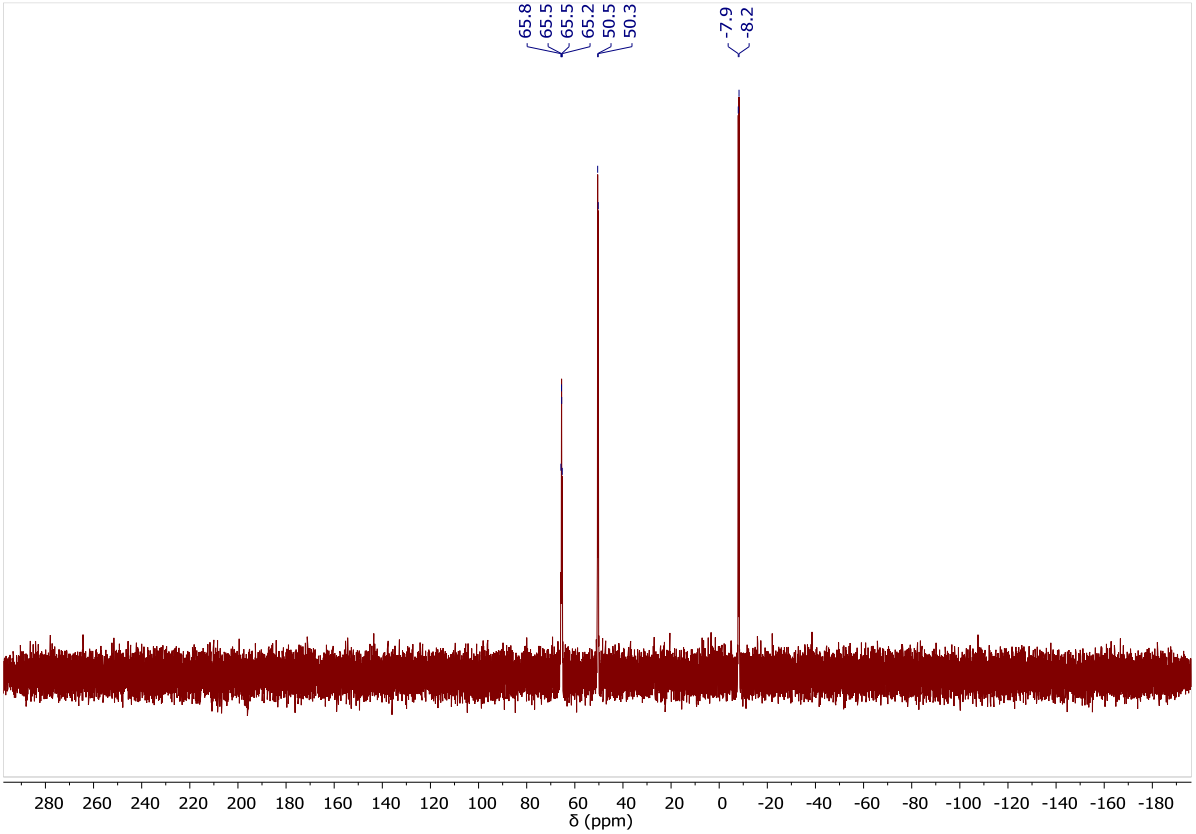

Figure S15 ^{31}P NMR of complex **3** in CD_2Cl_2 at 298 K.

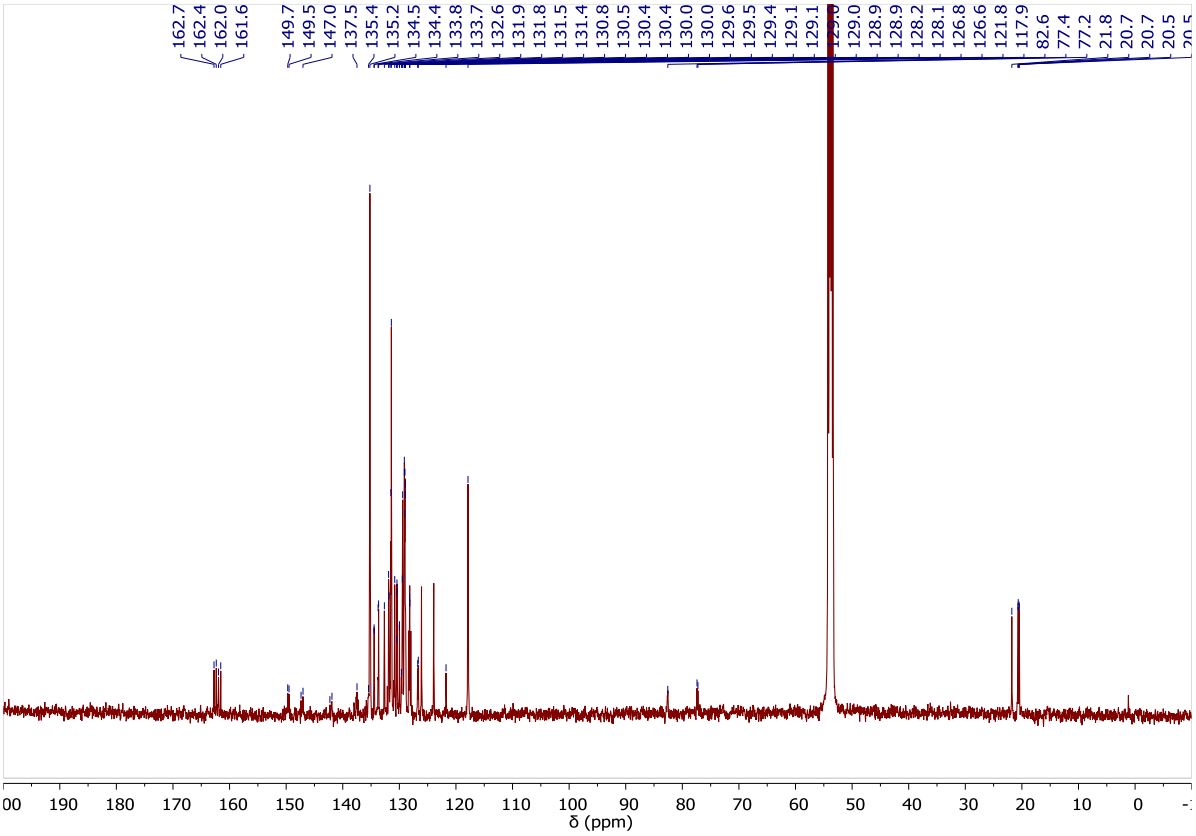

Figure S16 ^{13}C NMR of complex **3** in CD_2Cl_2 at 298 K.

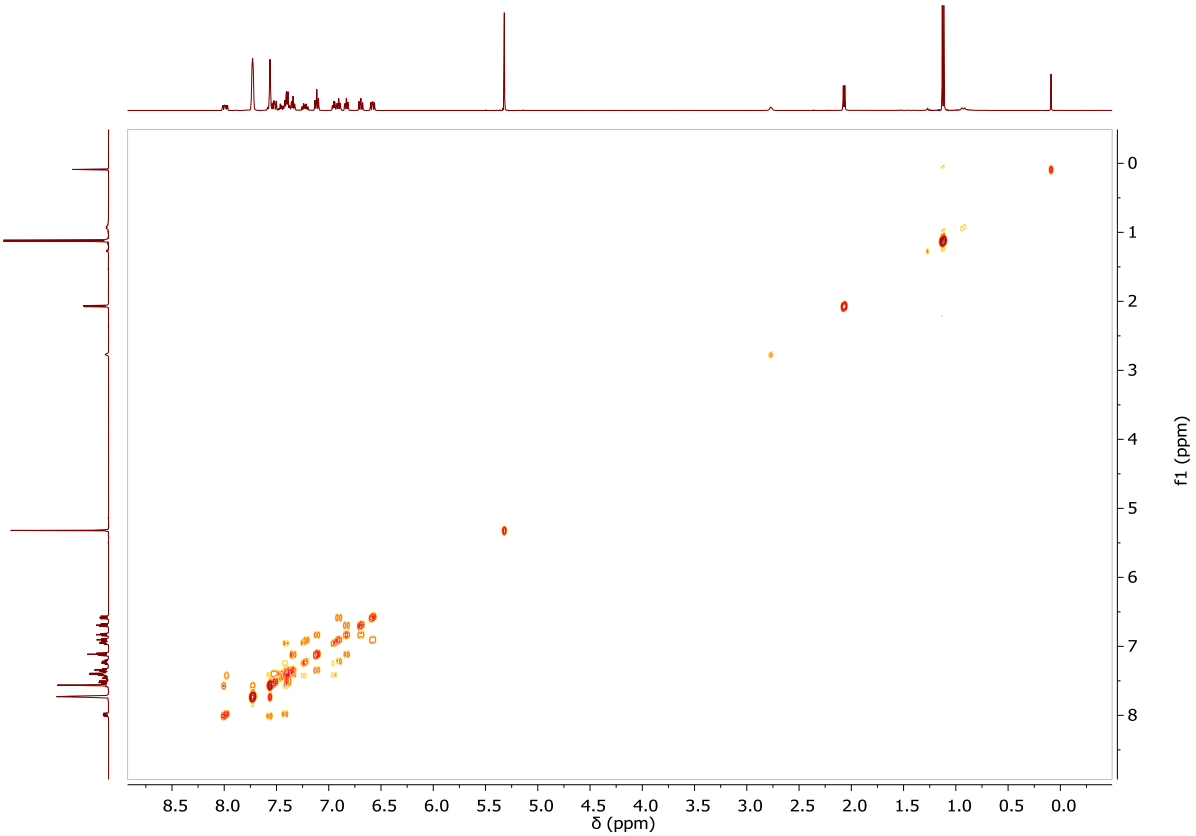

Figure S17 ^{1}H-^{1}H COSY NMR of complex **3** in CD_2Cl_2 at 298 K.

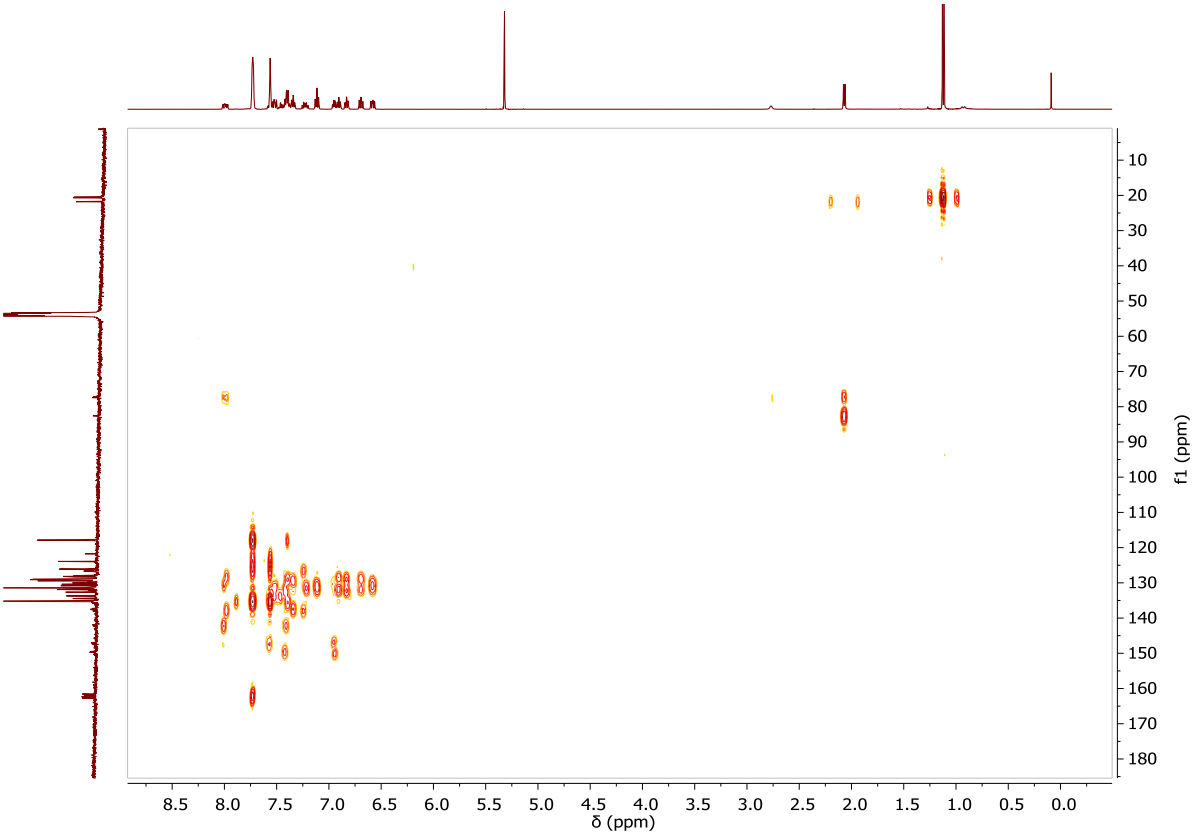

Figure S18 ^{1}H-^{13}C HMBC NMR of complex **3** in CD_2Cl_2 at 298 K.

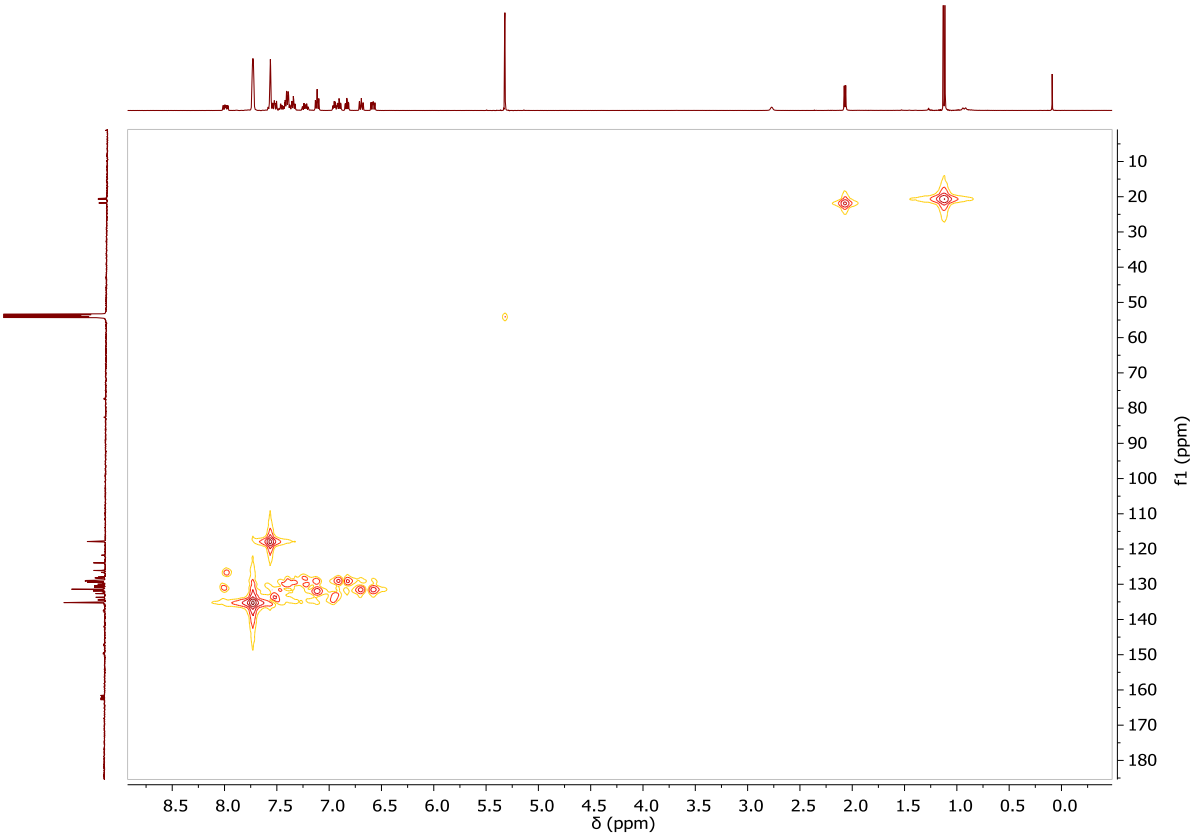

Figure S19 ^{1}H-^{13}C HMQC NMR of complex **3** in CD_2Cl_2 at 298 K.

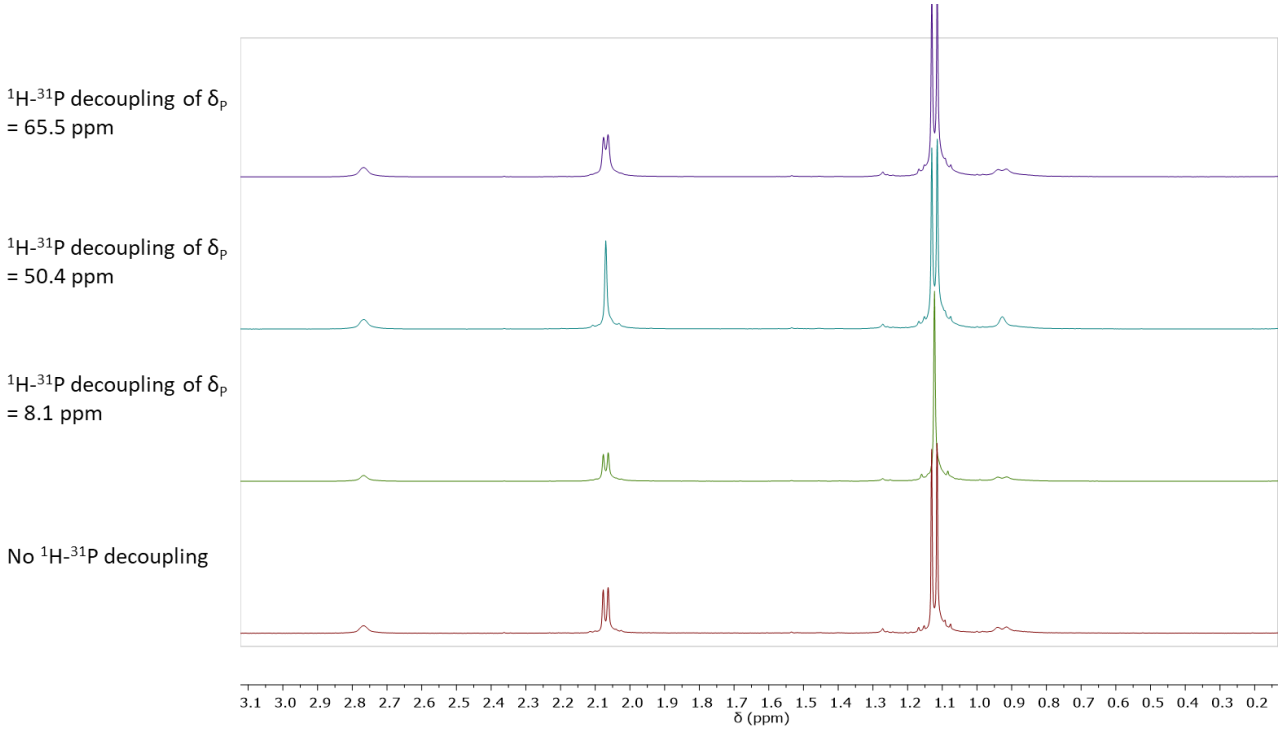

Figure S20 Comparison of ^{1}H and ^{1}H{^{31}P} NMR spectra of complex **3** in CD_2Cl_2 at 298 K highlighting the ^{1}H-^{31}P coupling of the PMe_3, N-H and Me resonances at δ_H 1.12, 0.93 and 2.07 ppm respectively.

NMR Spectra of complex 8a

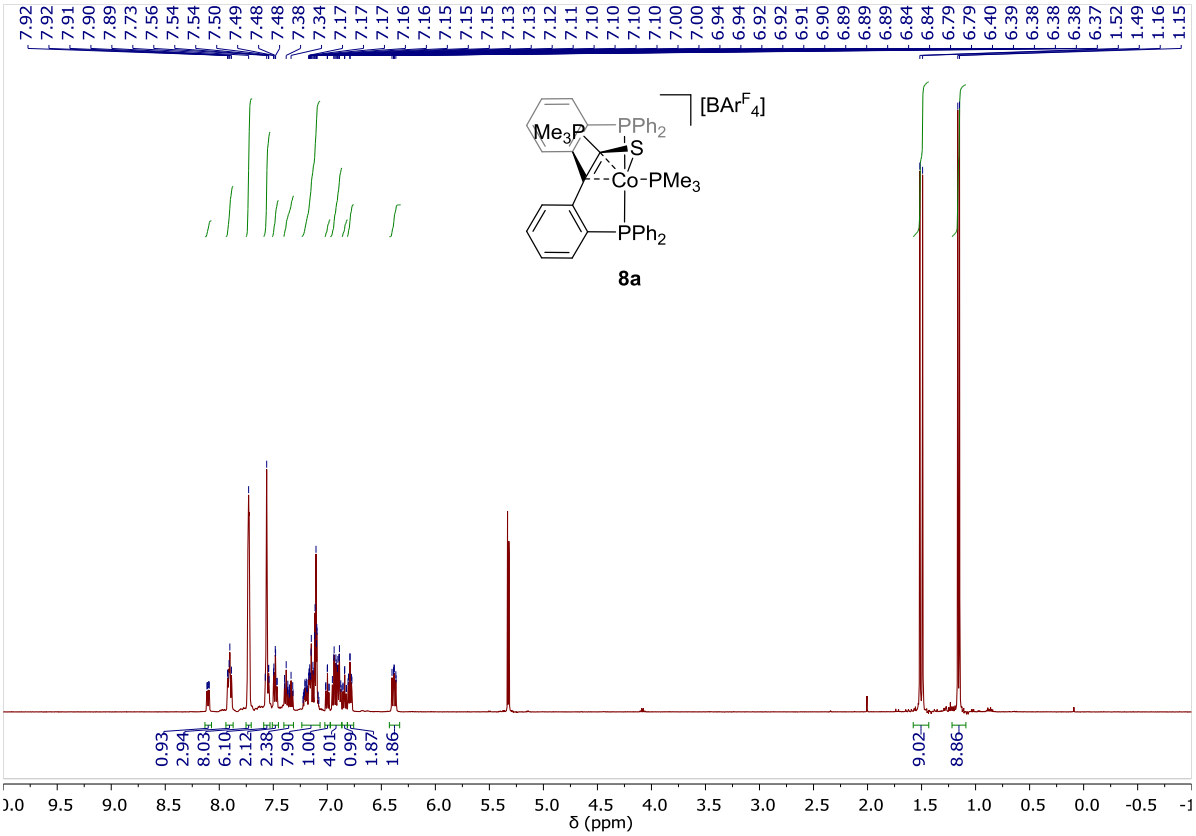

Figure S21 ^{1}H NMR of complex **8a** in CD_2Cl_2 at 298 K.

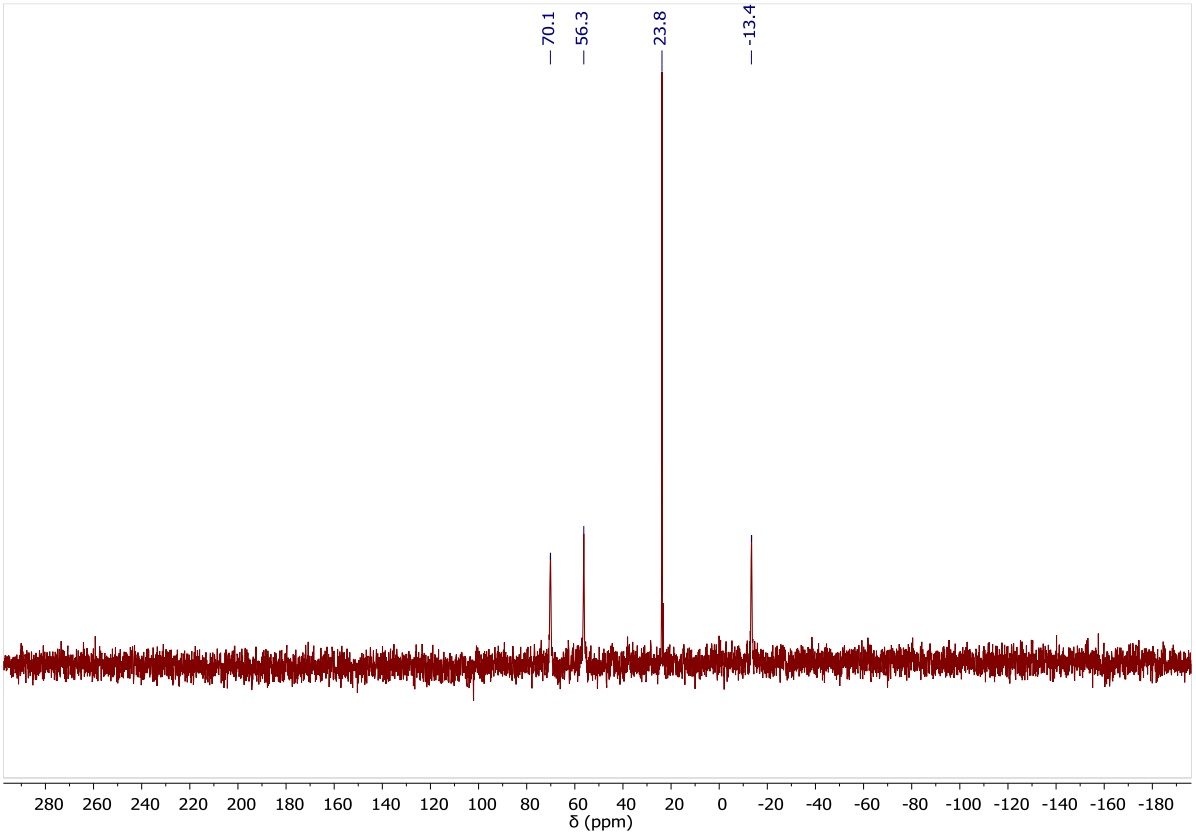

Figure S22 ^{31}P NMR of complex **8a** in CD_2Cl_2 at 298 K.

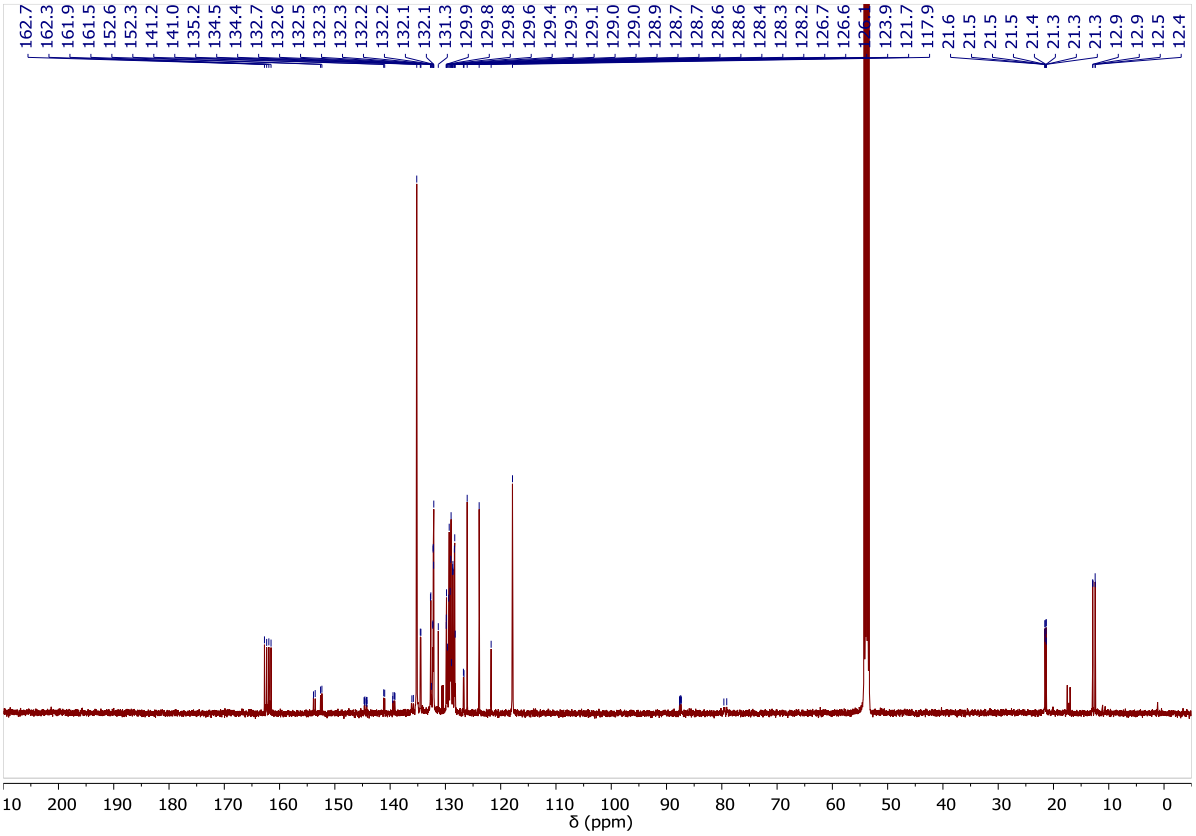

Figure S23 ^{13}C NMR of complex **8a** in CD_2Cl_2 at 298 K.

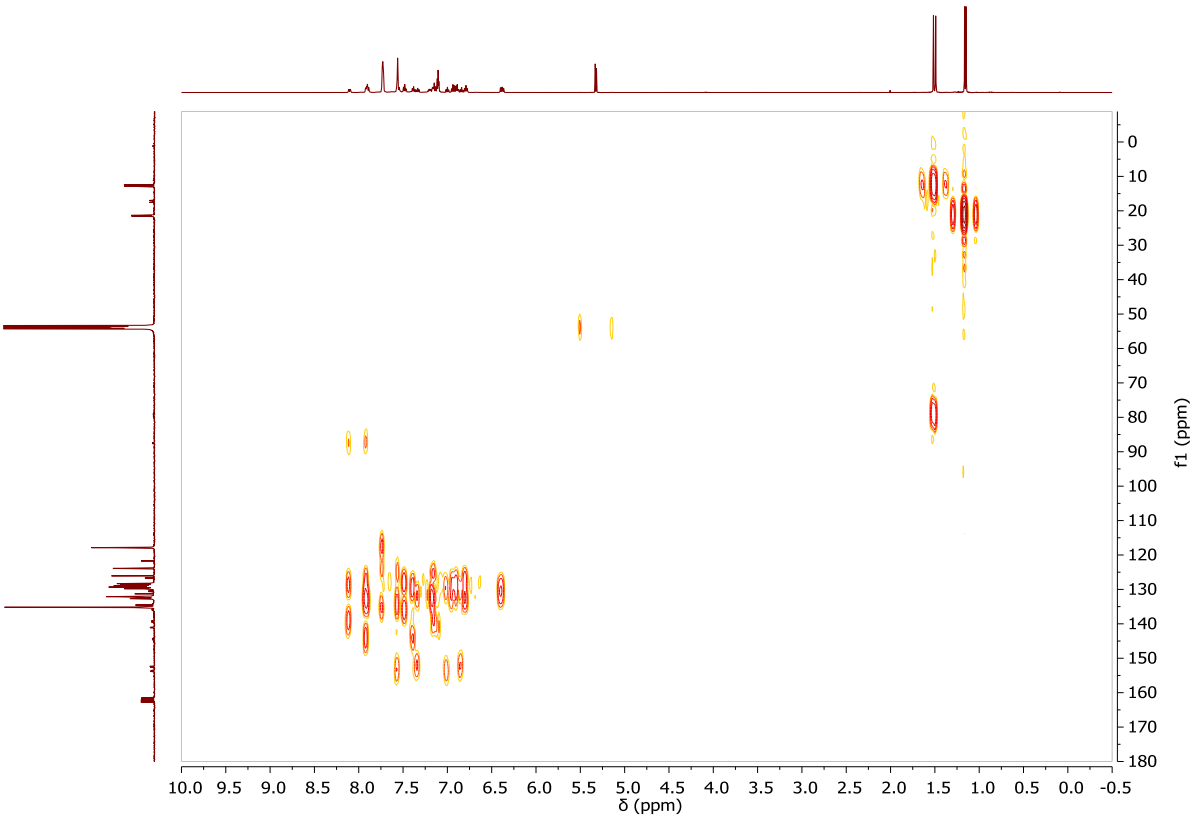

Figure S24 ^{1}H-^{13}C HMBC NMR of complex **8a** in CD_2Cl_2 at 298 K.

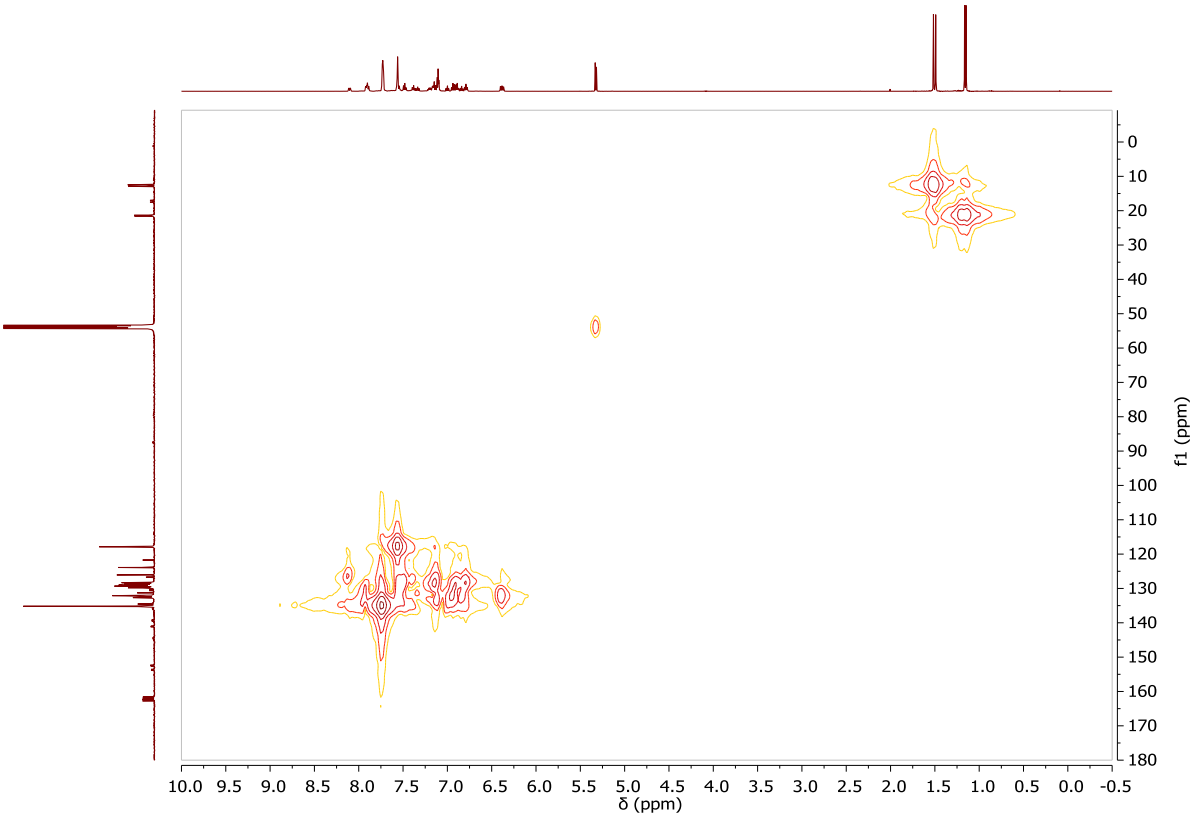

Figure S25 ^{1}H-^{13}C HMQC NMR of complex **8a** in CD_2Cl_2 at 298 K.

NMR Spectra of complex 8b

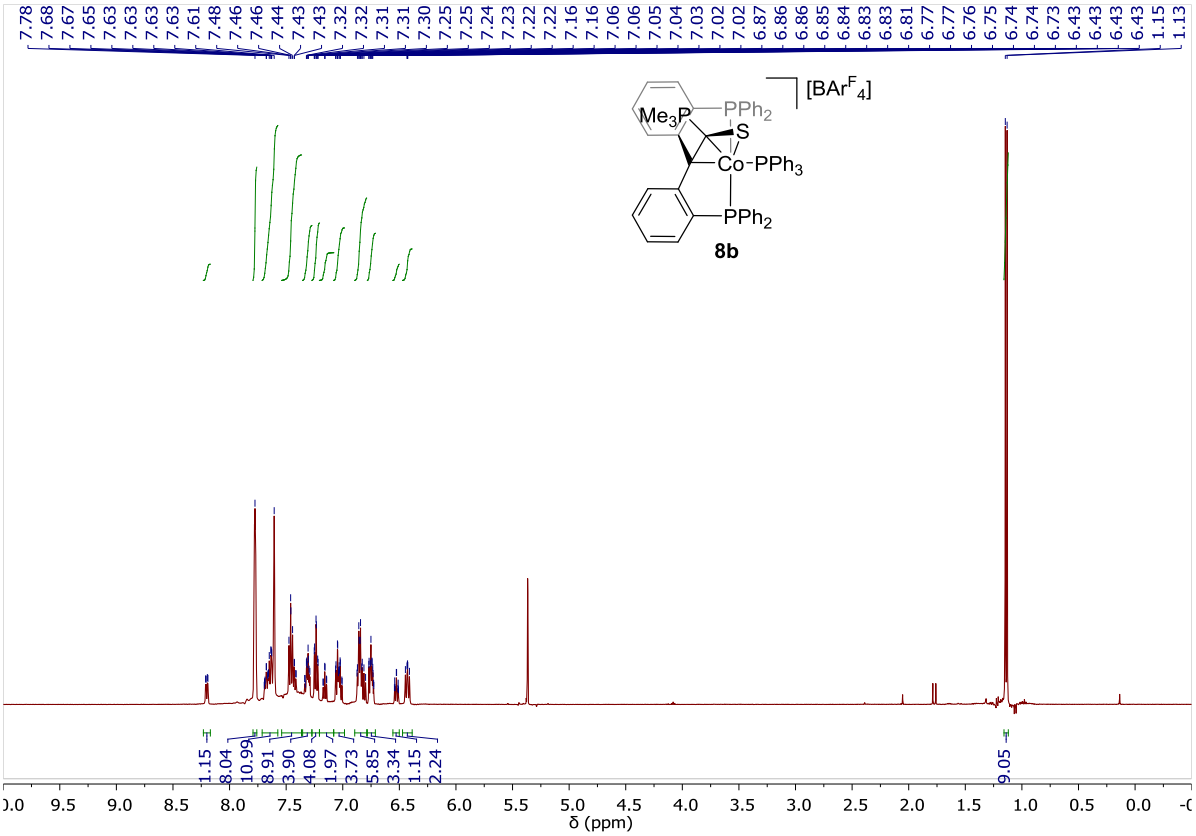

Figure S26 ^{1}H NMR of complex **8b** in CD_2Cl_2 at 298 K.

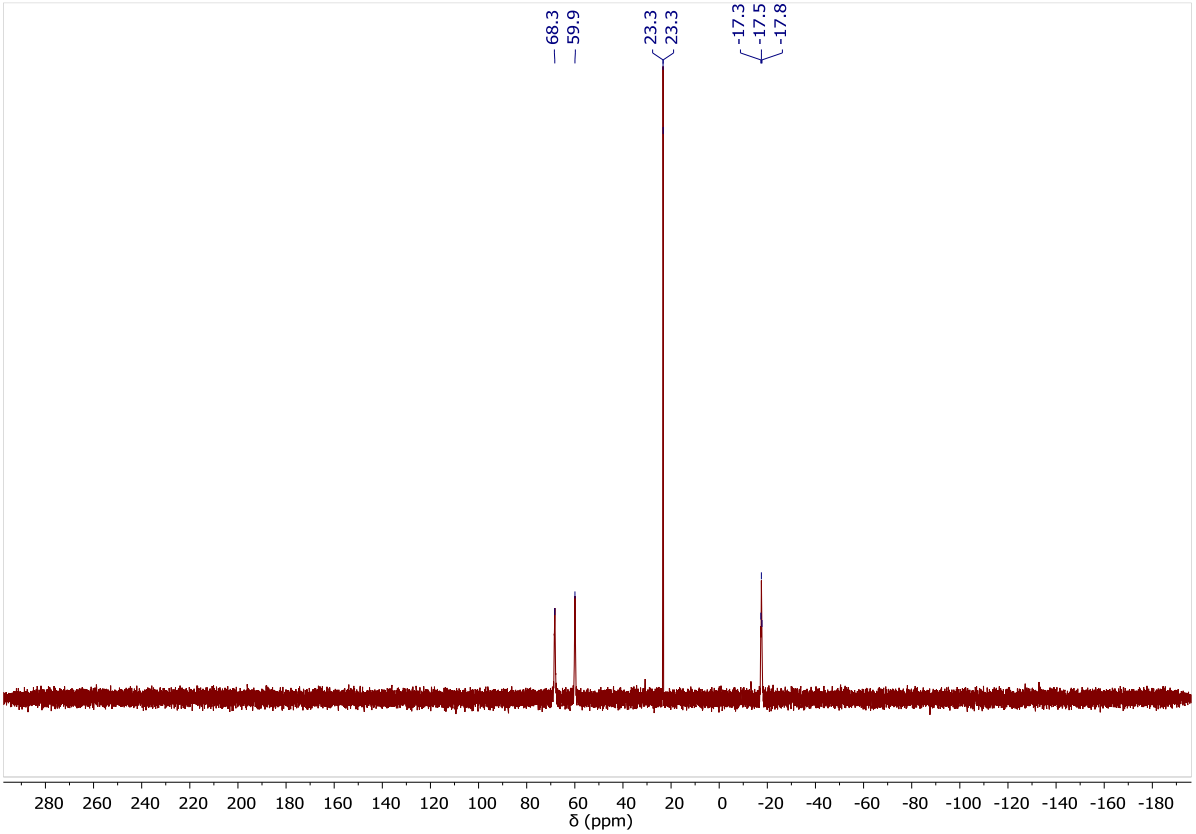

Figure S27 ^{31}P NMR of complex **8b** in CD_2Cl_2 at 298 K.

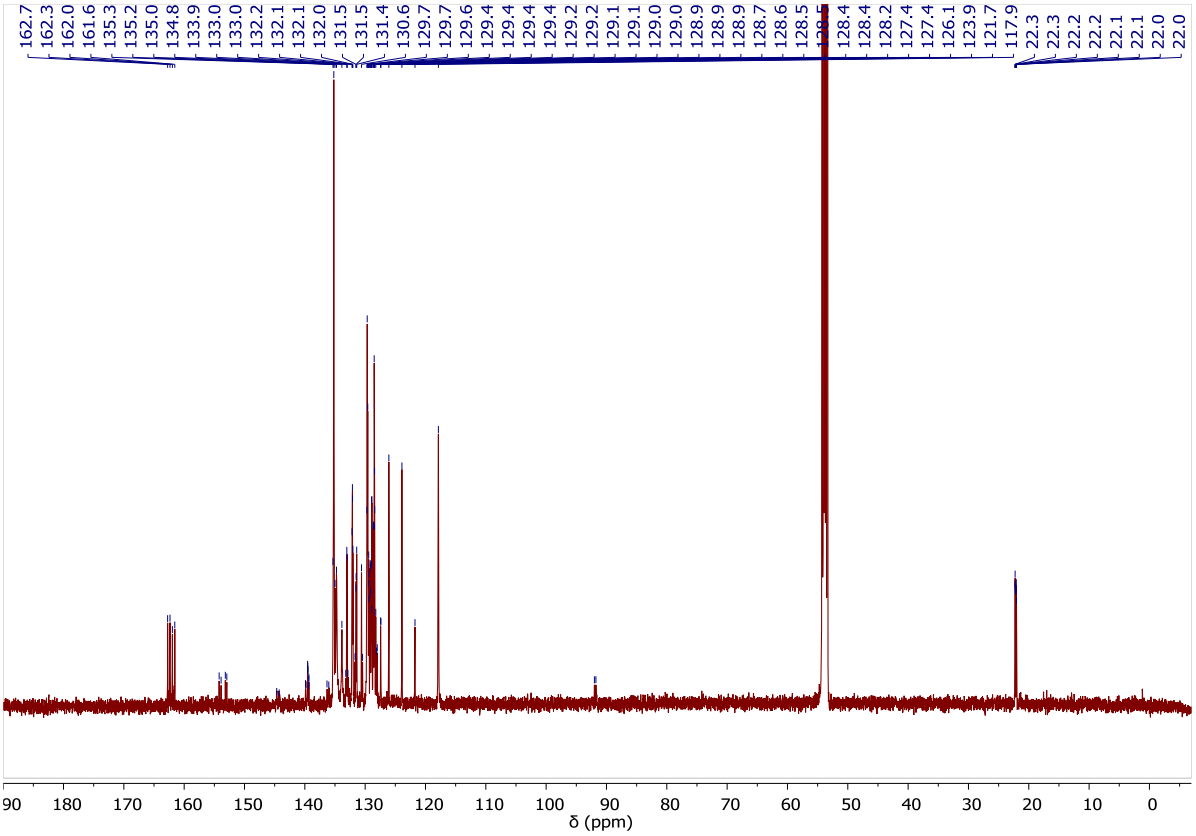

Figure S28 ^{13}C NMR of complex **8b** in CD_2Cl_2 at 298 K.

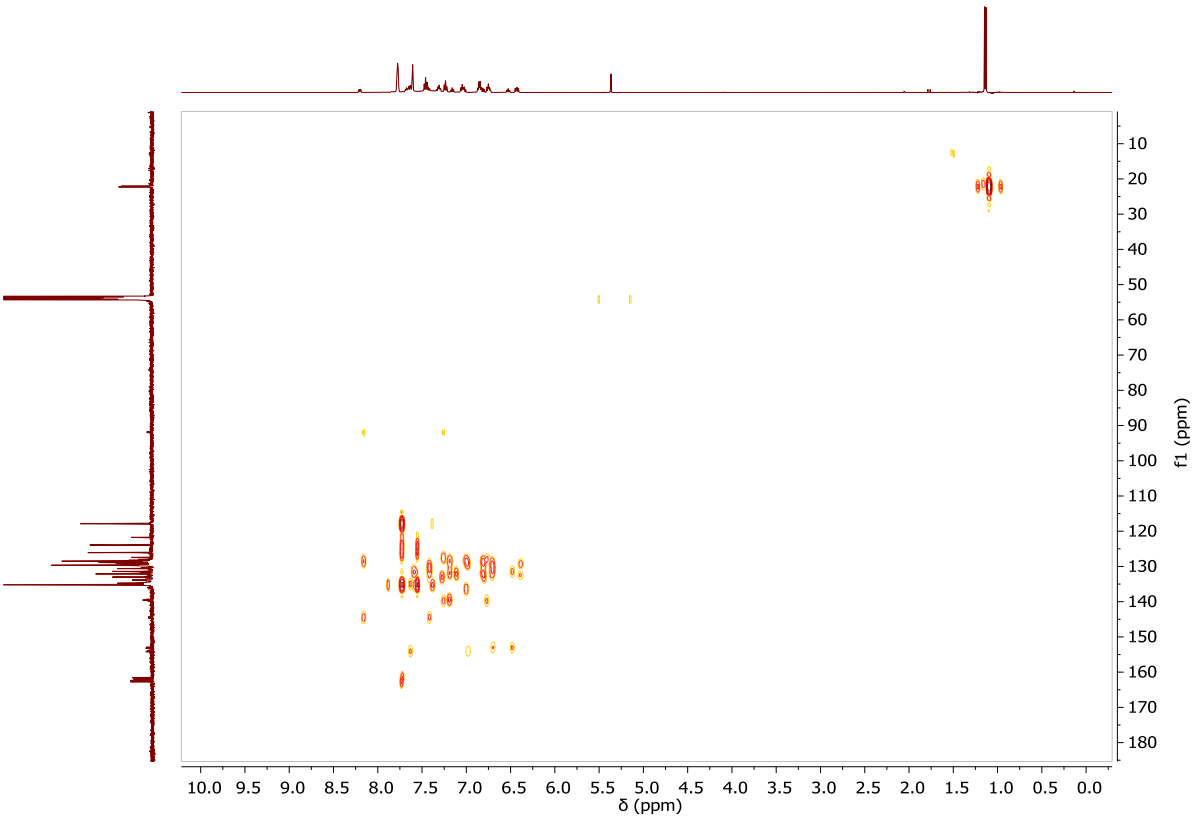

Figure S29 ^{1}H-^{13}C HMBC NMR of complex **8b** in CD_2Cl_2 at 298 K.

NMR Spectra of complex 9

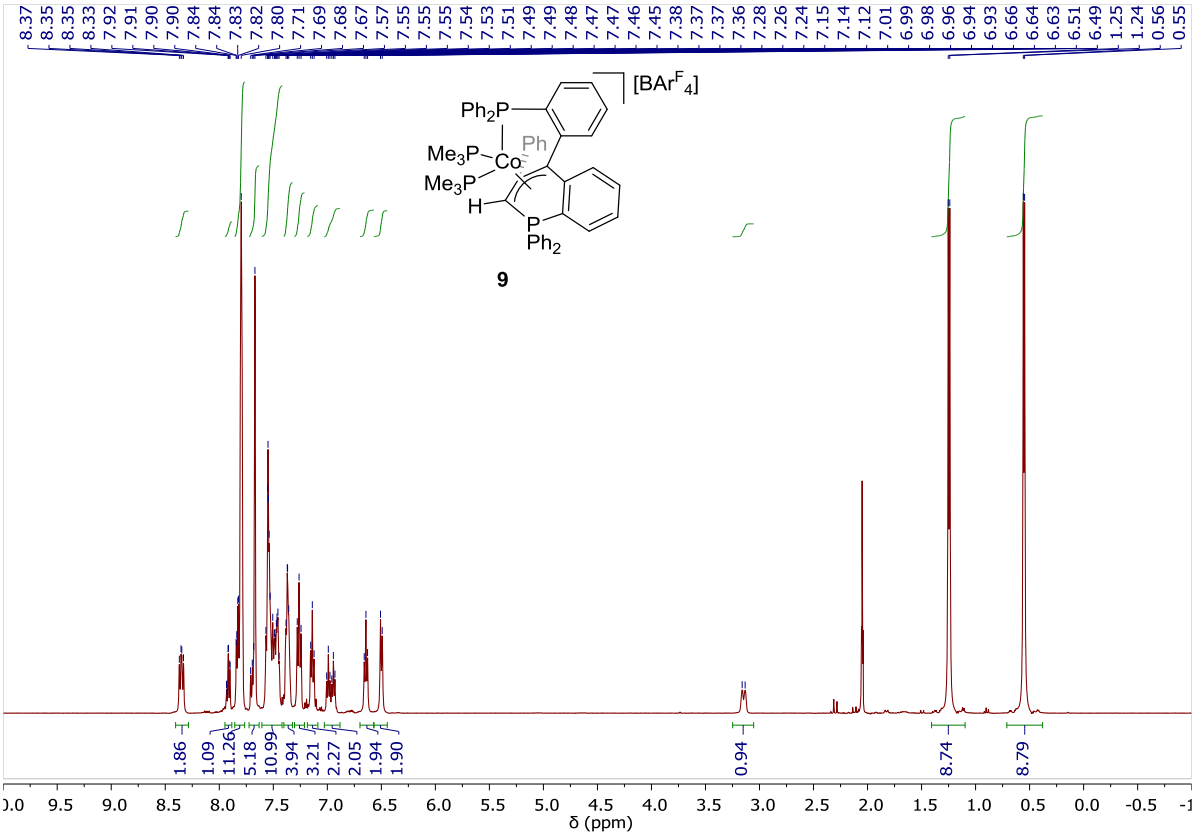

Figure S30 ^{1}H NMR of complex **9** in Acetone-d_6 at 298 K.

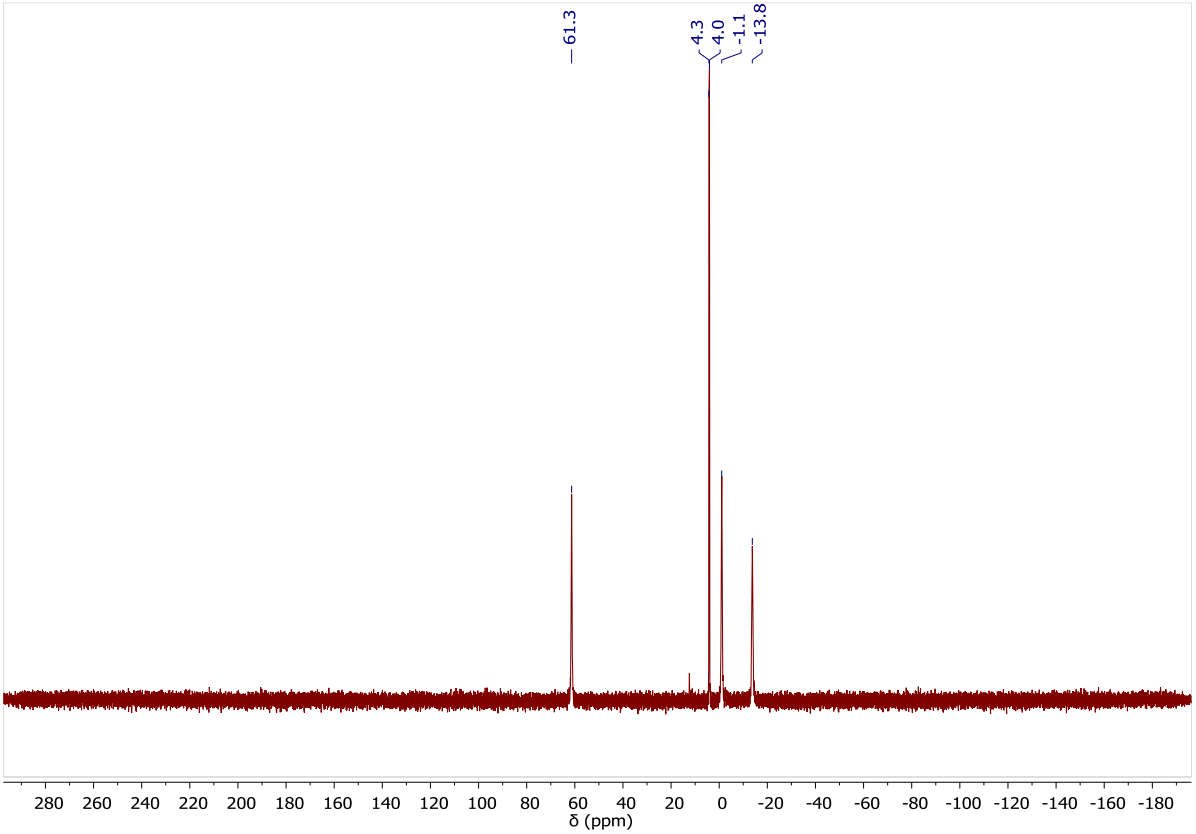

Figure S31 ^{31}P NMR of complex **9** in Acetone-d_6 at 298 K.

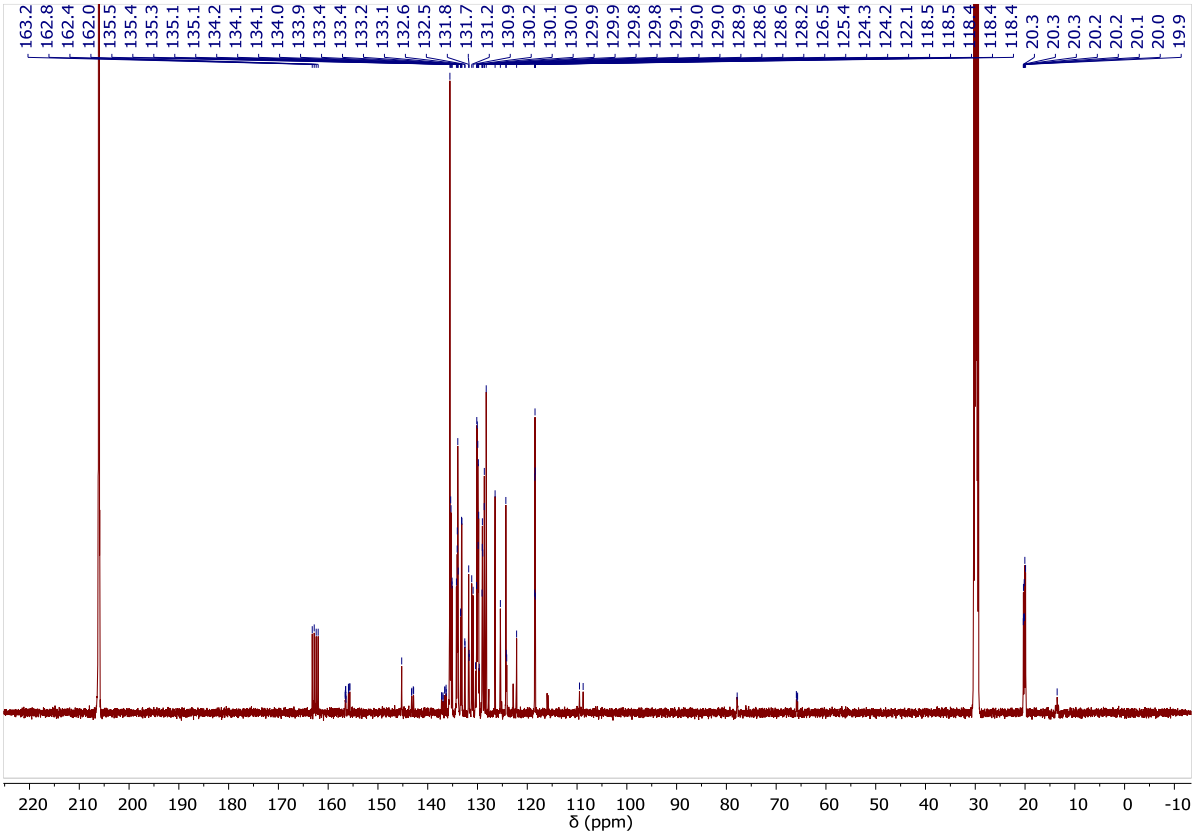

Figure S32 ^{13}C NMR of complex **9** in Acetone-d_6 at 298 K.

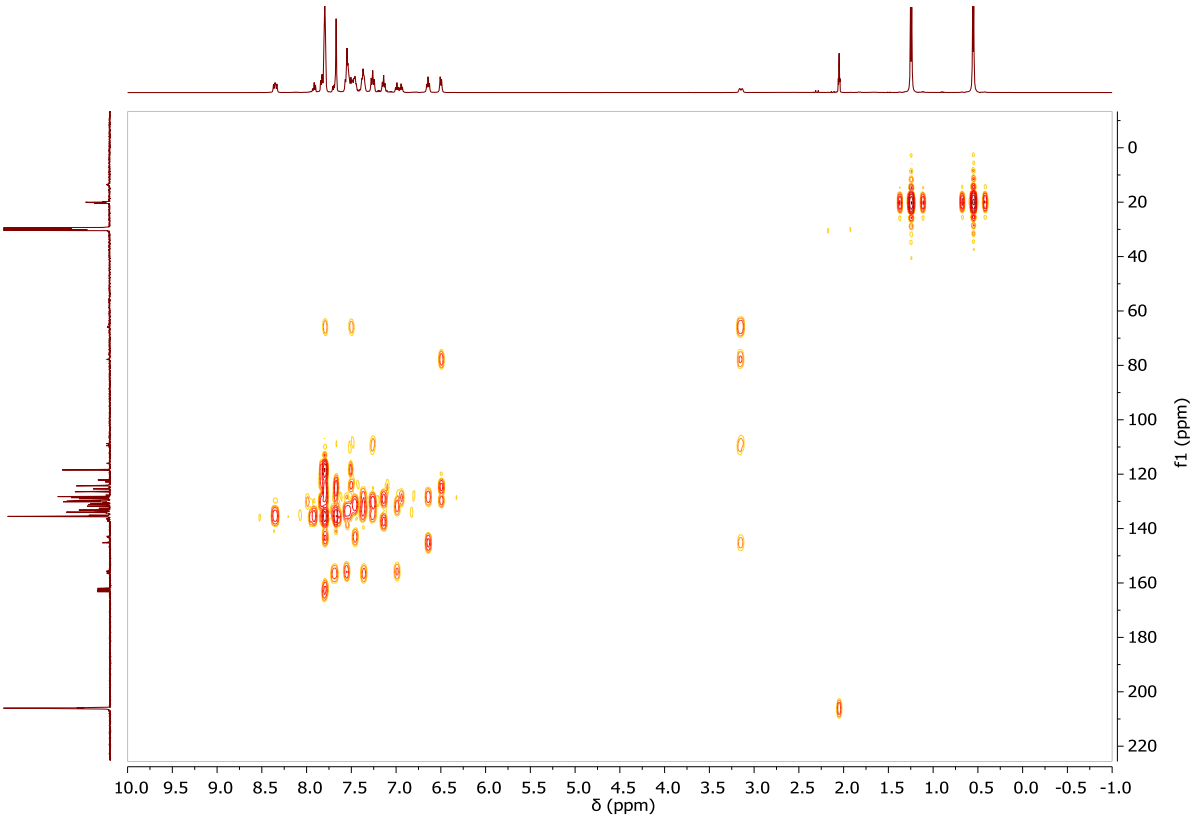

Figure S33 ^{1}H-^{13}C HMBC NMR of complex **9** in Acetone-d_6 at 298 K.

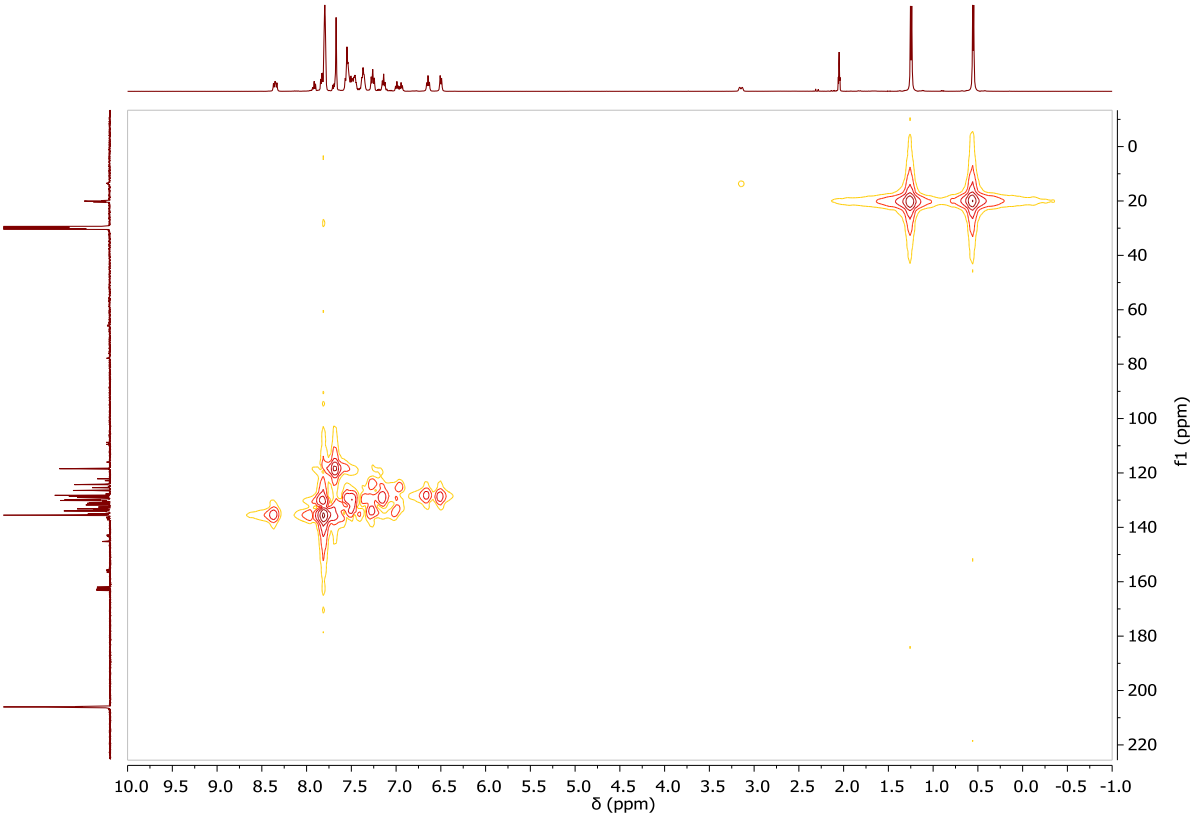

Figure S34 ^{1}H-^{13}C HMQC NMR of complex **9** in Acetone-d_6 at 298 K.

NMR Spectra of complex 10

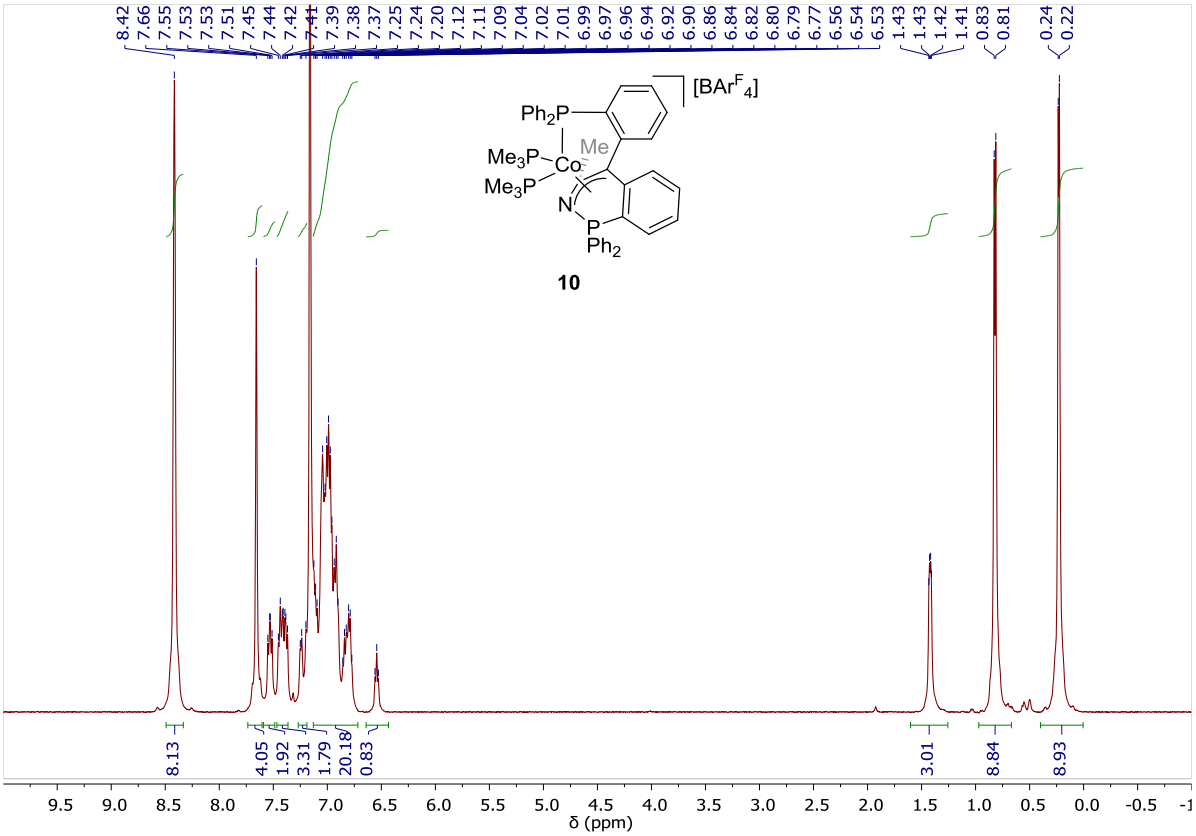

Figure S35 ^{1}H NMR of complex **10** in C_6D_6 at 298 K.

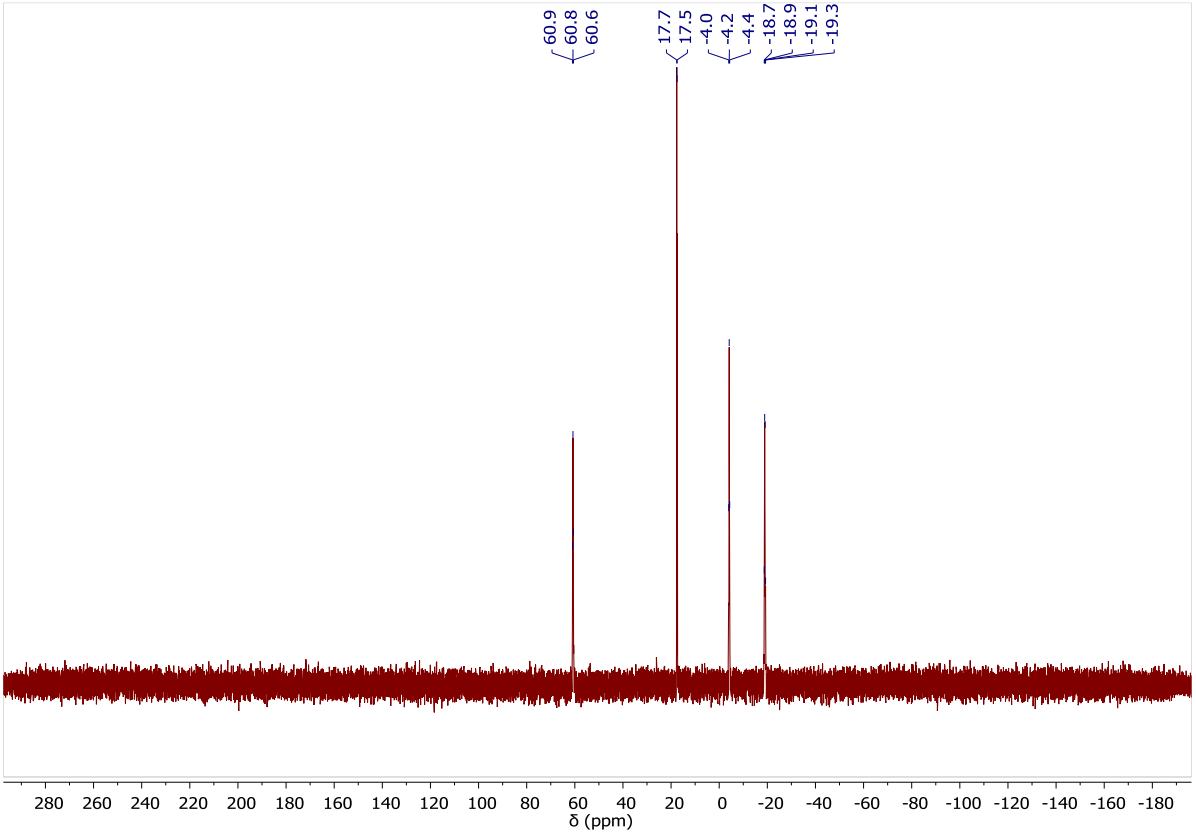

Figure S36 ^{31}P NMR of complex **10** in C_6D_6 at 298 K.

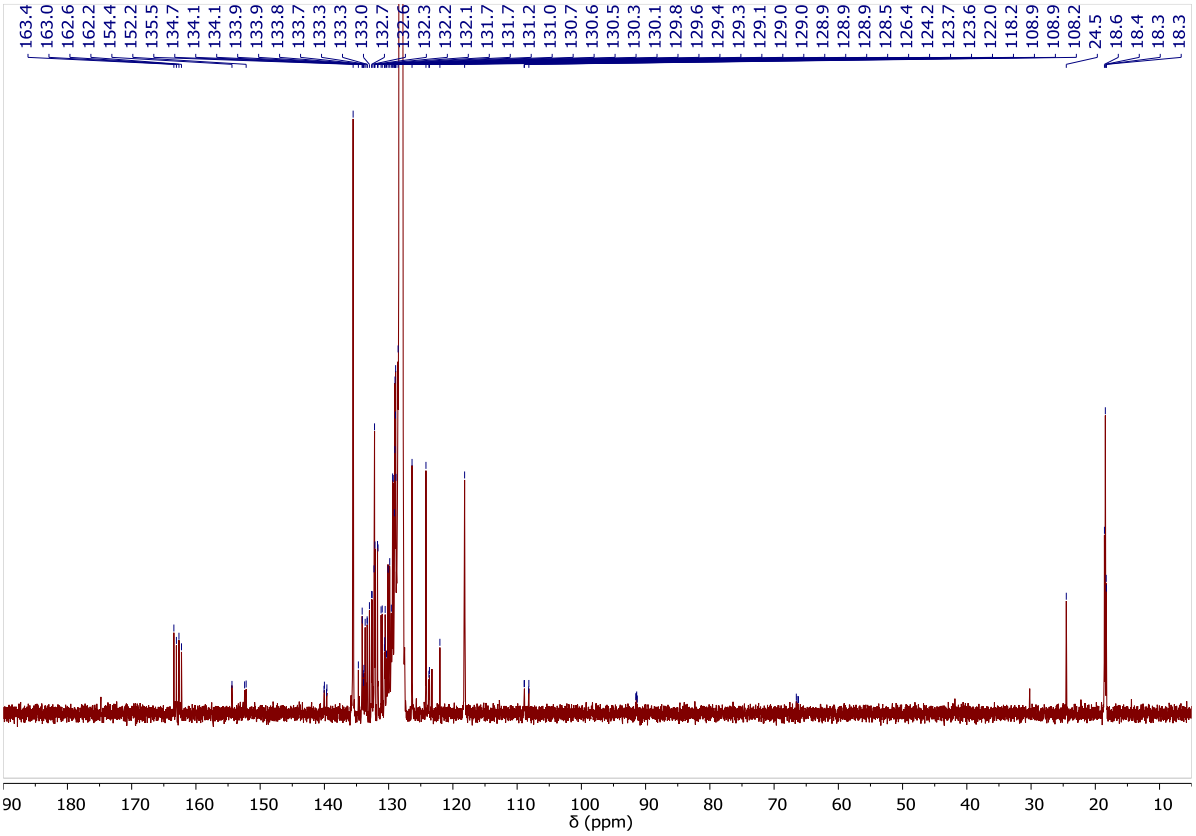

Figure S37 ^{13}C NMR of complex **10** in C_6D_6 at 298 K.

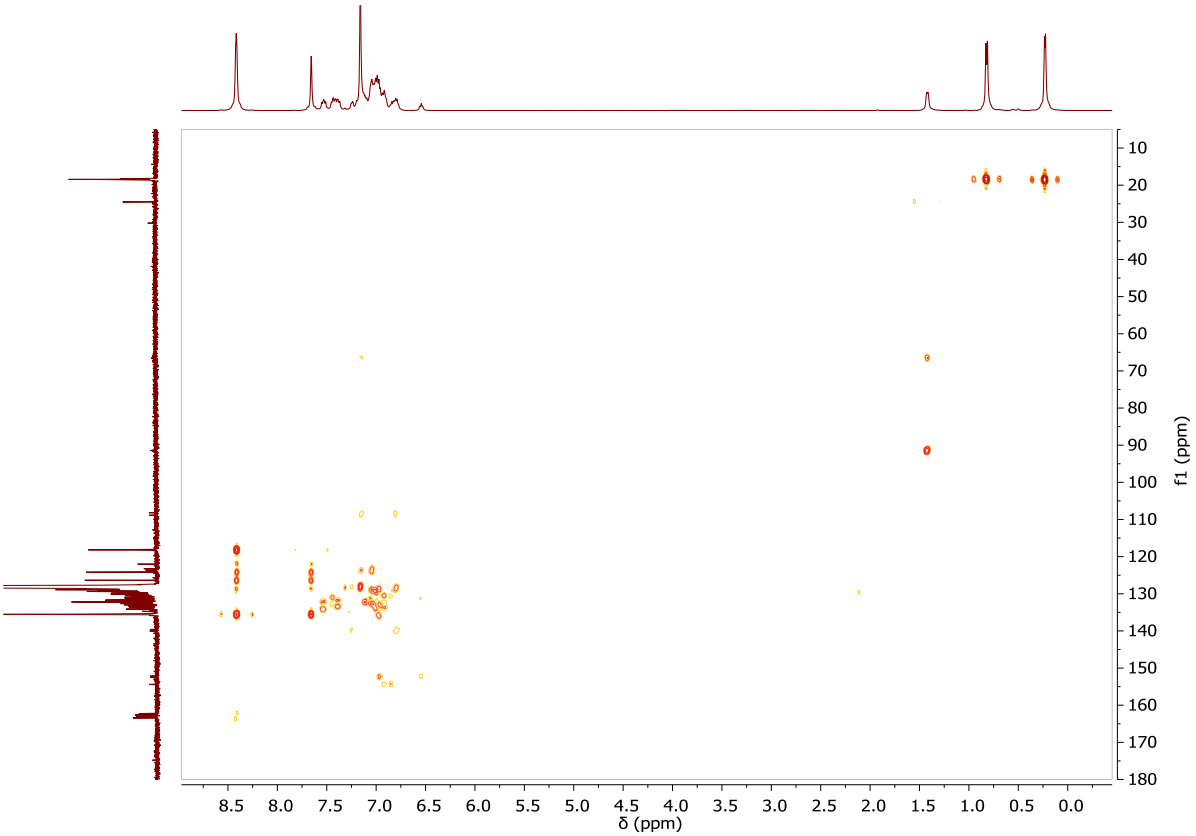

Figure S38 ^{1}H-^{13}C HMBC NMR of complex **10** in C_6D_6 at 298 K.

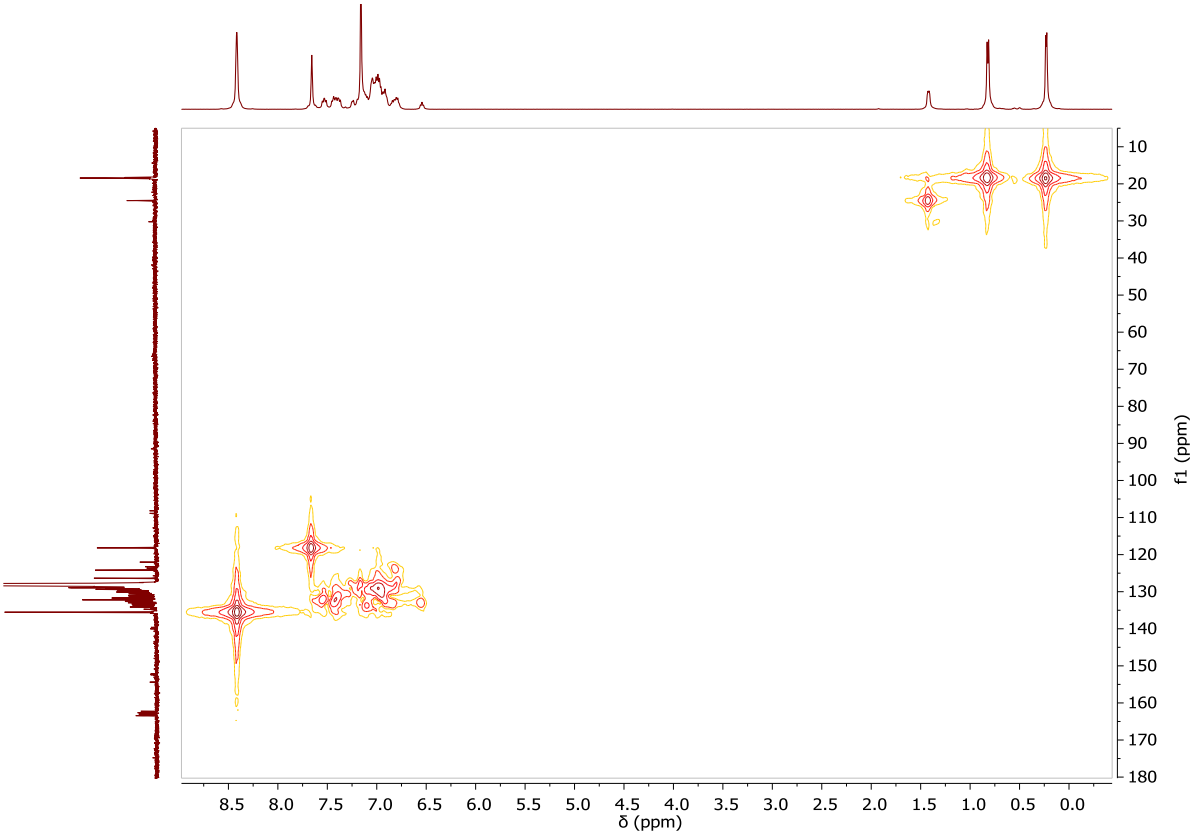

Figure S39 ^{1}H-^{13}C HMQC NMR of complex **10** in C_6D_6 at 298 K.

NMR Spectra of complex V

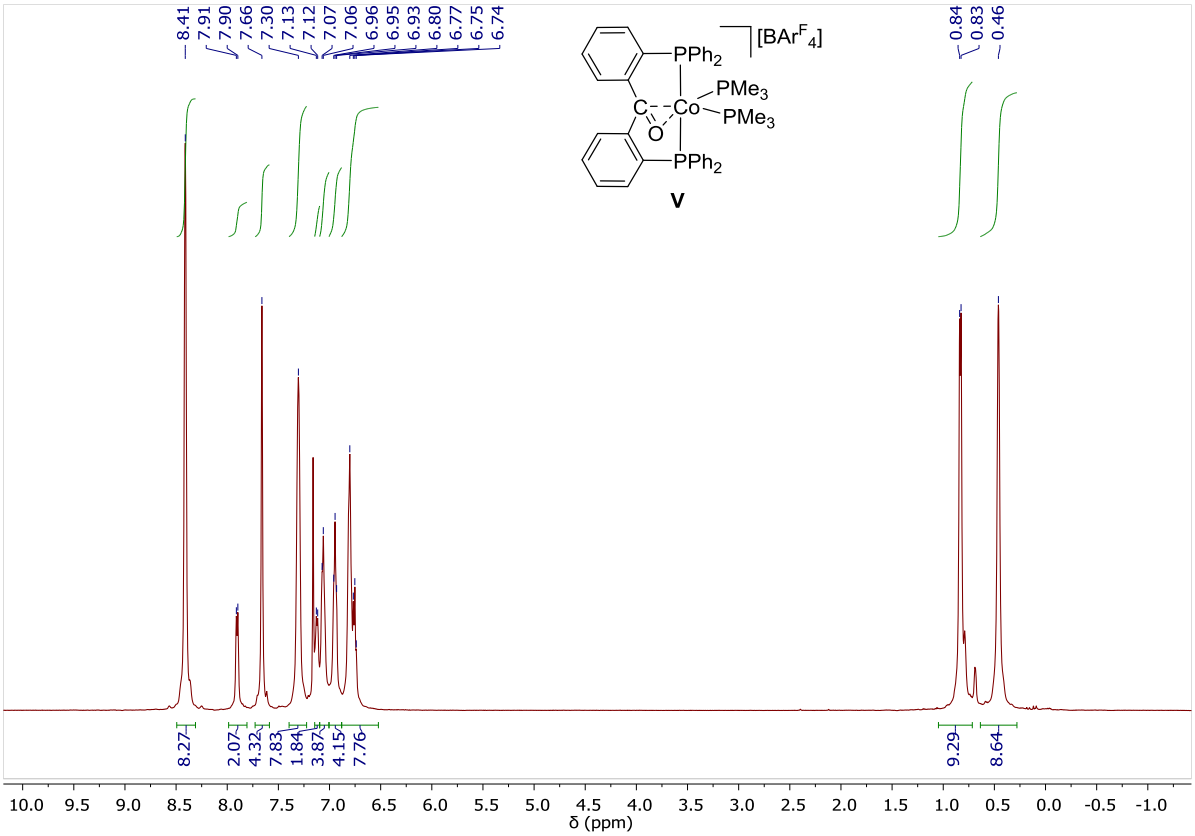

Figure S40 ^{1}H NMR of complex **V** in C_6D_6 at 298 K.

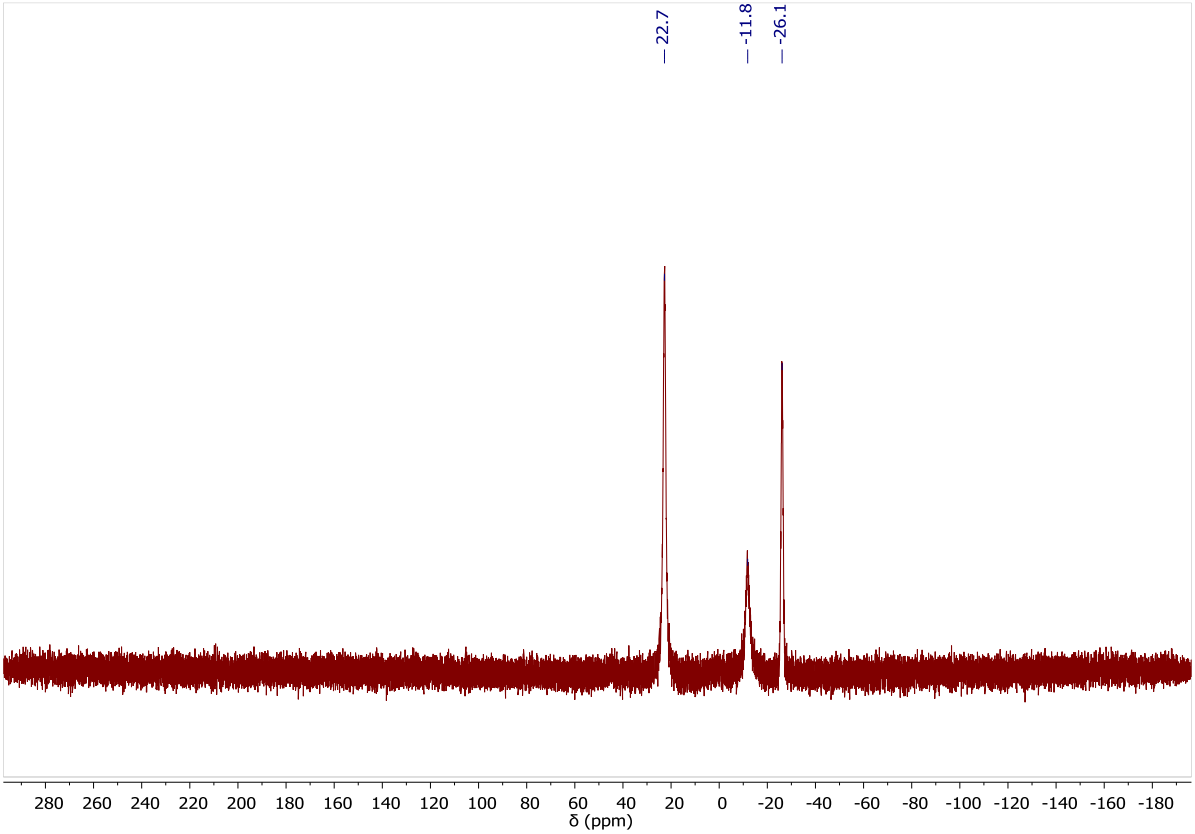

Figure S41 ^{31}P NMR of complex **V** in C_6D_6 at 298 K.

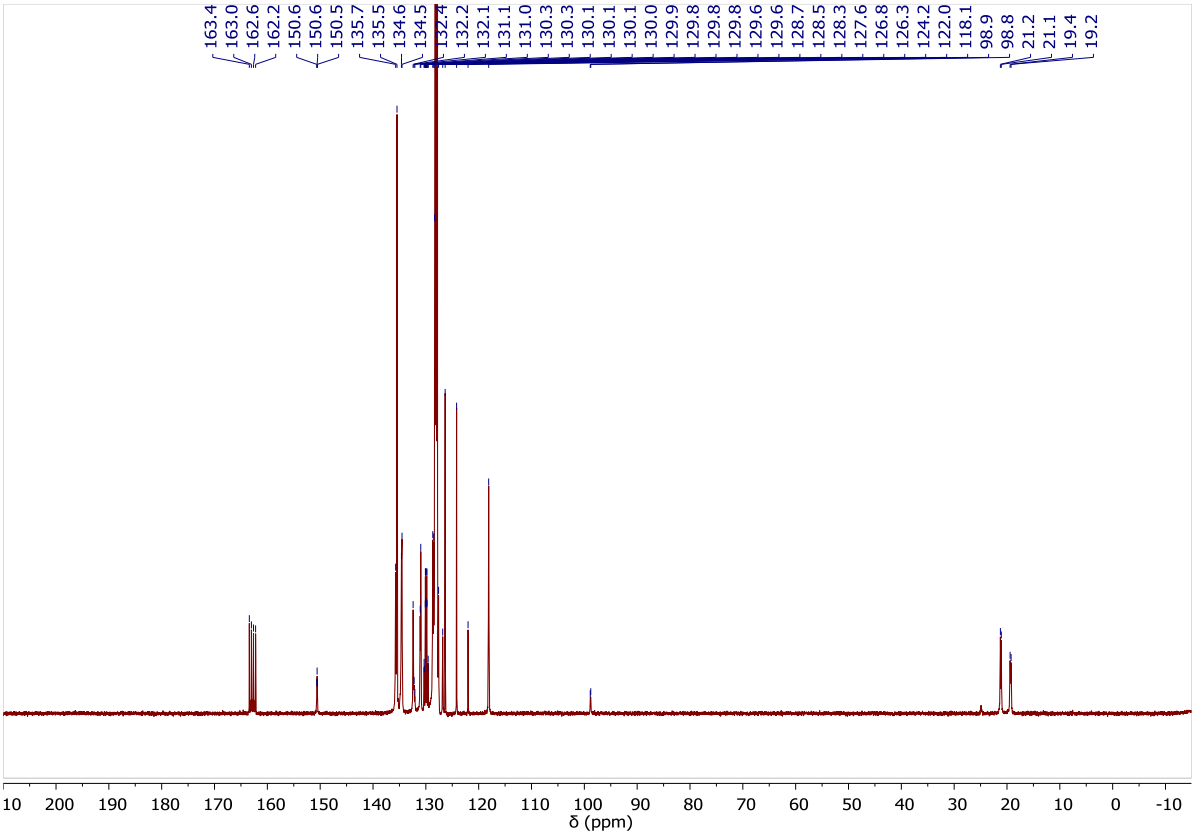

Figure S42 ^{13}C NMR of complex **V** in C_6D_6 at 298 K.

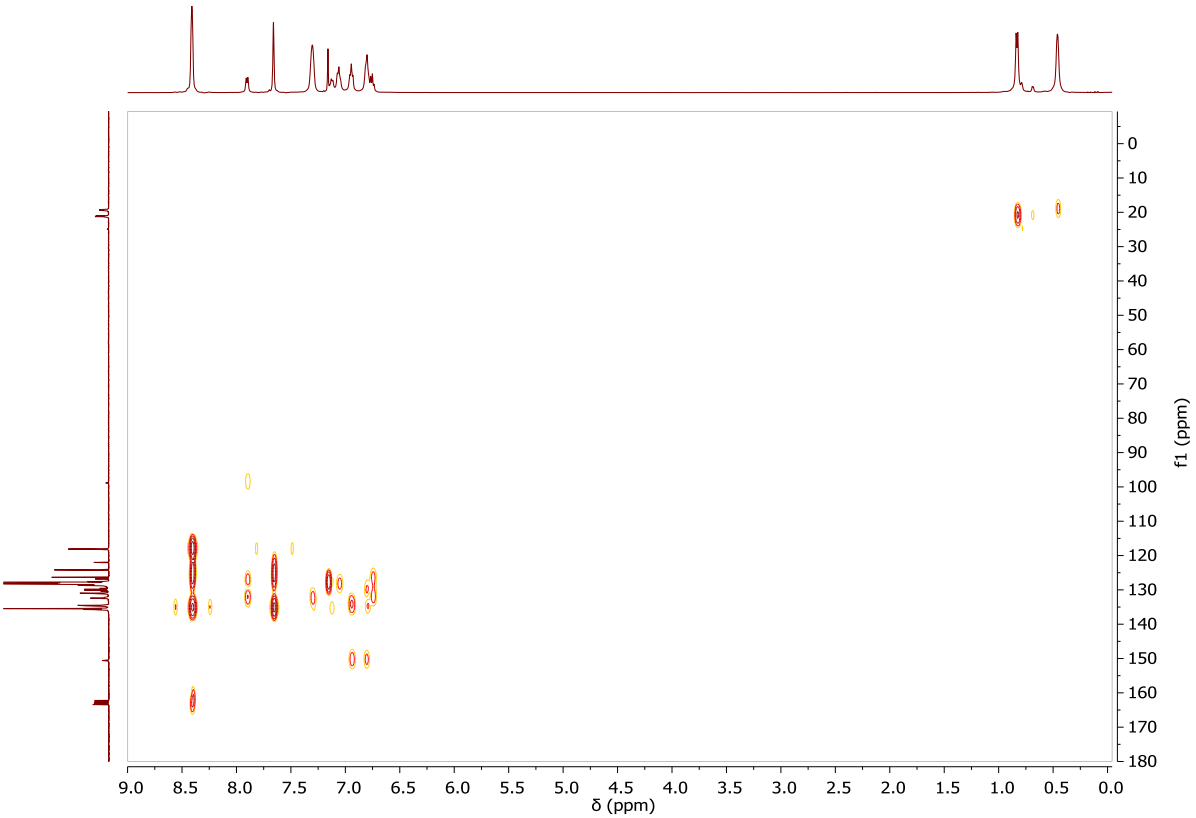

Figure S43 ^{1}H-^{13}C HMBC NMR of complex **V** in C_6D_6 at 298 K.

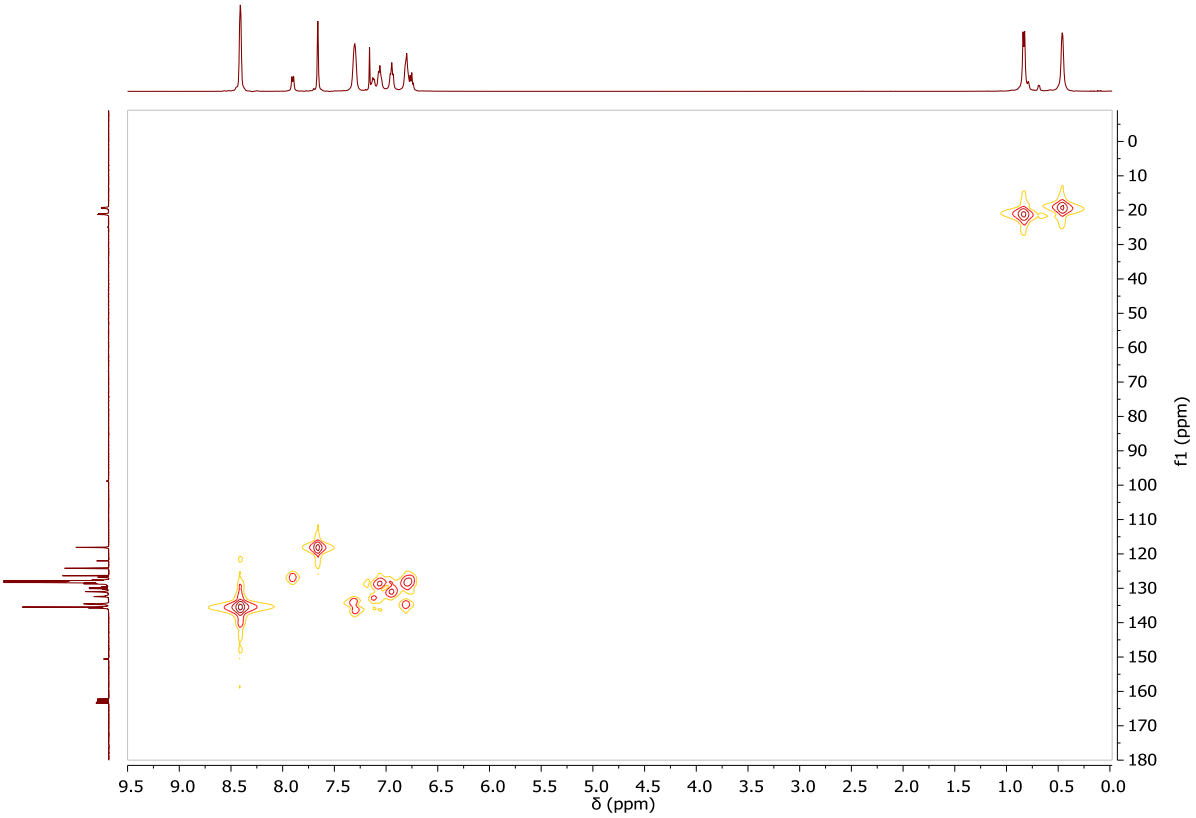

Figure S44 ^{1}H-^{13}C HMQC NMR of complex **V** in C_6D_6 at 298 K.

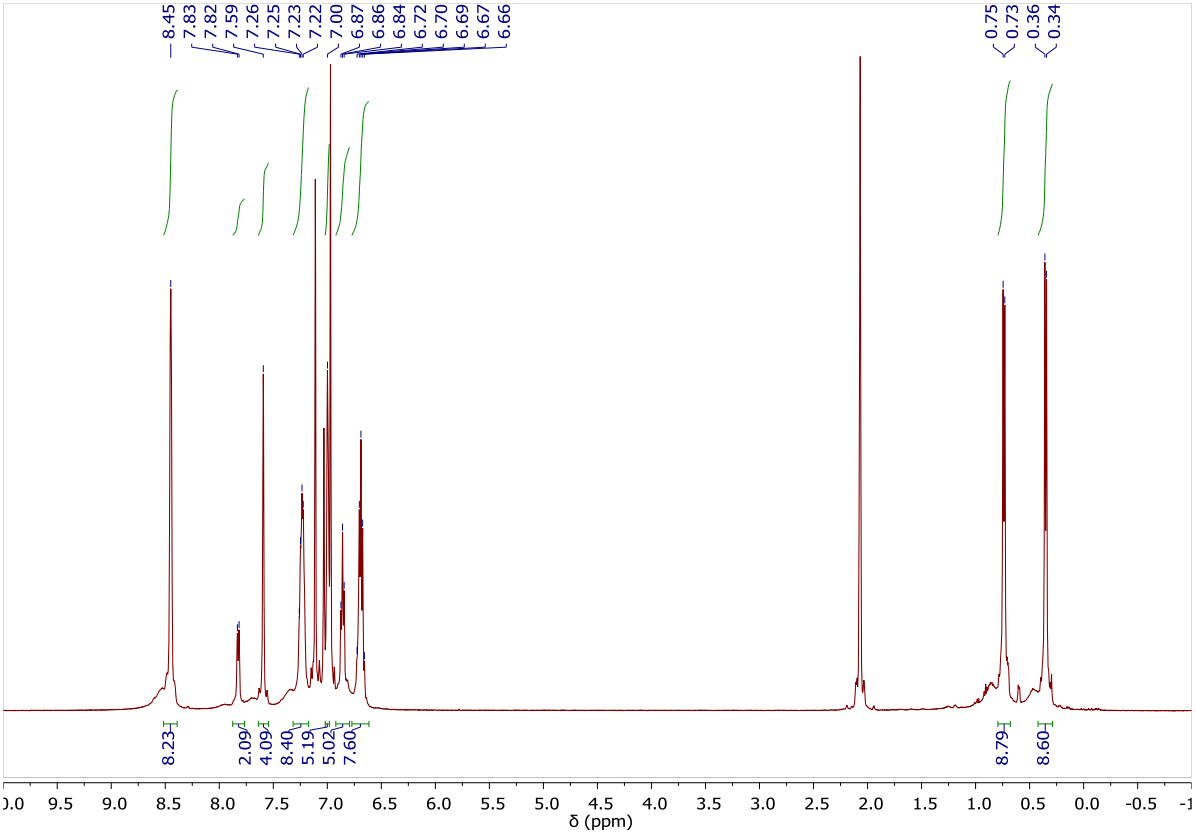

Figure S45 ^{1}H NMR of complex **V** in C_6D_6 at 253 K.

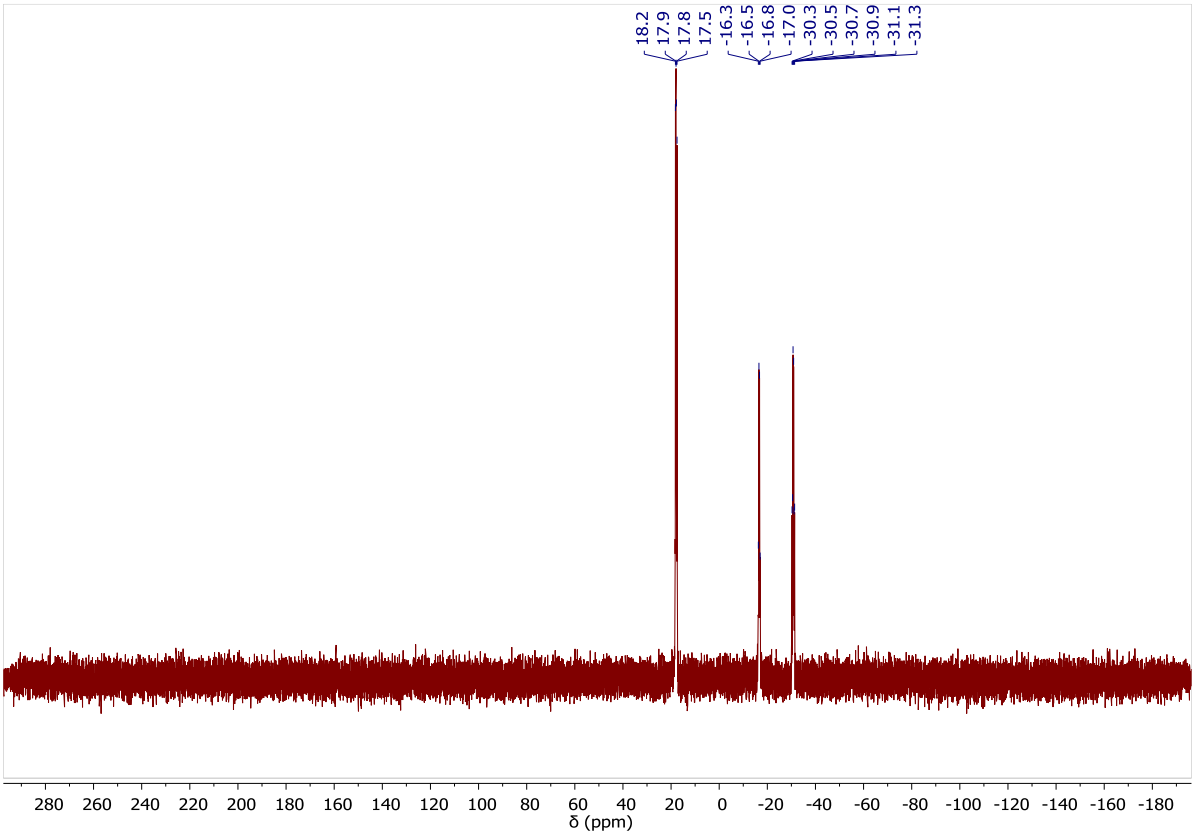

Figure S46 ^{31}P NMR of complex **V** in C_6D_6 at 253 K.

NMR Spectra of reduced bisphosphine ligand $(Ph_2PC_6H_4)_2CH_2$

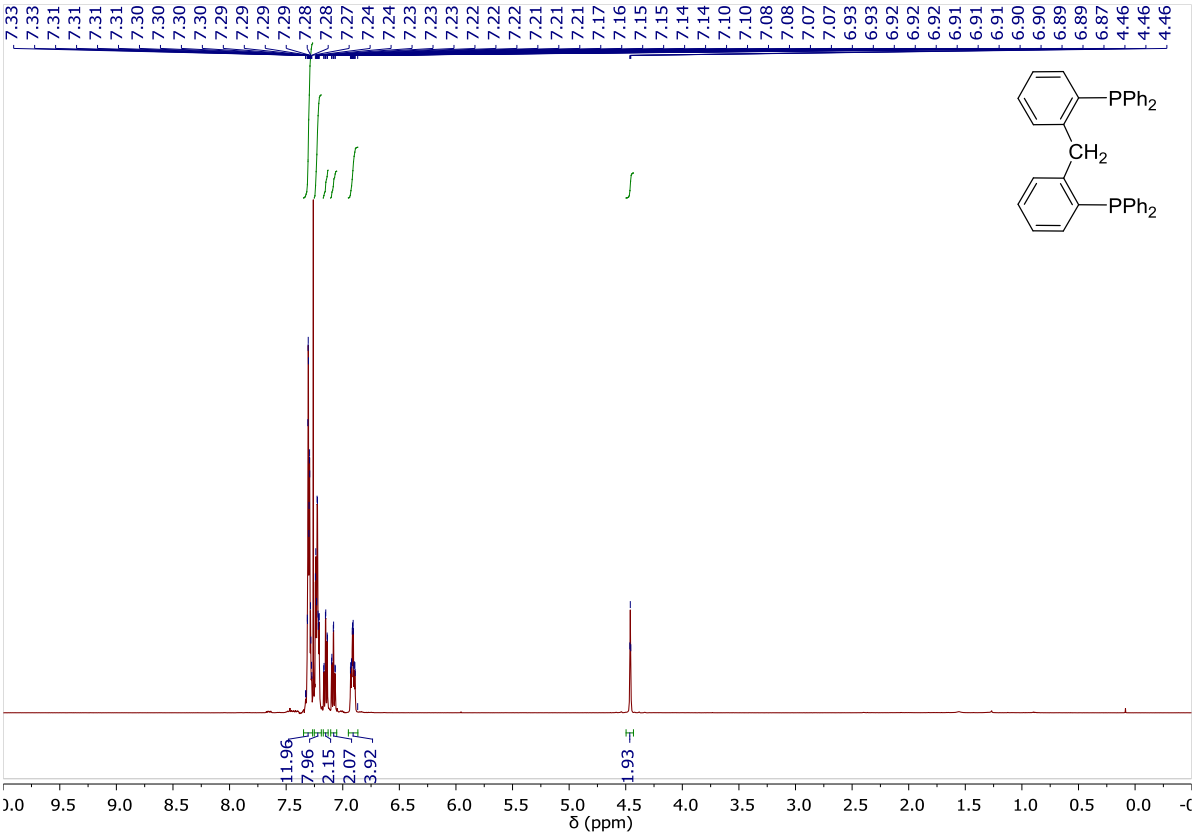

Figure S47 ^{1}H NMR of reduced bisphosphine ligand $(Ph_2PC_6H_4)_2CH_2$ in $CDCl_3$ at 298 K.

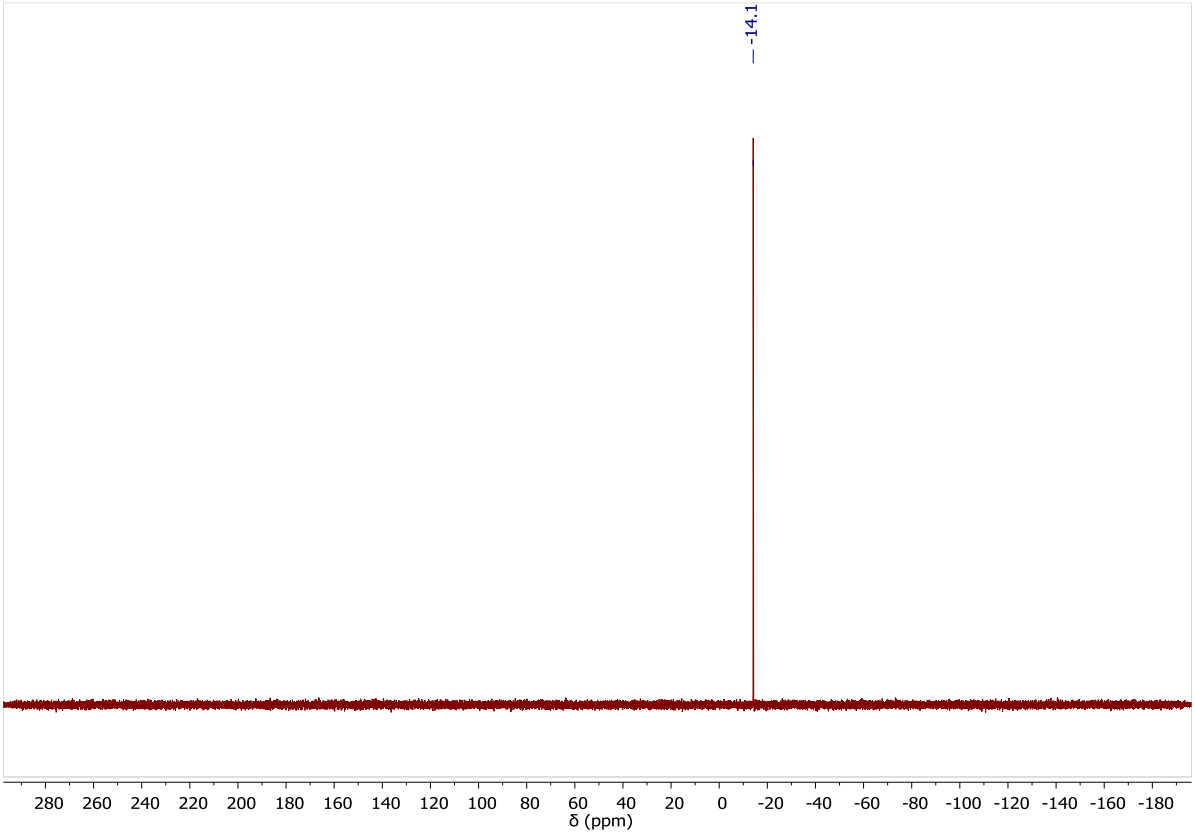

Figure S48 ^{31}P NMR of reduced bisphosphine ligand $(Ph_2PC_6H_4)_2CH_2$ in $CDCl_3$ at 298 K.

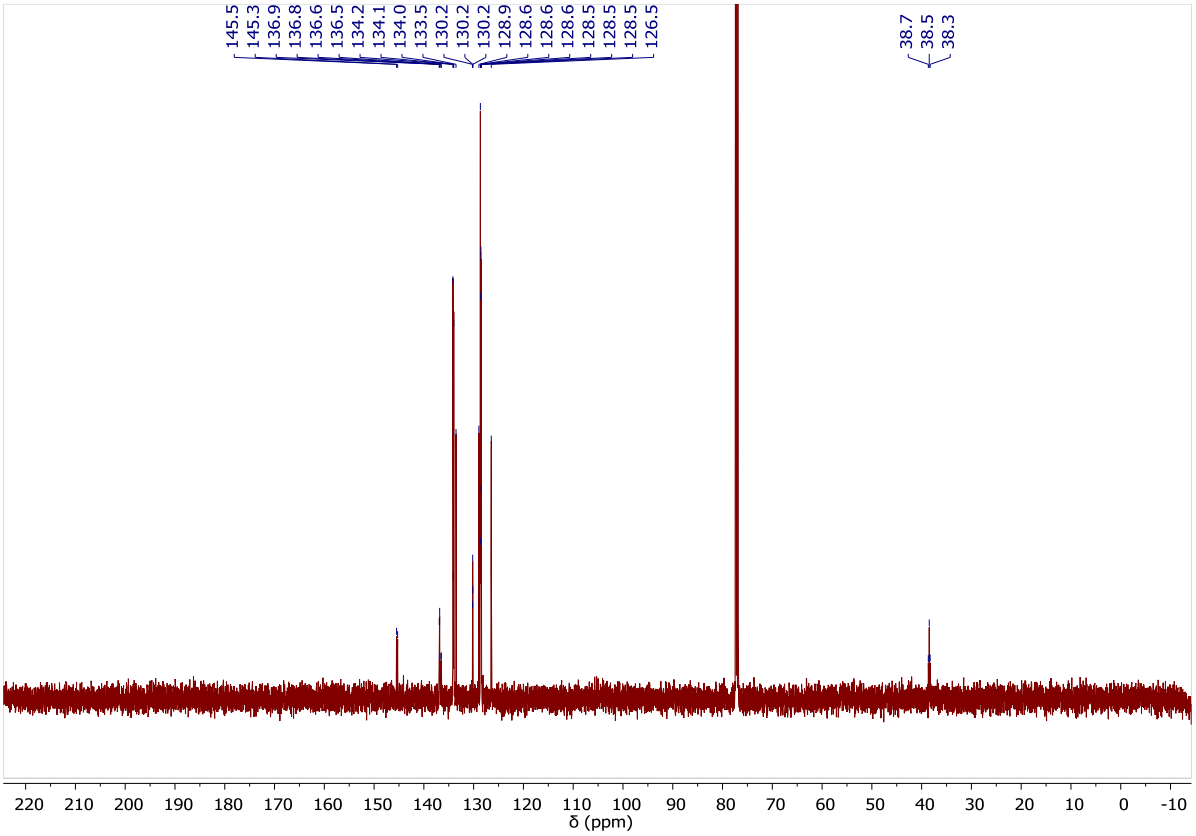

Figure S49 ^{13}C NMR of reduced bisphosphine ligand $(Ph_2PC_6H_4)_2CH_2$ in $CDCl_3$ at 298 K.

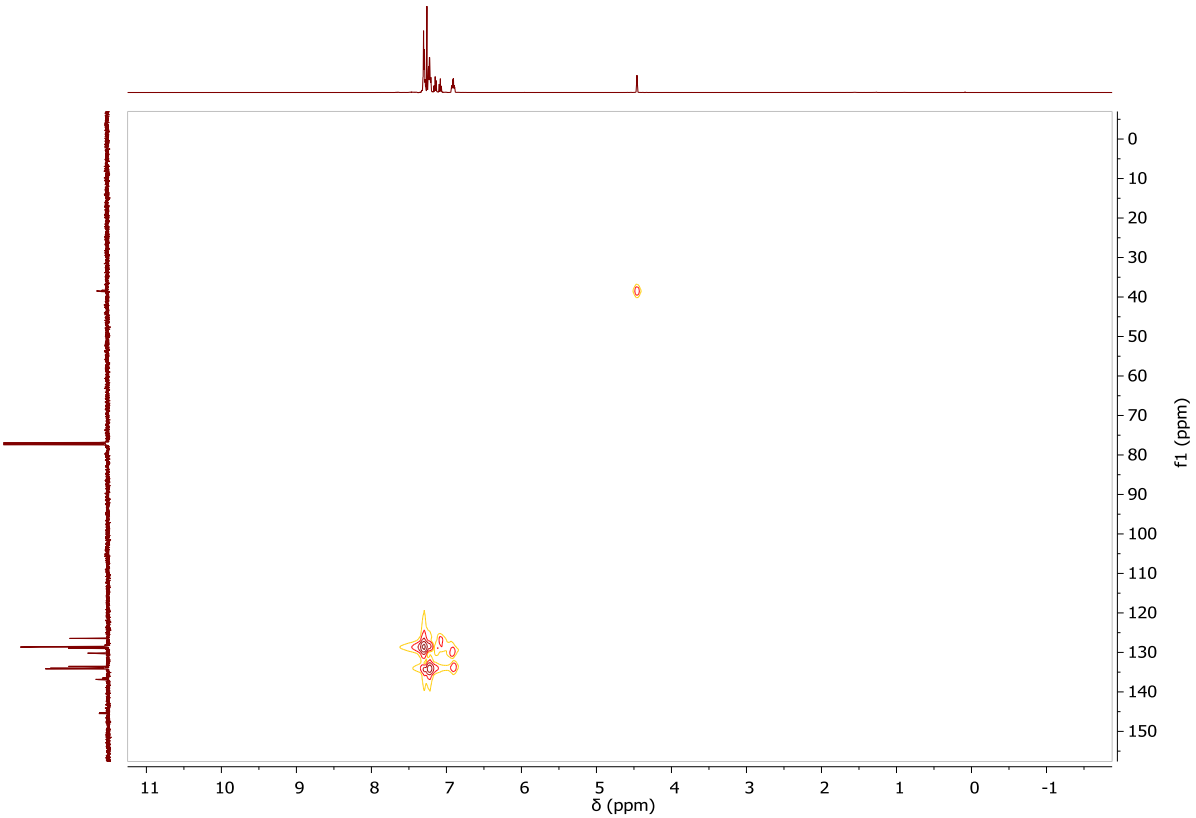

Figure S50 ^{1}H-^{13}C HMQC NMR of reduced bisphosphine ligand $(Ph_2PC_6H_4)_2CH_2$ in $CDCl_3$ at 298 K.

NMR Spectra of A^{Me}

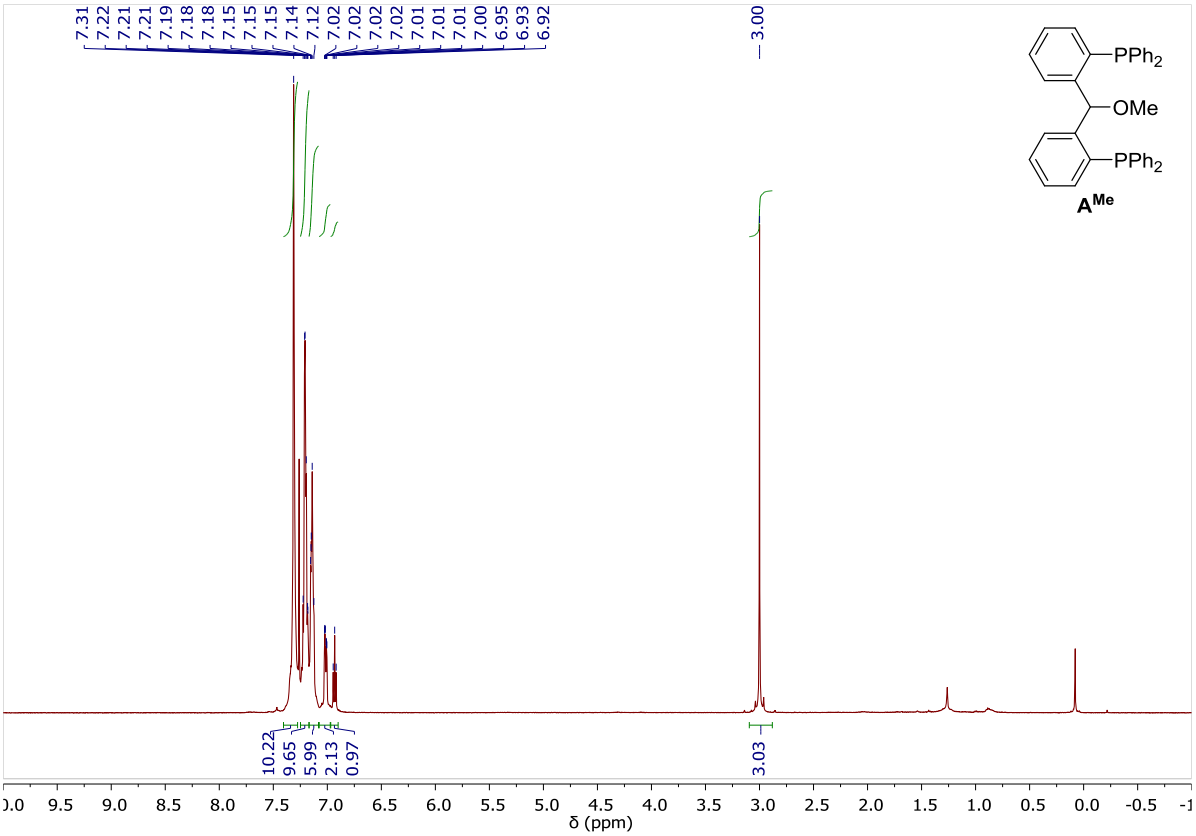

Figure S51 ^{1}H NMR of **A^{Me}** in $CDCl_3$ at 298 K.

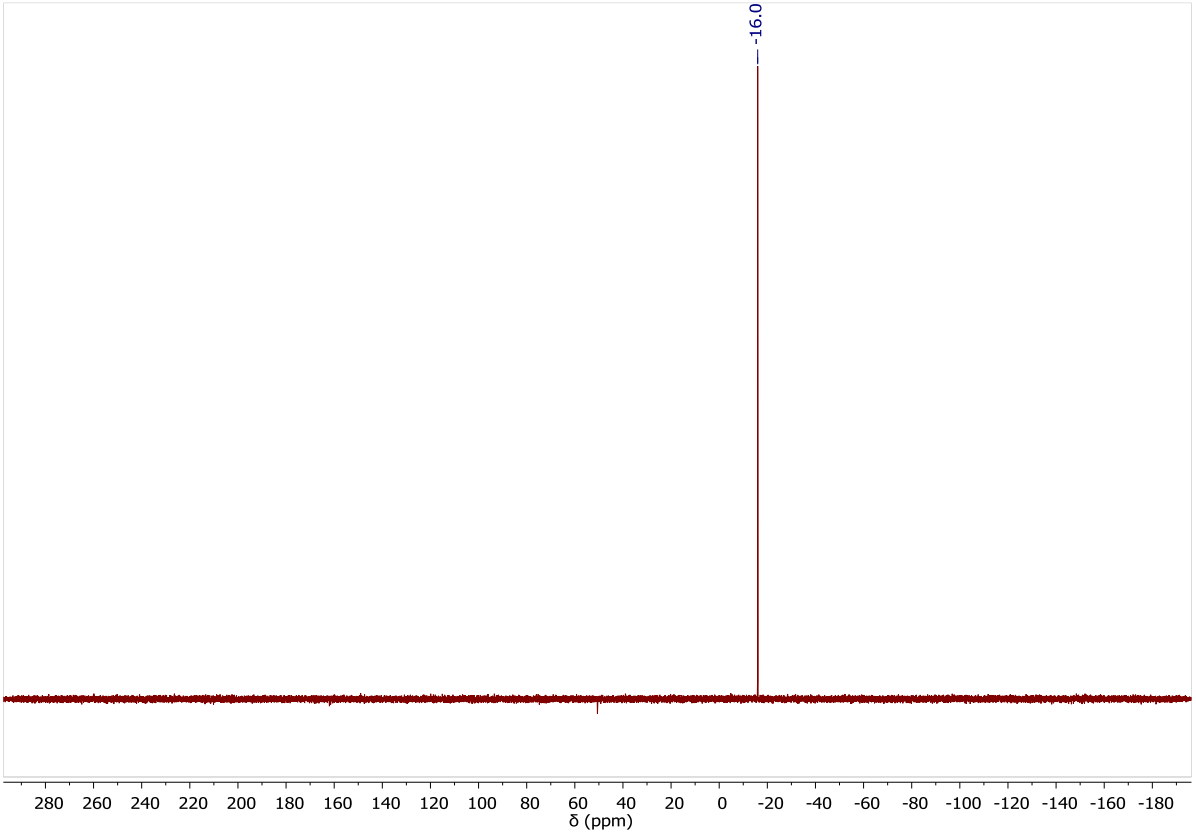

Figure S52 ^{31}P NMR of **A^{Me}** in $CDCl_3$ at 298 K.

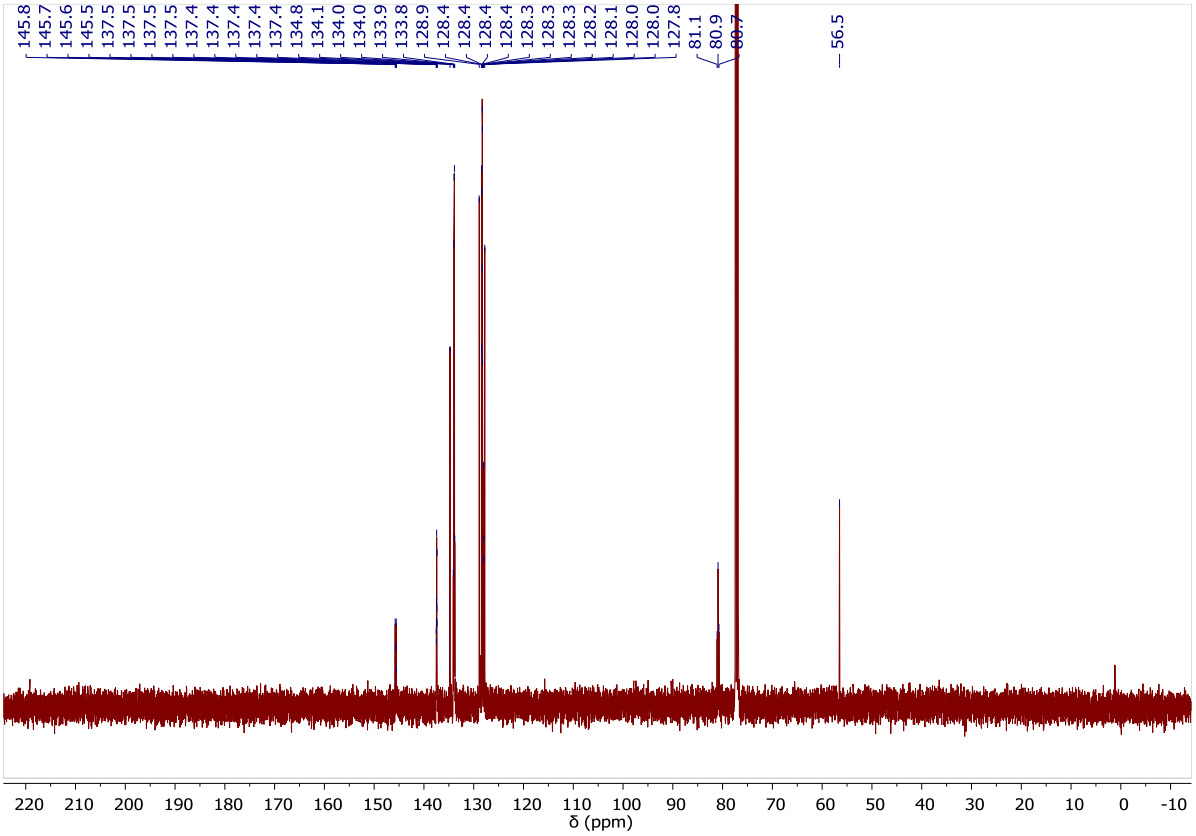

Figure S53 ^{13}C NMR of $\mathbf{A}^{\mathbf{Me}}$ in $CDCl_3$ at 298 K.

NMR Spectra of A^{TIPS}

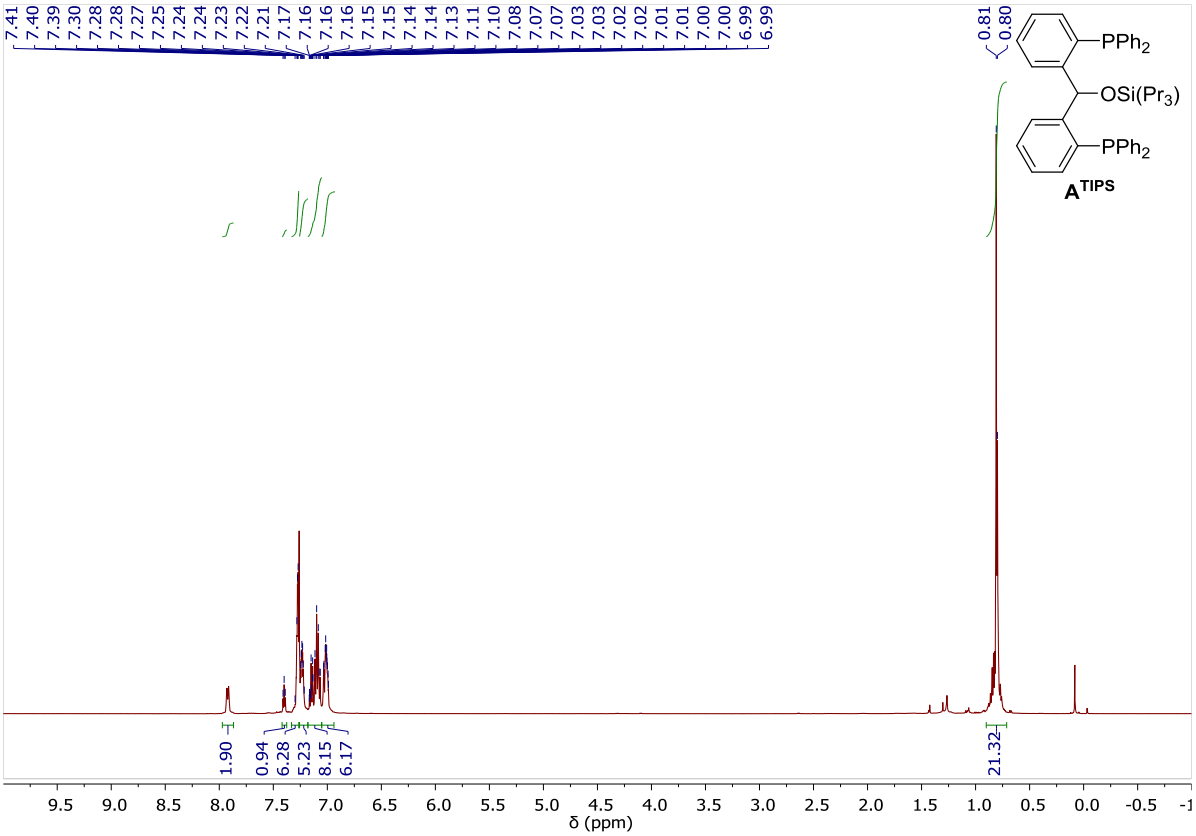

Figure S54 ^{1}H NMR of $\mathbf{A^{TIPS}}$ in $CDCl_3$ at 298 K.

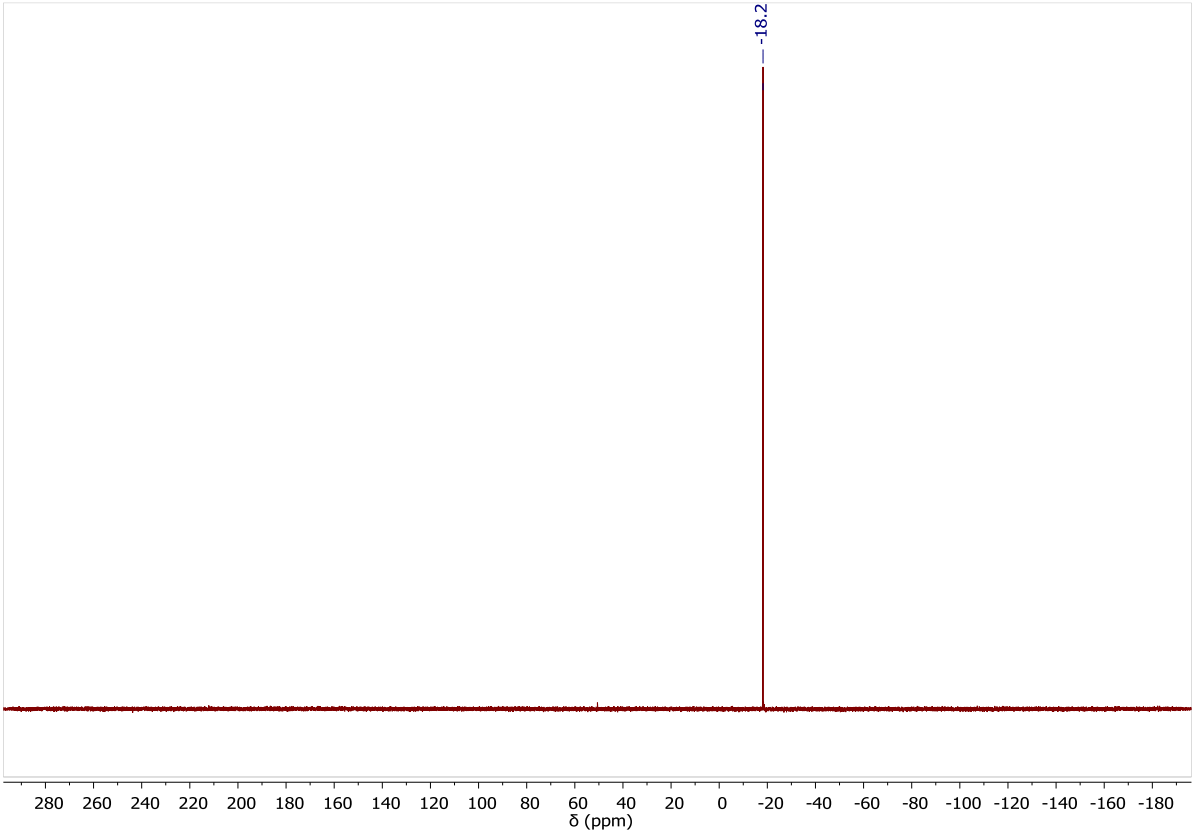

Figure S55 ^{31}P NMR of $\mathbf{A^{TIPS}}$ in $CDCl_3$ at 298 K.

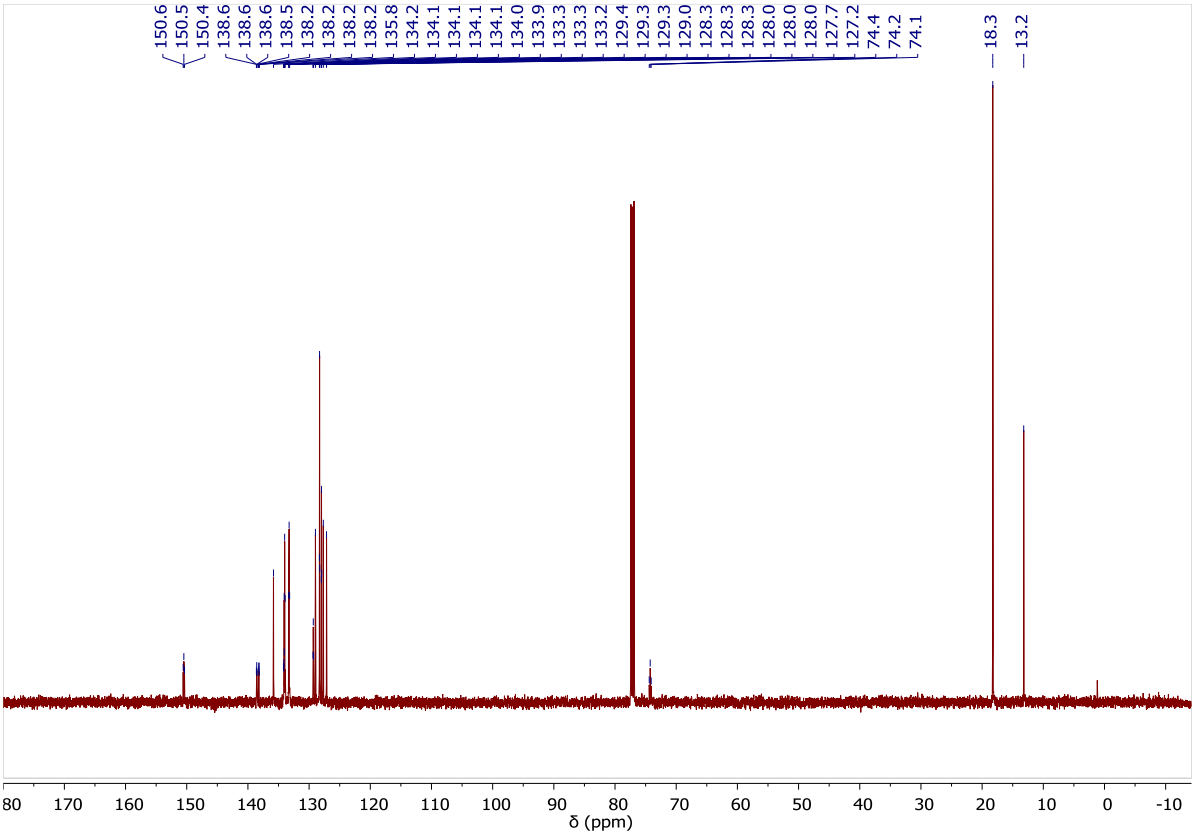

Figure S56 ^{13}C NMR of $\mathbf{A}^{\mathbf{TIPS}}$ in $CDCl_3$ at 298 K.

NMR Spectra for the reaction between complex 1 and H_2

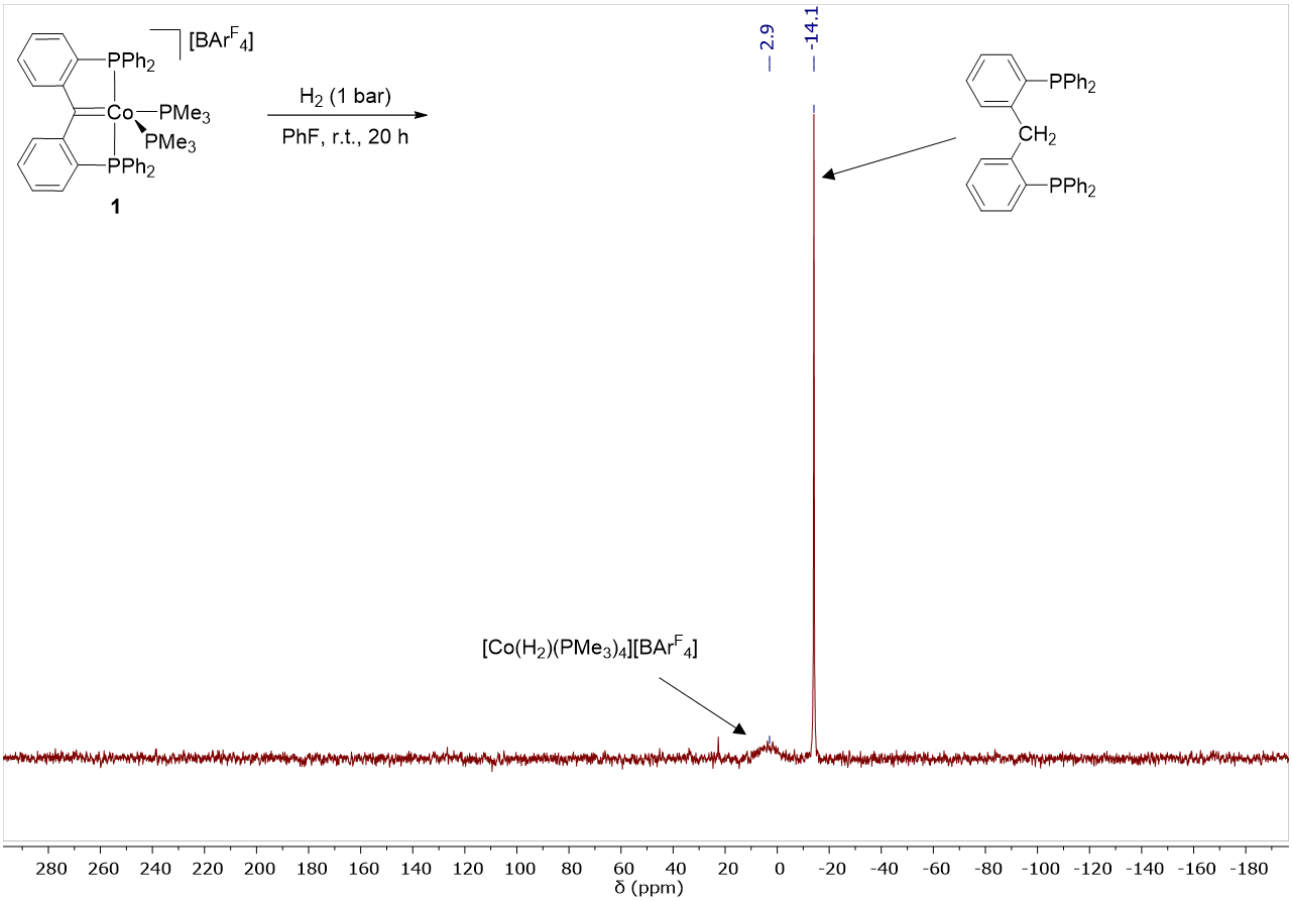

Figure S57 ^{31}P NMR after reacting complex **1** with H_2 in fluorobenzene at 298 K.

NMR Spectra of $[Co(H_2)(PMe_3)_4][BAr^F{}_4]$

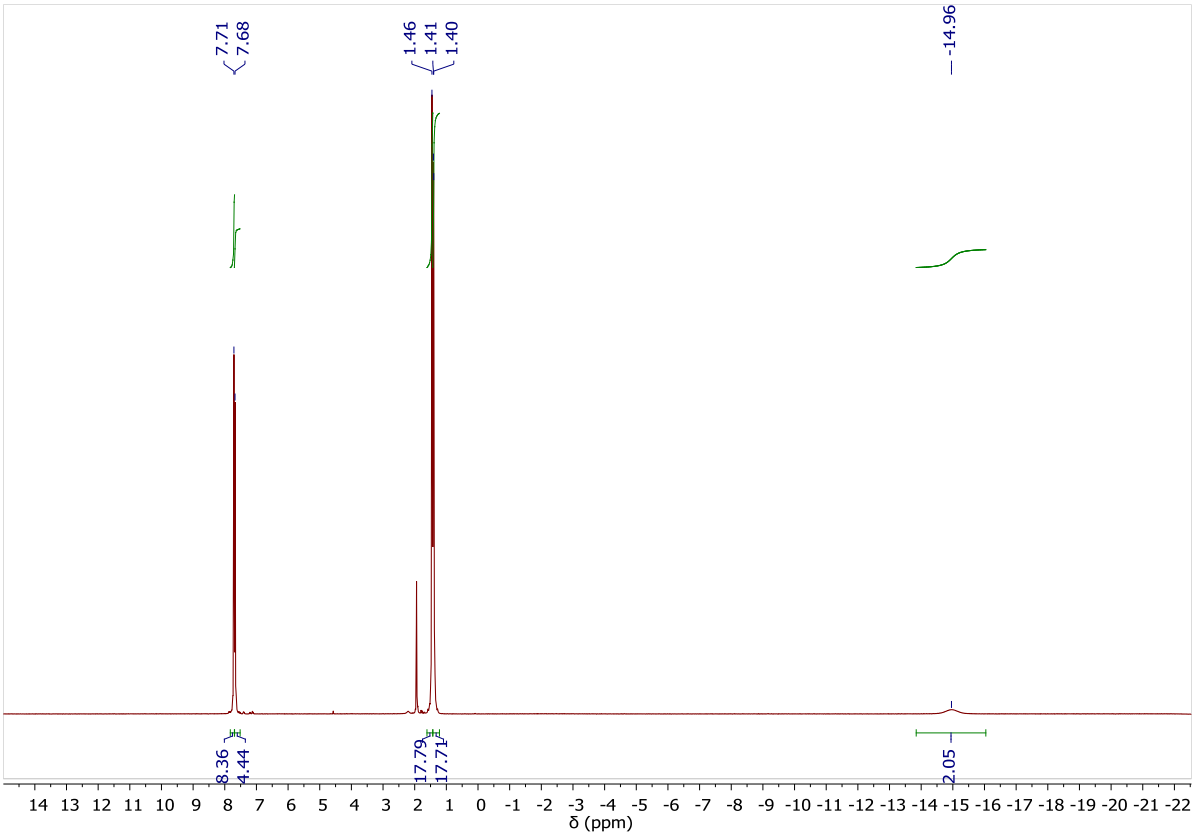

Figure S58 ^{1}H NMR of $[Co(H_2)(PMe_3)_4][BAr^F{}_4]$ in CD_3CN at 298 K.

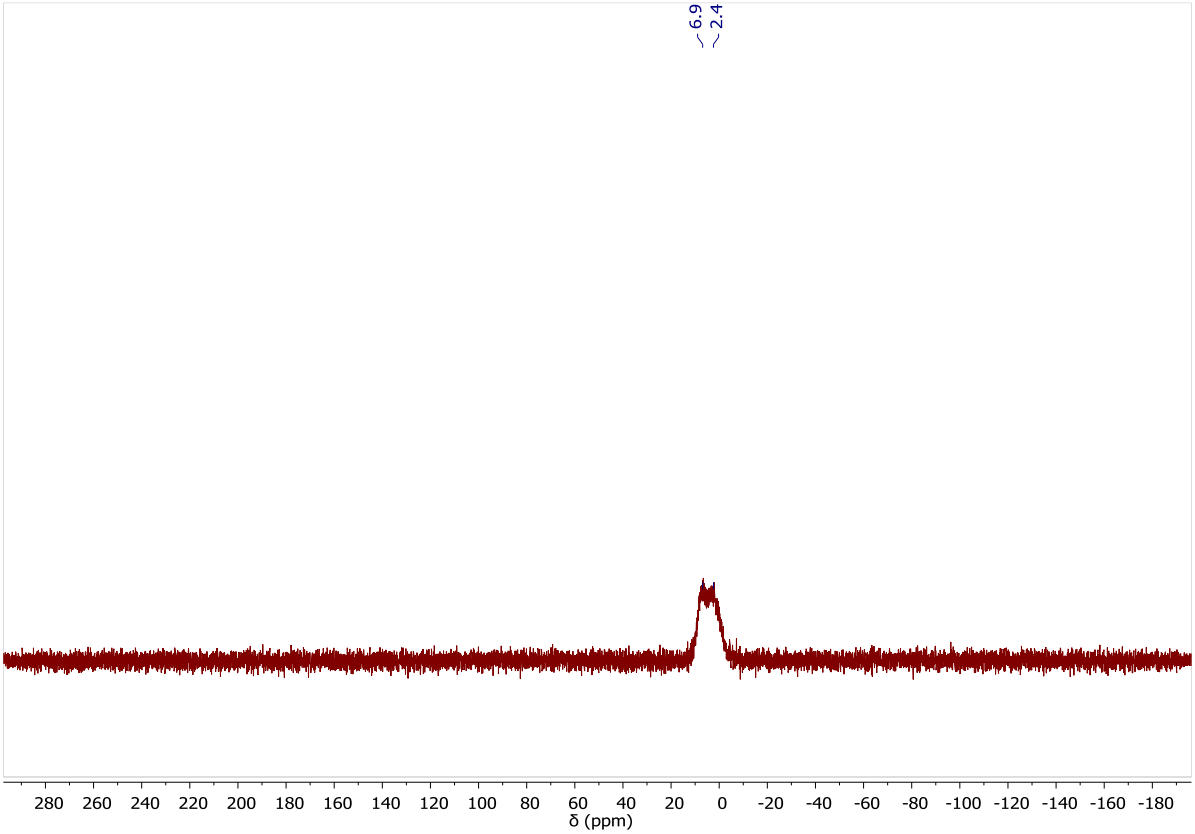

Figure S59 ^{31}P NMR of $[Co(H_2)(PMe_3)_4][BAr^F{}_4]$ in CD_3CN at 298 K.

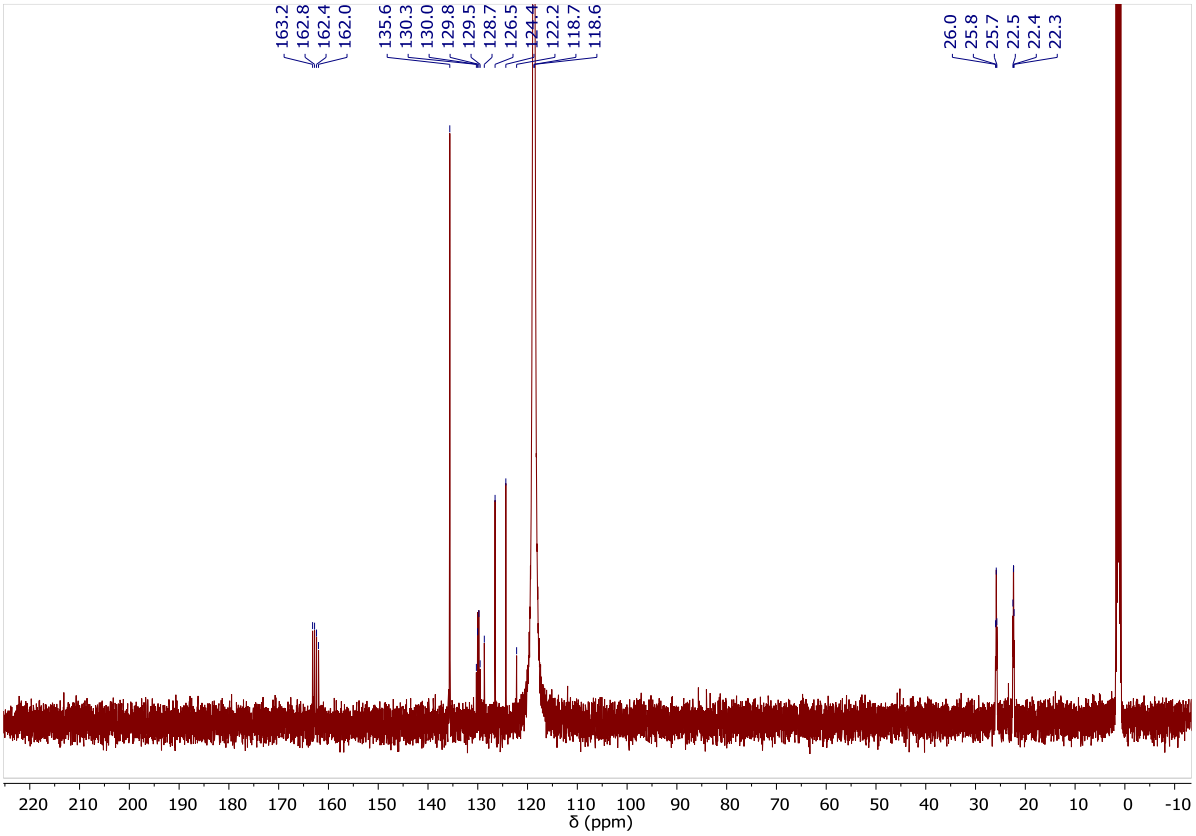

Figure S60 ^{13}C NMR of $[Co(H_2)(PMe_3)_4][BAr^F{}_4]$ in CD_3CN at 298 K.

NMR Spectra for the reaction between complex 1 and $[H(OEt_2)_2][BAr^F_4]$

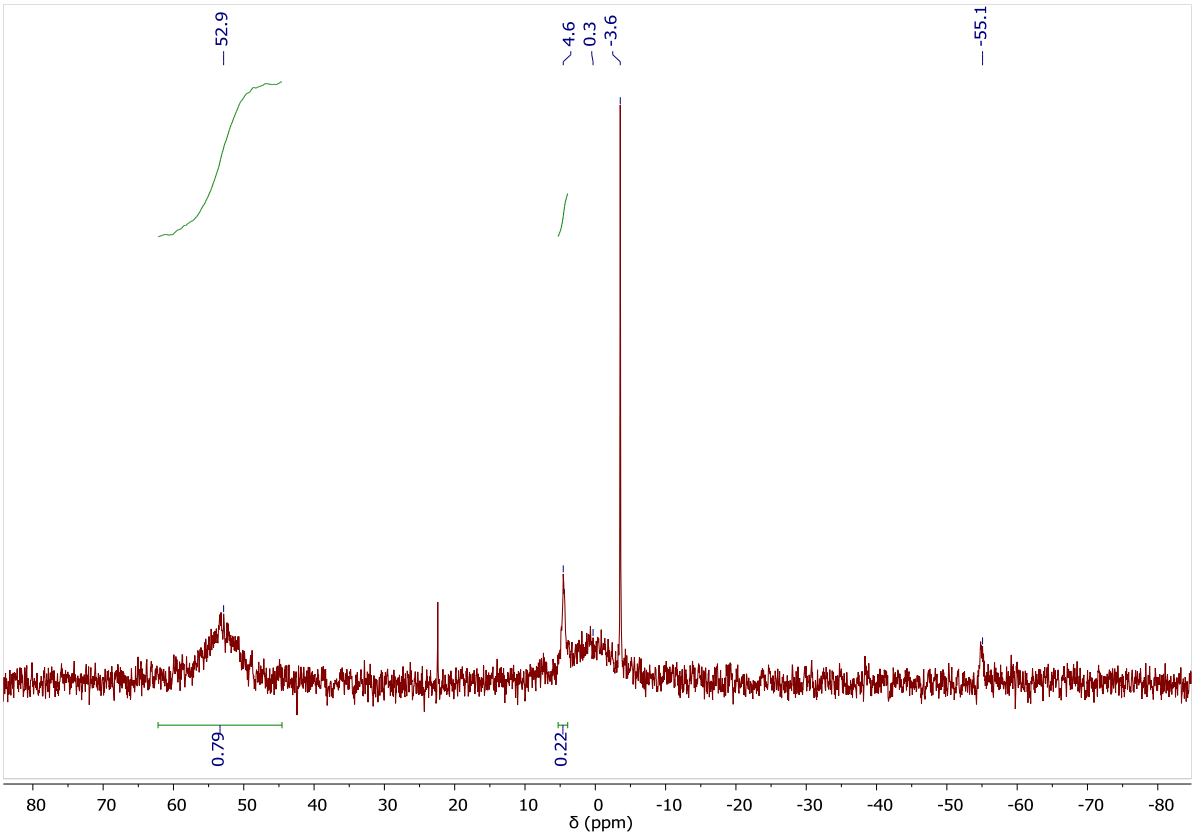

Figure S61 ^{31}P NMR after reacting **1** with $[H(OEt_2)_2][BAr^F_4]$ in fluorobenzene at 298 K, with approx. 22% conversion.

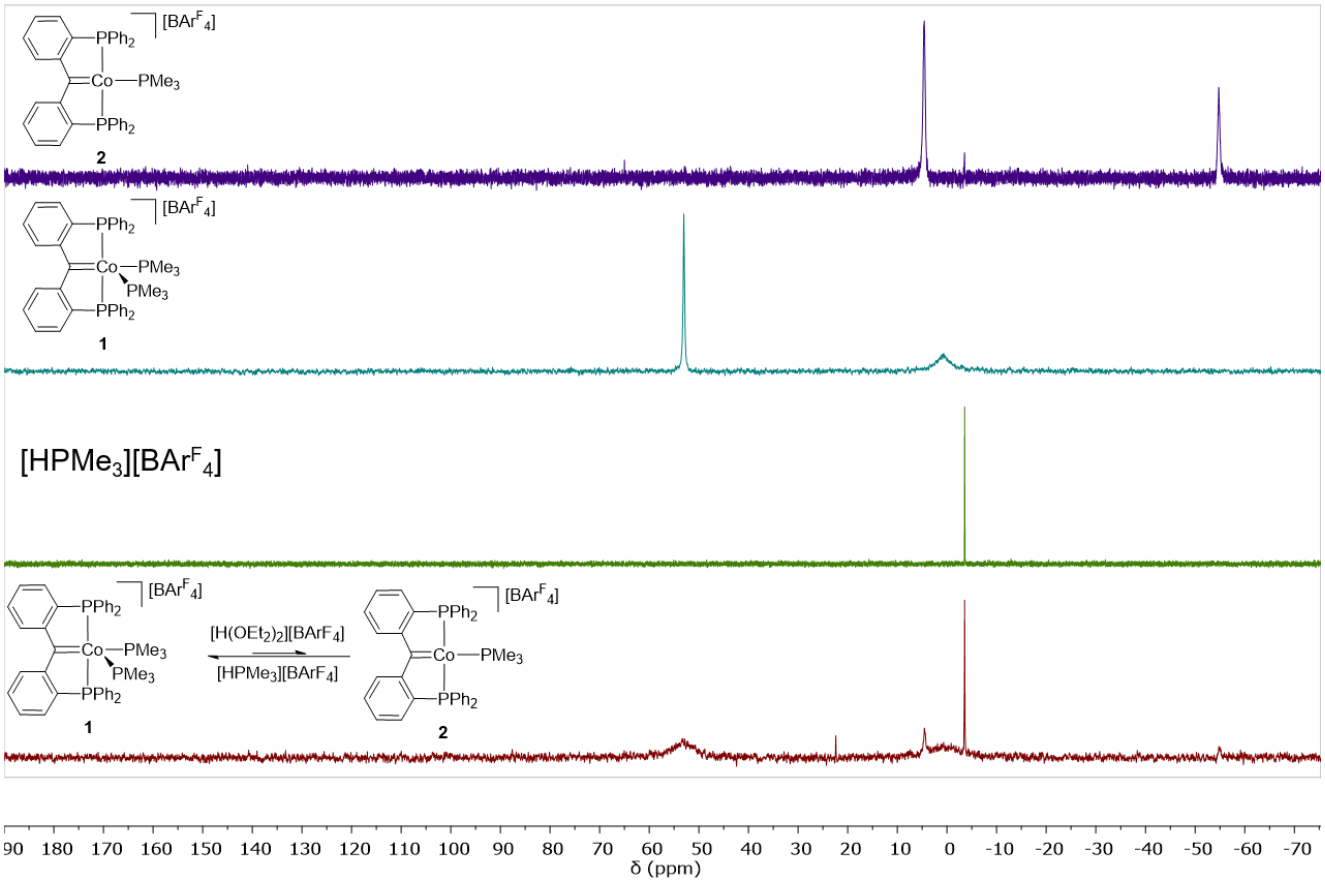

Figure S62 Comparison of the ^{31}P NMR spectrum of the reaction between complex **1** and $[H(OEt_2)_2][BAr^F_4]$ in fluorobenzene, with their starting materials and products at 298 K.

NMR Spectra for the reaction when heating intermediate III to form complex 1

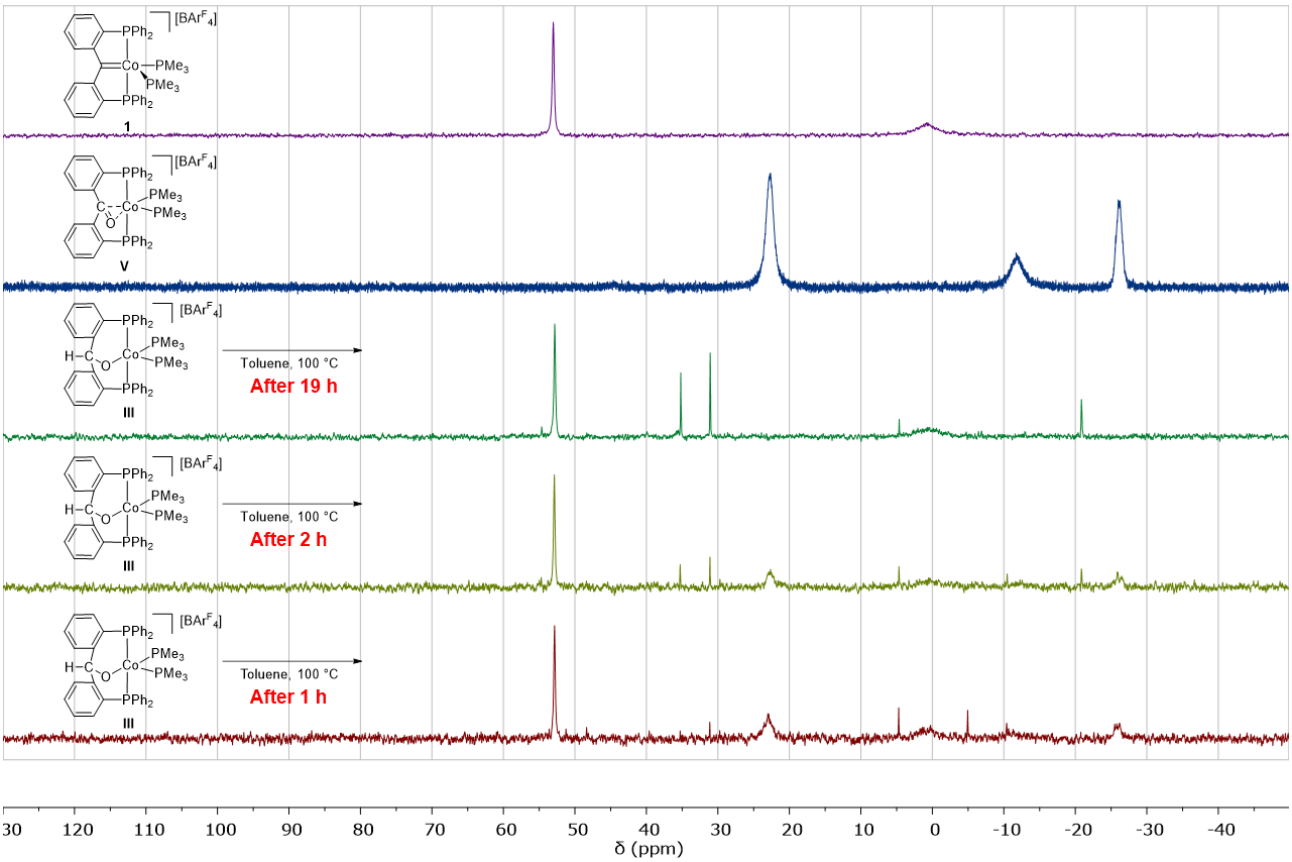

Figure S63 Comparison of the ^{31}P NMR spectrum of the reaction when heating intermediate **III** in fluorobenzene, showing the formations of complexes **1** and intermediate **V**.

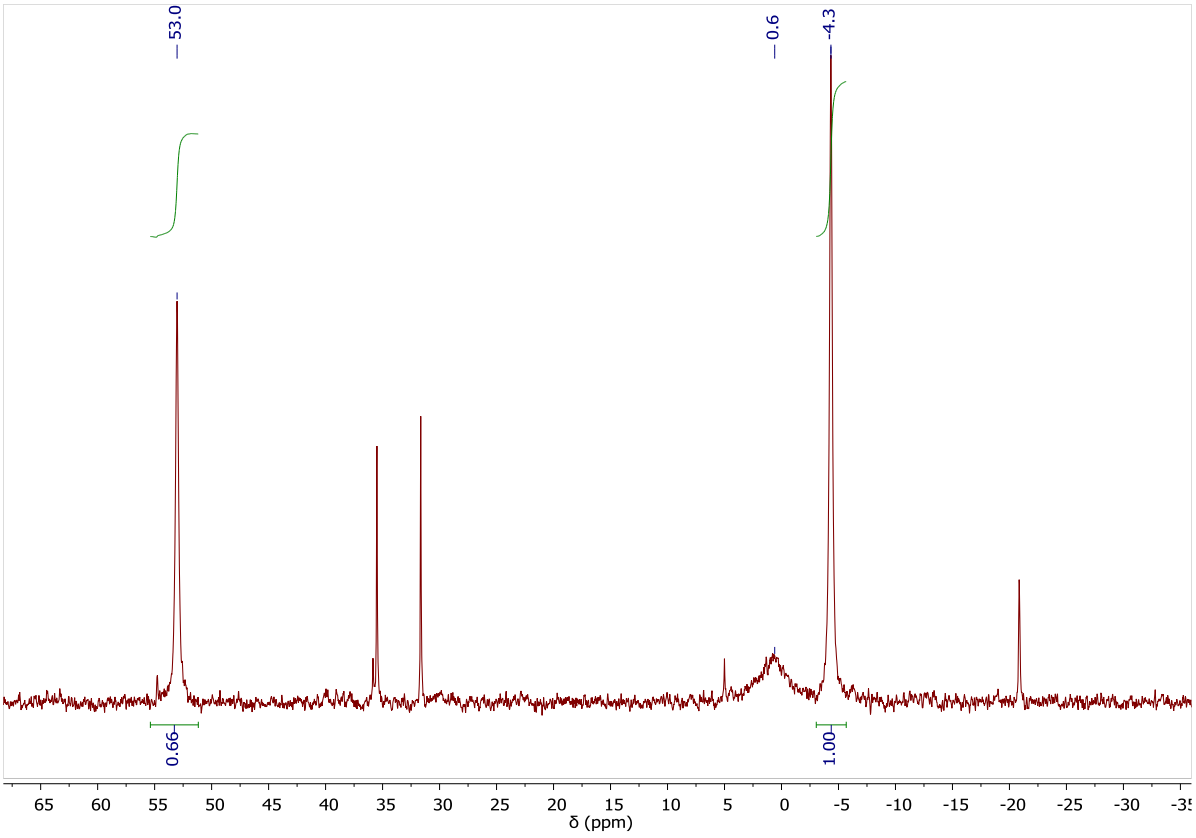

Figure S64 ^{31}P NMR spectrum of the end-point of the reaction when heating intermediate **III** in fluorobenzene, with one equivalent of added PPh_3 (at -4.3 ppm) as an internal standard to determine the yield of complex **1** formed (33%).

NMR Spectra for the reaction between complex V and H_2

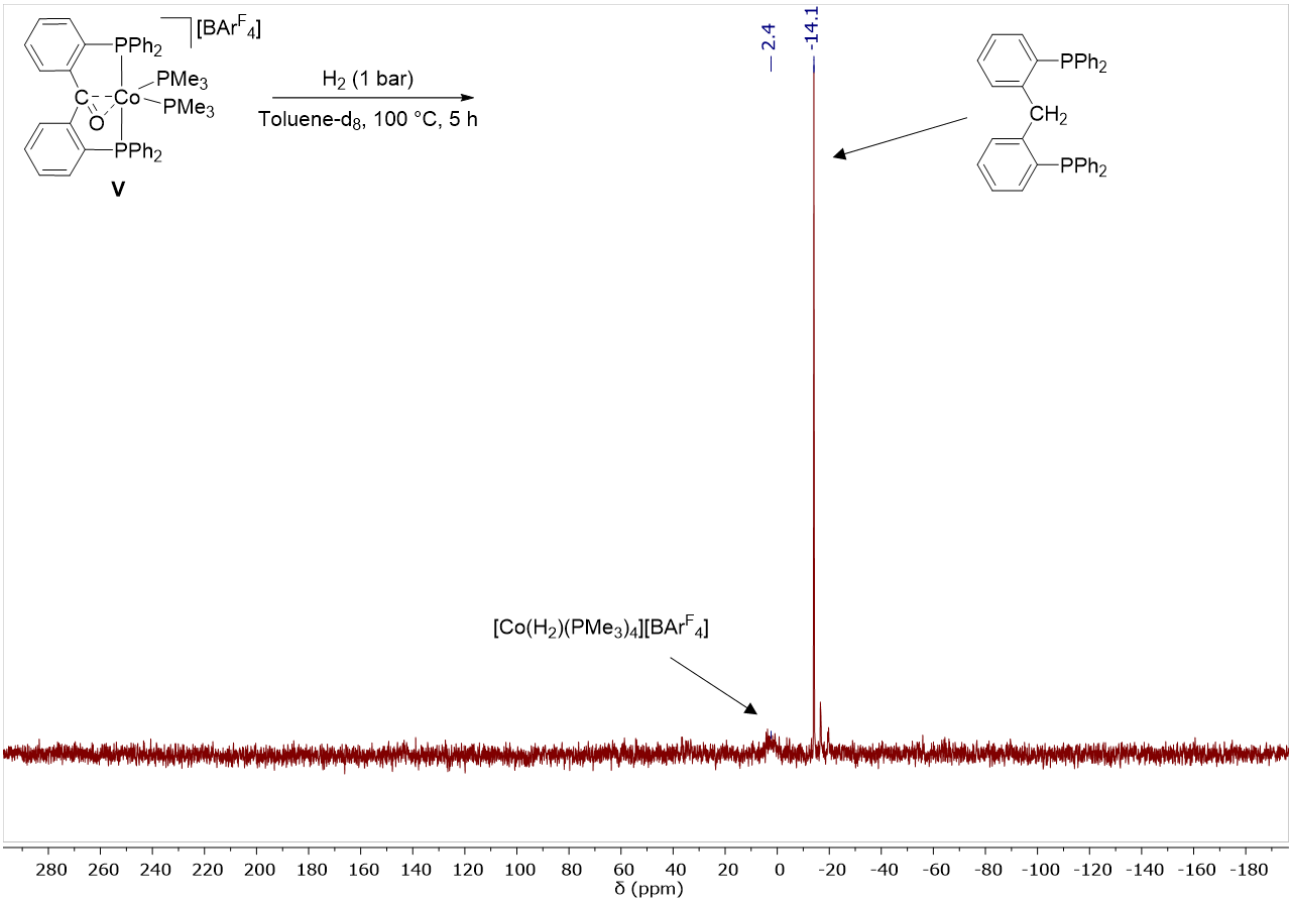

Figure S65 ^{31}P NMR after reacting complex **V** with H_2 in fluorobenzene showing the formation reduced bisphosphine ligand $(Ph_2PC_6H_4)_2CH_2$ and $[Co(H_2)(PMe_3)_4][BAr^F_4]$.

HRMS (ESI-TOF) Spectra

Mass spectrum of complex 1

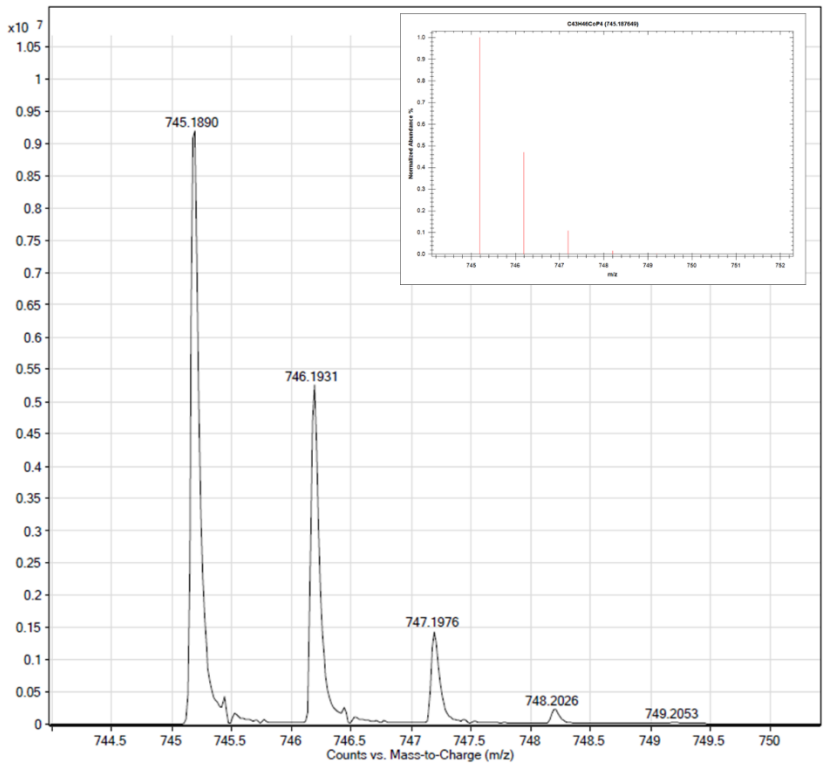

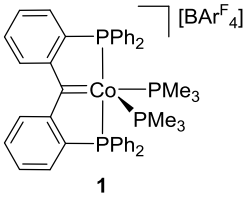

1

Figure S66 Positive mode HRMS (ESI-TOF) spectrum of $[M]^+$ ion of **1**. Inset shows expected isotope pattern.

Mass spectrum of complex 2

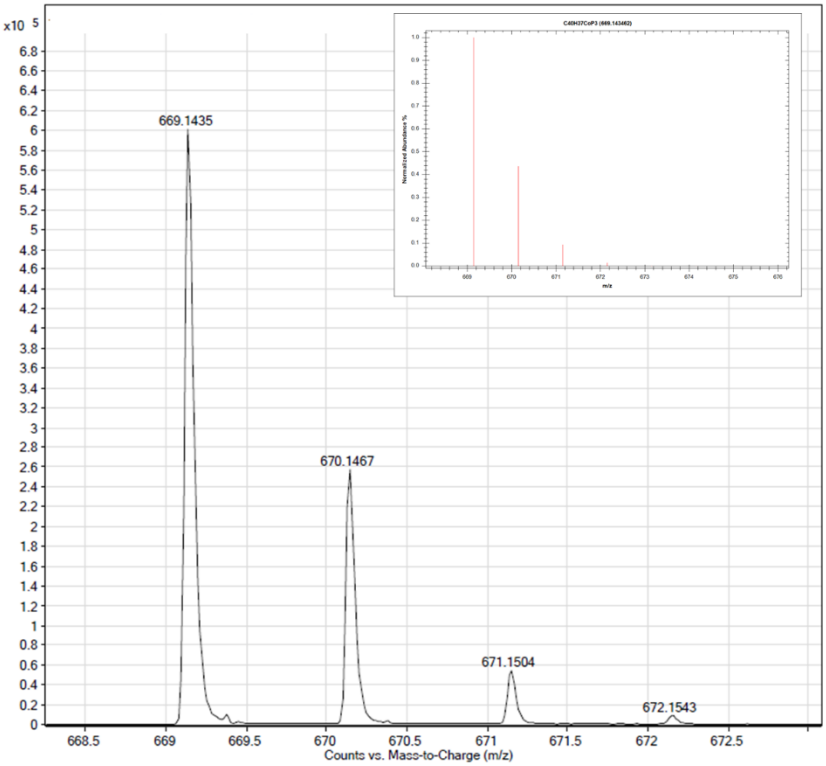

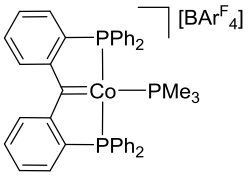

2

Figure S67 Positive mode HRMS (ESI-TOF) spectrum of $[M]^+$ ion of **2**. Inset shows expected isotope pattern.

Mass spectrum of complex 3

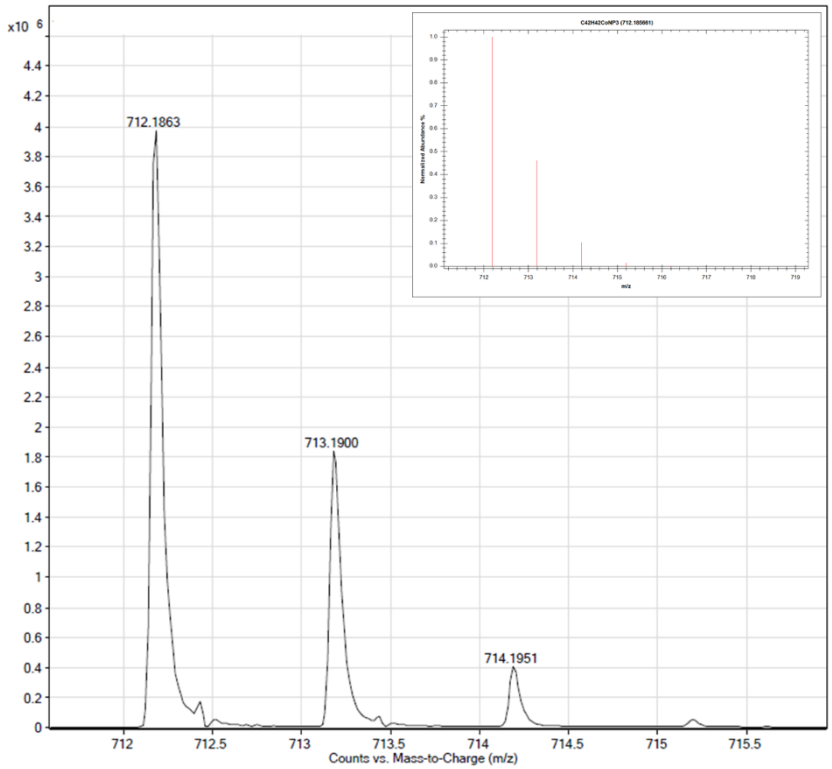

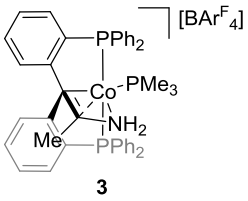

3

Figure S68 Positive mode HRMS (ESI-TOF) spectrum of $[M]^+$ ion of **3**. Inset shows expected isotope pattern.

Mass spectrum of complex 4

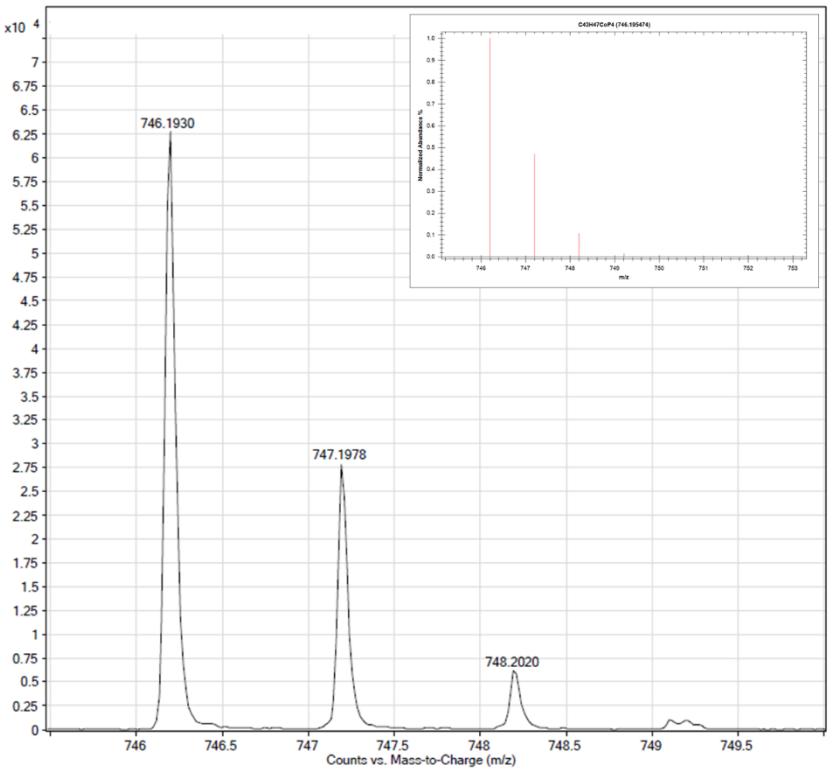

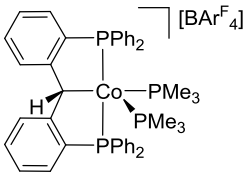

4

Figure S69 Positive mode HRMS (ESI-TOF) spectrum of $[M]^+$ ion of **4**. Inset shows expected isotope pattern.

Mass spectrum of complex 5

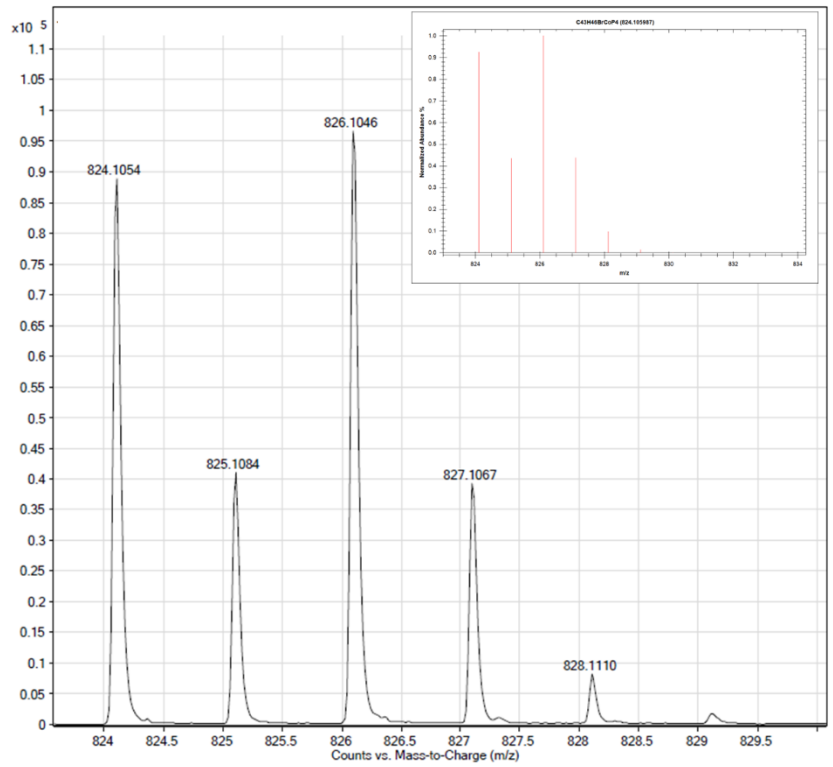

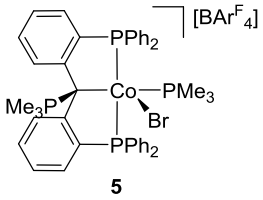

5

Figure S70 Positive mode HRMS (ESI-TOF) spectrum of $[M]^+$ ion of **5**. Inset shows expected isotope pattern.

Mass spectrum of the initial complex formed in the preparation of 6

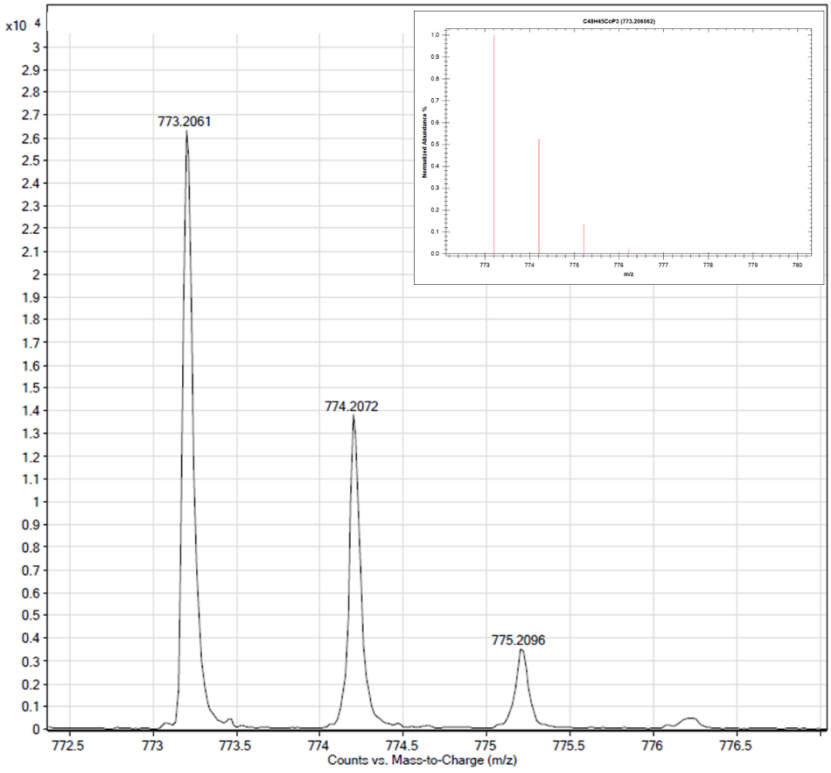

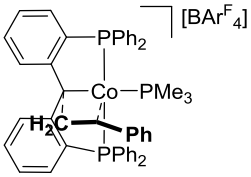

Figure S71 Positive mode HRMS (ESI-TOF) spectrum of $[M]^+$ ion of the initial complex formed in the preparation of **6** after 12 hours, before loss of H_2 (0.5 equivalents) has occurred. Inset shows expected isotope pattern.

Mass spectrum of complex 6

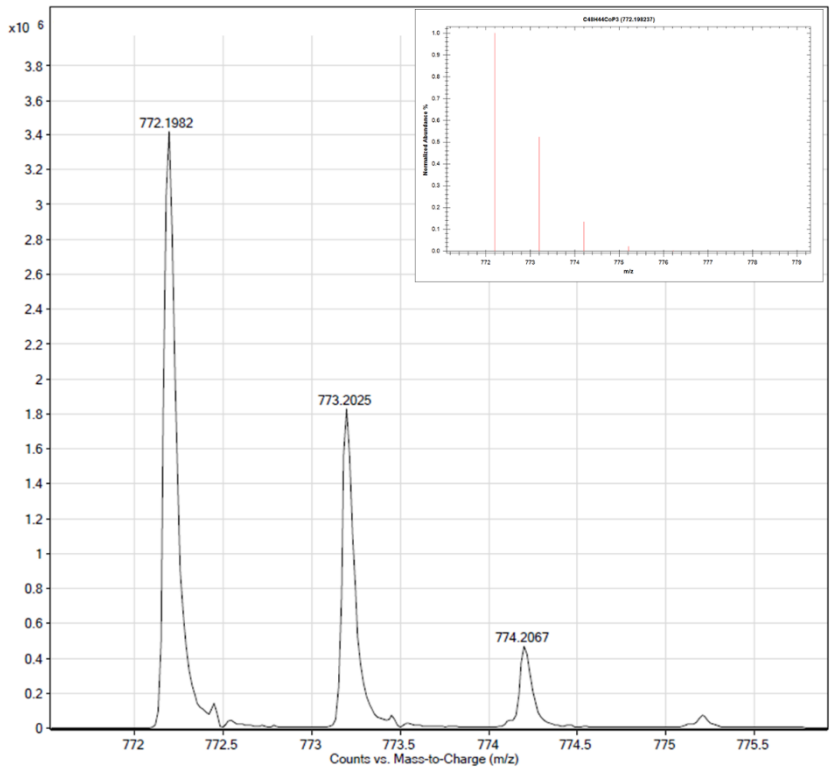

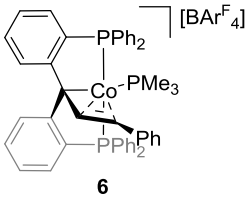

6

Figure S72 Positive mode HRMS (ESI-TOF) spectrum of $[M]^+$ ion of **6**. Inset shows expected isotope pattern.

Mass spectrum of the initial complex formed in the preparation of 7

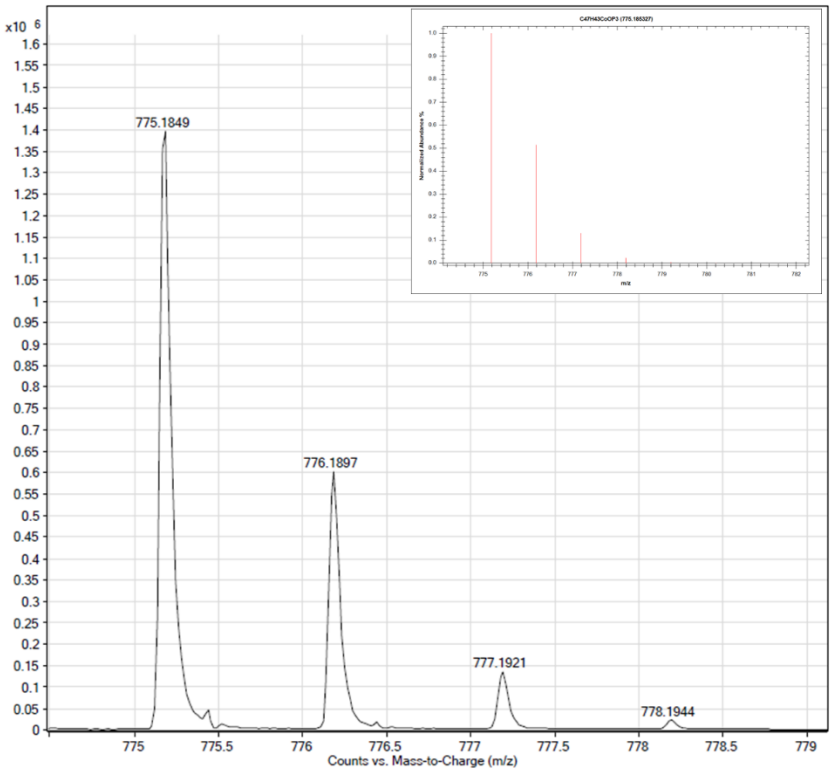

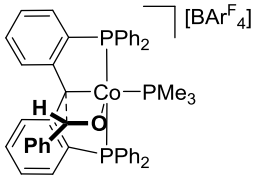

Figure S73 Positive mode HRMS (ESI-TOF) spectrum of $[M]^+$ ion of the initial complex formed in the preparation of **7** after 12 hours, before loss of H_2 (0.5 equivalents) has occurred. Inset shows expected isotope pattern.

Mass spectrum of complex 7

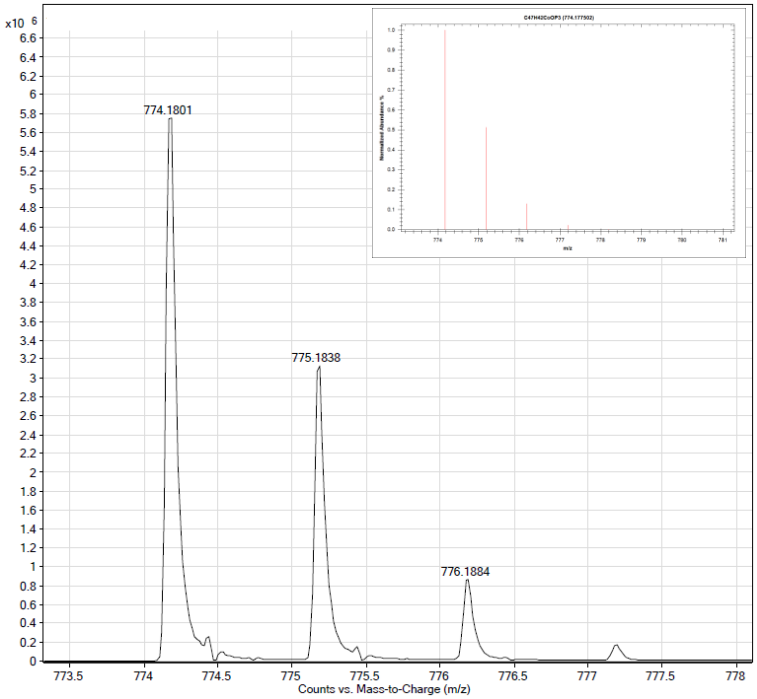

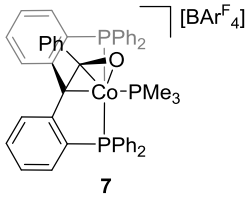

7

Figure S74 Positive mode HRMS (ESI-TOF) spectrum of $[M]^+$ ion of **7**. Inset shows expected isotope pattern.

Mass spectrum of complex 8a

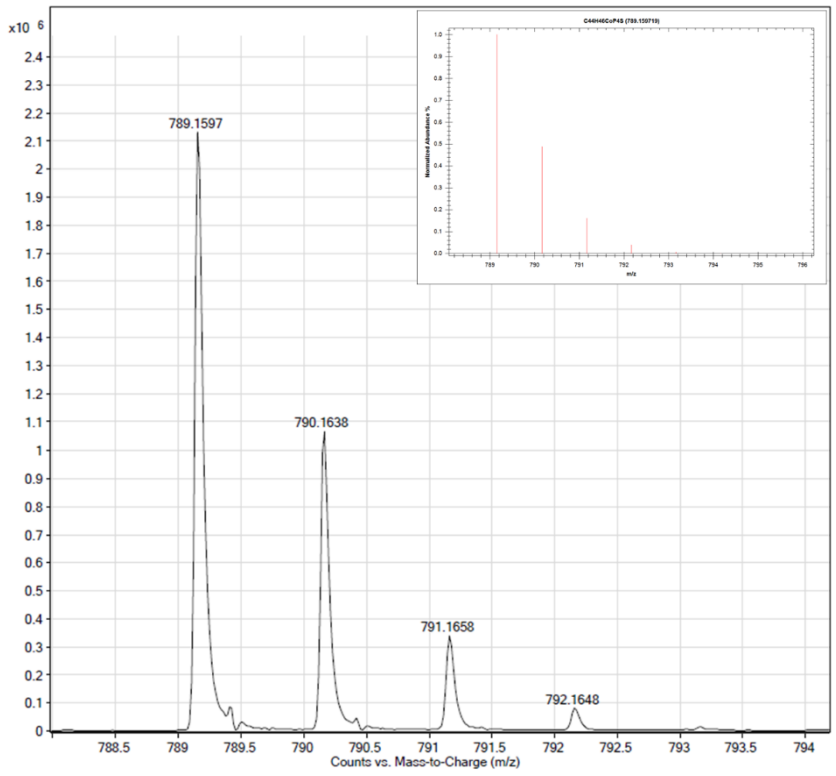

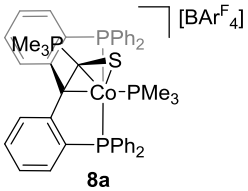

8a

Figure S75 Positive mode HRMS (ESI-TOF) spectrum of $[M]^+$ ion of **8a**. Inset shows expected isotope pattern.

Mass spectrum of complex 8b

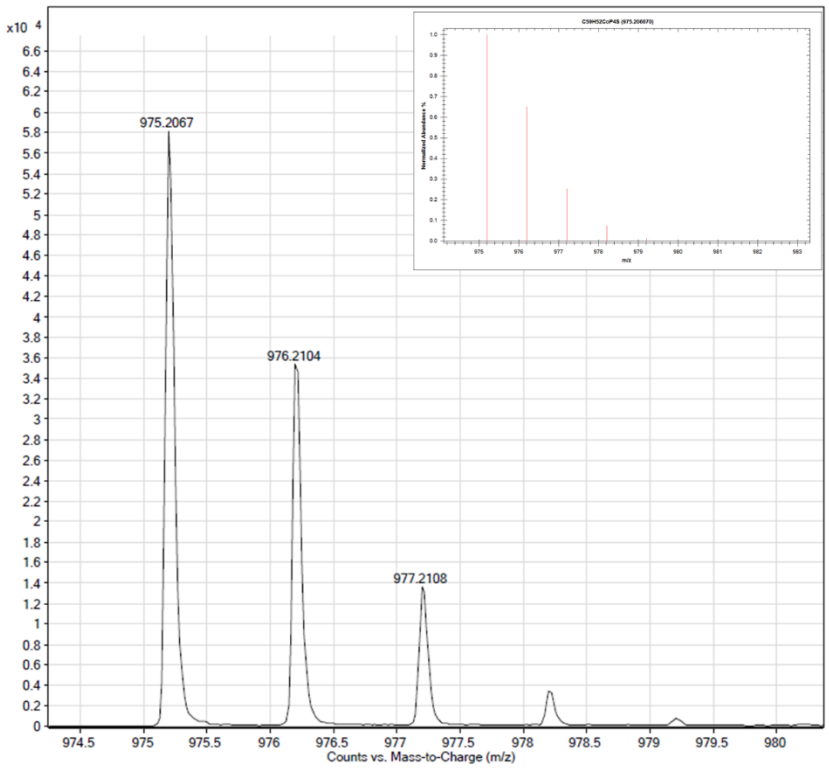

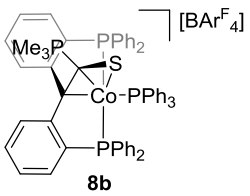

8b

Figure S76 Positive mode HRMS (ESI-TOF) spectrum of $[M]^+$ ion of **8b**. Inset shows expected isotope pattern.

Mass spectrum of complex 9

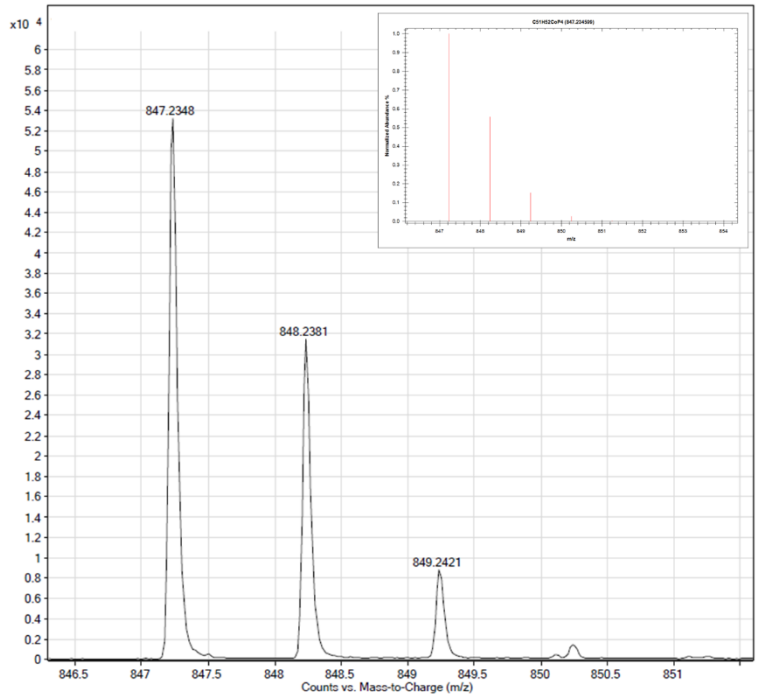

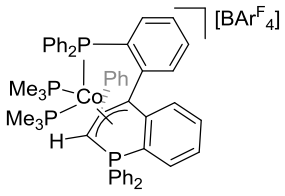

9

Figure S77 Positive mode HRMS (ESI-TOF) spectrum of $[M]^+$ ion of **9**. Inset shows expected isotope pattern.

Mass spectrum of complex 10

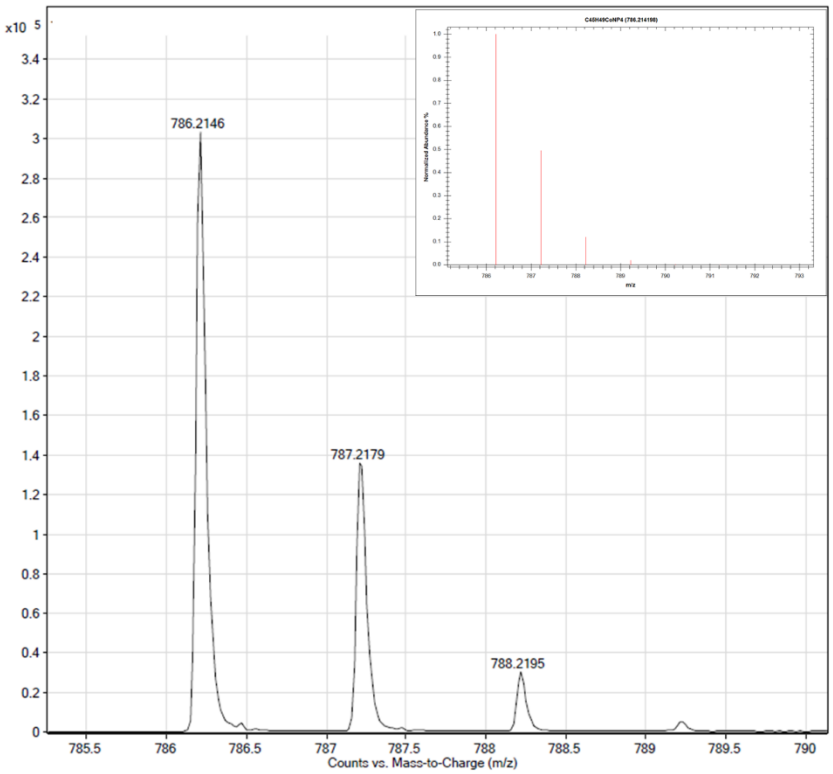

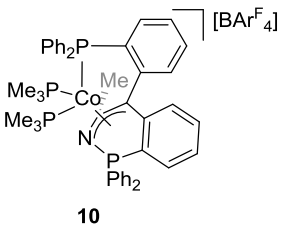

10

Figure S78 Positive mode HRMS (ESI-TOF) spectrum of $[M]^+$ ion of **10**. Inset shows expected isotope pattern.

Mass spectrum of complex III

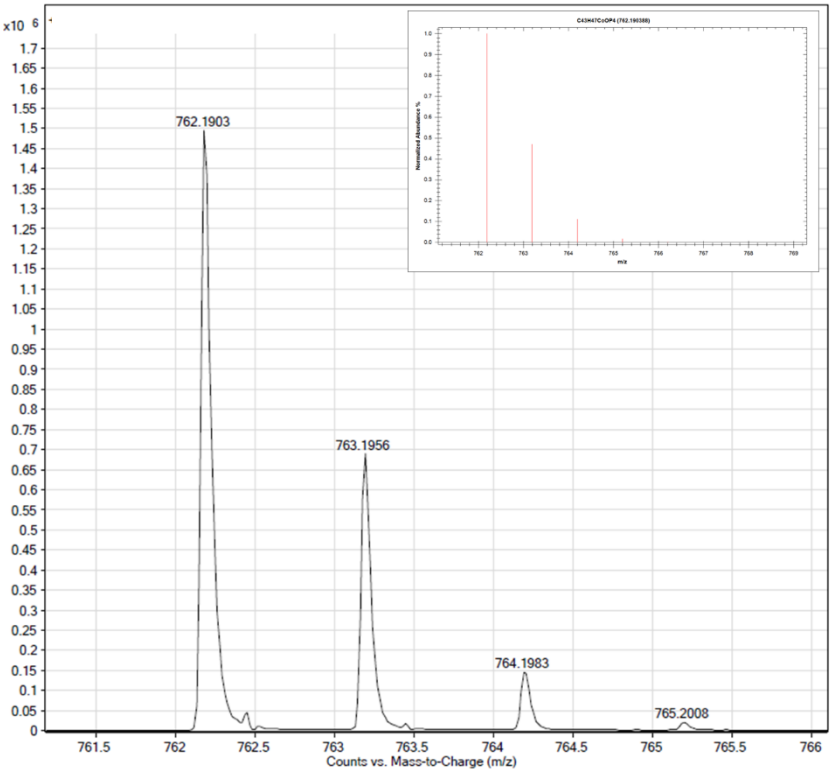

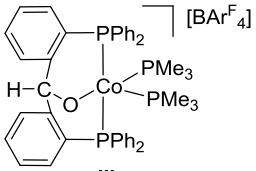

III

Figure S79 Positive mode HRMS (ESI-TOF) spectrum of $[M]^+$ ion of **III**. Inset shows expected isotope pattern.

Mass spectrum of complex V

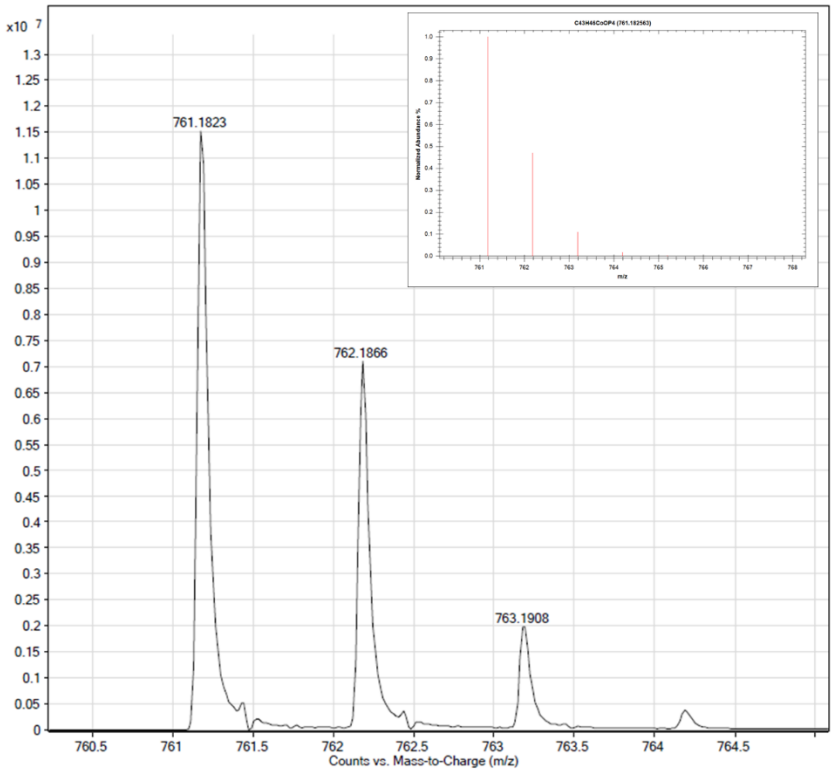

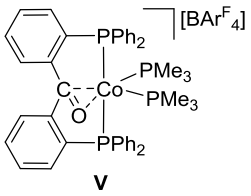

V

Figure S80 Positive mode HRMS (ESI-TOF) spectrum of $[M]^+$ ion of **V**. Inset shows expected isotope pattern.

Mass spectrum of reduced bisphosphine ligand $(Ph_2PC_6H_4)_2CH_2$

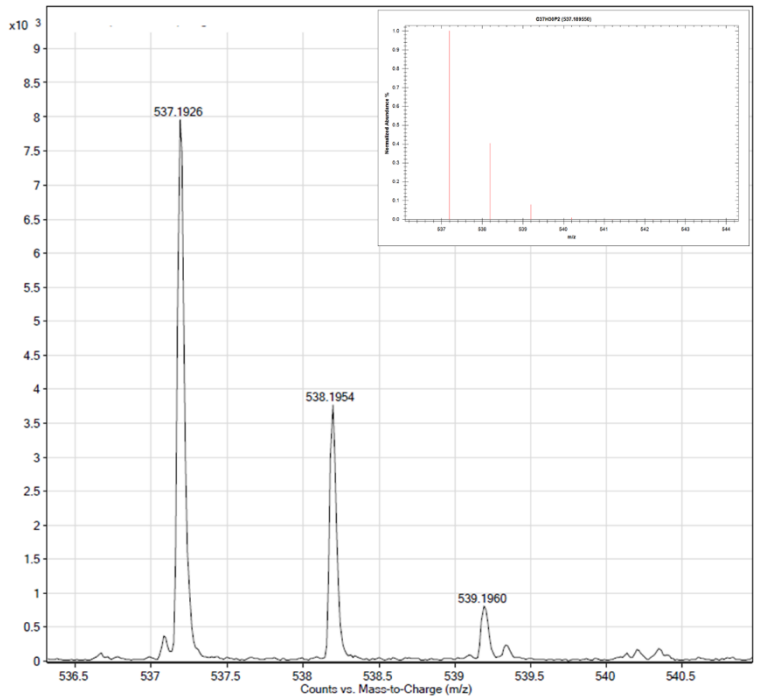

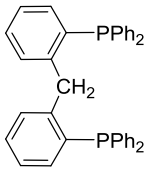

Figure S81 Positive mode HRMS (ESI-TOF) spectrum of $[M+H]^+$ ion of reduced bisphosphine ligand $(Ph_2PC_6H_4)_2CH_2$. Inset shows expected isotope pattern.

Mass spectrum of A^{Me}

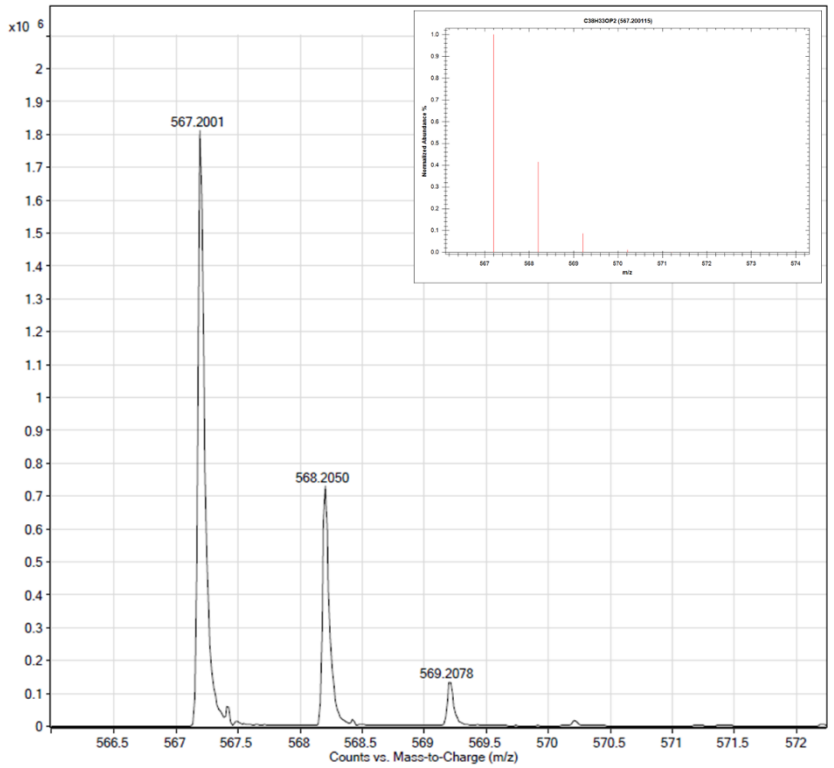

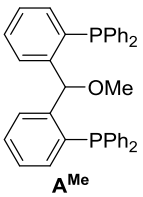

A^{Me}

Figure S82 Positive mode HRMS (ESI-TOF) spectrum of $[M+H]^+$ ion of $\mathbf{A^{Me}}$. Inset shows expected isotope pattern.

Mass spectrum of A^{TIPS}

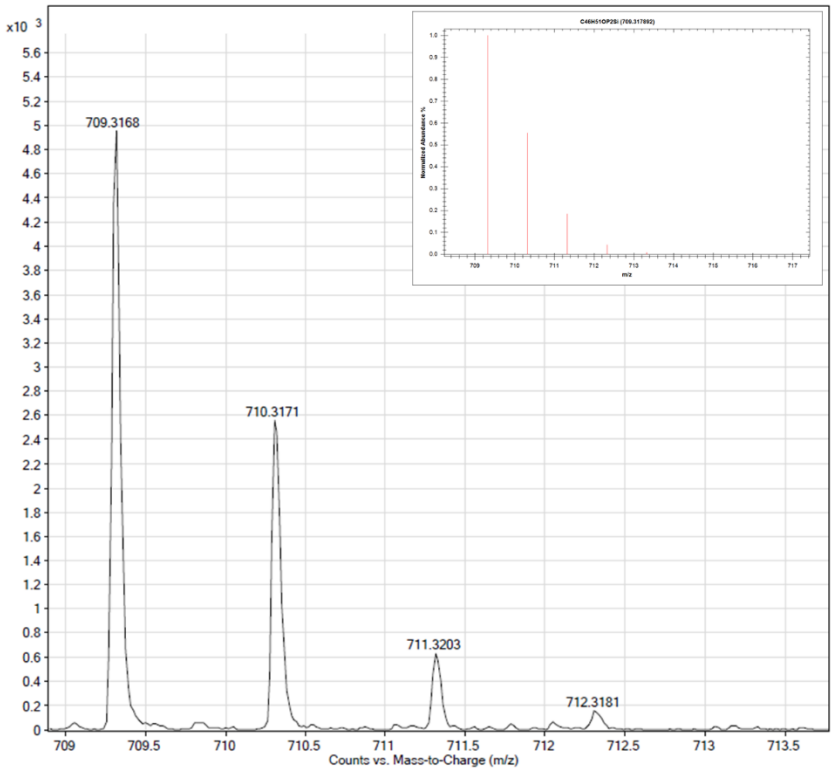

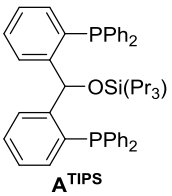

A^{TIPS}

Figure S83 Positive mode HRMS (ESI-TOF) spectrum of $[M+H]^+$ ion of $\mathbf{A^{TIPS}}$. Inset shows expected isotope pattern.

Mass spectrum of reduced ligand with incorporated MeCN

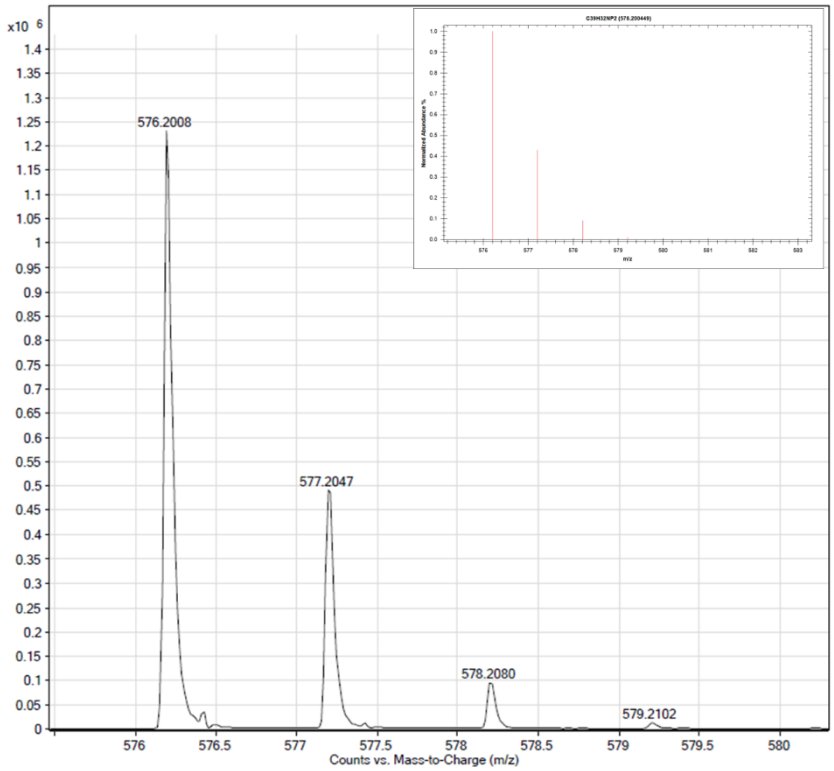

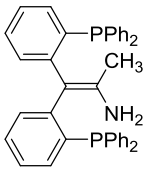

Figure S84 Positive mode HRMS (ESI-TOF) spectrum of $[M-H]^+$ ion of the reduced ligand with incorporated MeCN, observed when **1** is treated with H_2 (1 bar) in MeCN solvent. Inset shows expected isotope pattern.

Mass spectrum of $[Co(PMe_3)_4][BAr^F{}_4]$

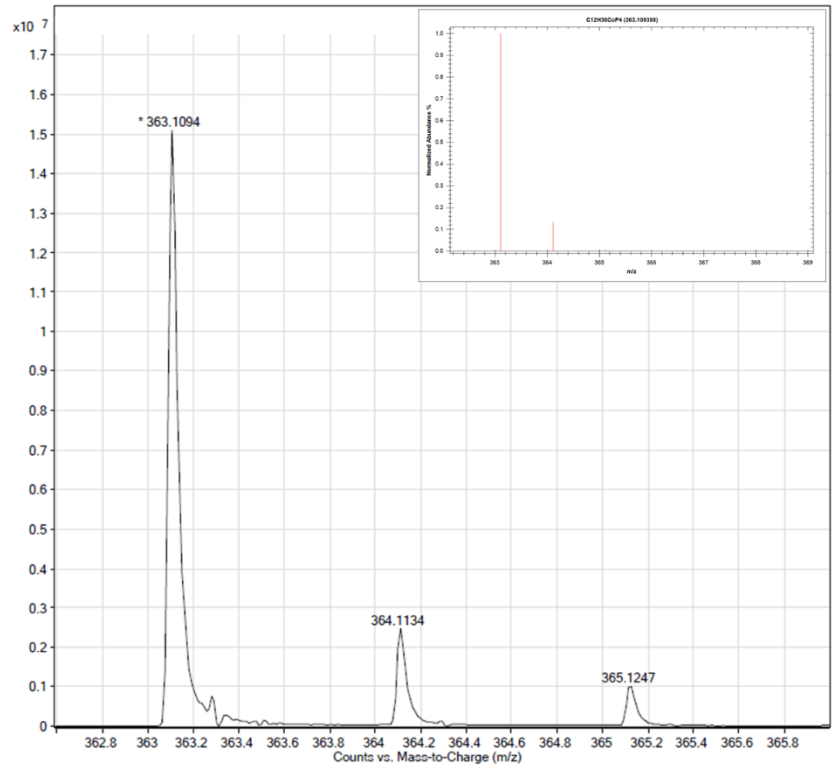

Figure S85 Positive mode HRMS (ESI-TOF) spectrum of $[M]^+$ ion of $[Co(PMe_3)_4][BAr^F{}_4]$. Inset shows expected isotope pattern.

Mass spectrum of $[Co(H_2)(PMe_3)_4][BAr^F{}_4]$

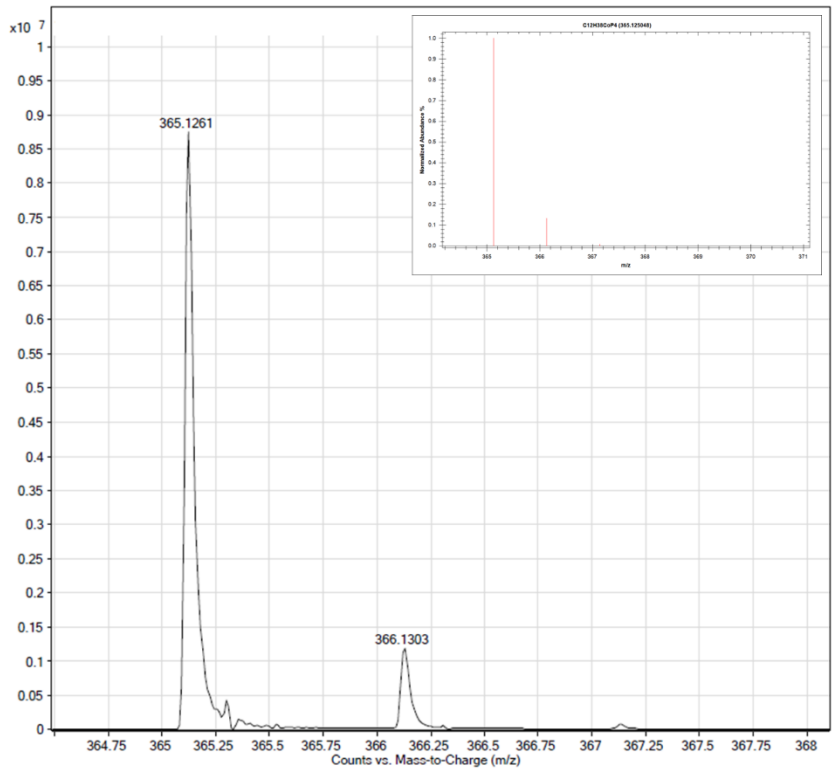

Figure S86 Positive mode HRMS (ESI-TOF) spectrum of $[M]^+$ ion of $[Co(H_2)(PMe_3)_4][BAr^F{}_4]$. Inset shows expected isotope pattern.

Mass spectrum of the solution from the reaction between complex 1 and HBr

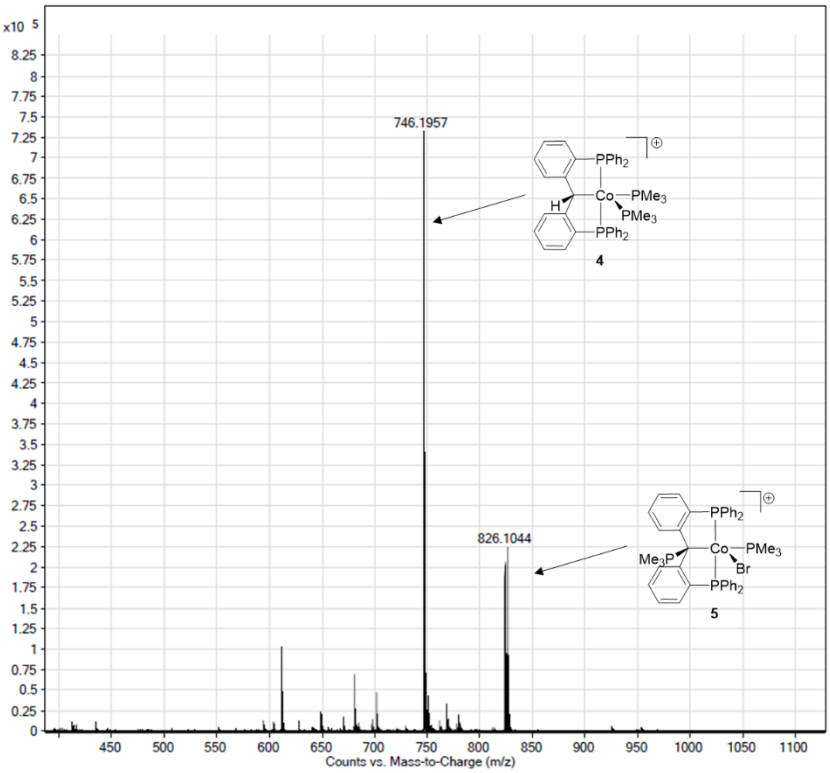

Figure S87 Positive mode HRMS (ESI-TOF) spectrum of $[M]^+$ ions of **4** and **5**, from the reaction between complex **1** and HBr.

Infrared spectrum of complex 7

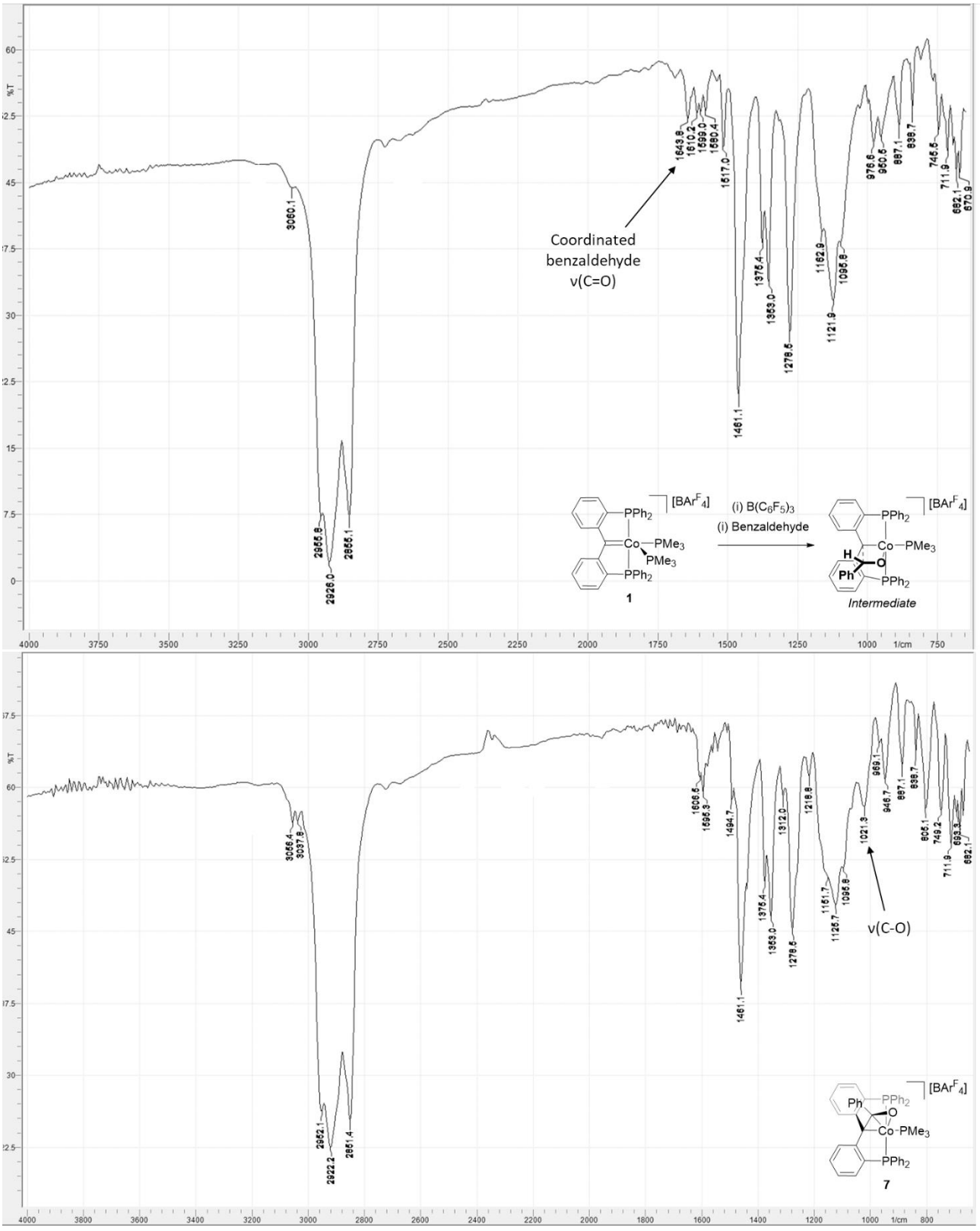

Figure S88 IR spectra in nujol of the evaporated initial reaction mixture in the preparation of complex **7** (top), and a sample of complex **7** (bottom). The observed frequency for the *ν*(C=O) stretching band in the top spectrum is typical of a Co-coordinated benzaldehyde.[14]

Infrared spectrum of complex III

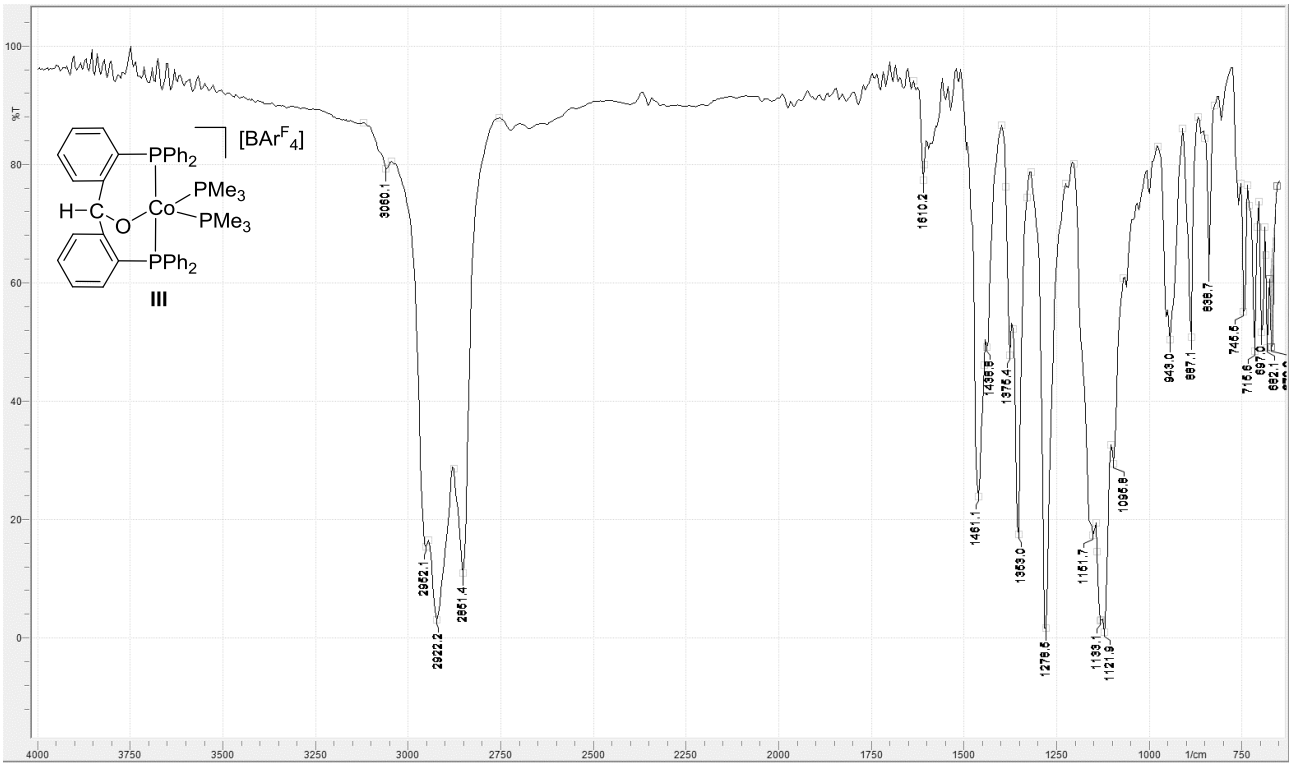

Figure S89 IR spectrum of complex **III** in nujol.

Infrared spectrum of complex [Co(H$_2$)(PMe$_3$)$_4$][BAr$^F_4$]

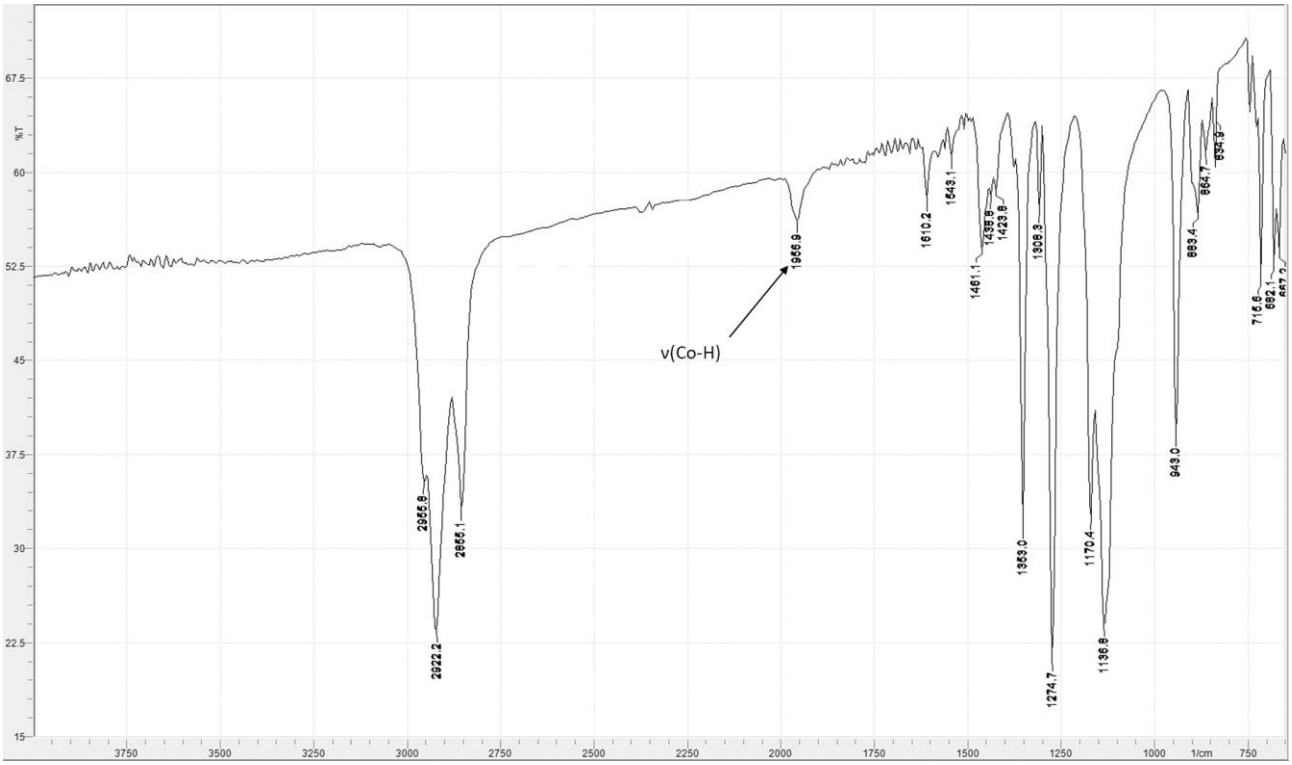

Figure S90 IR spectrum of [Co(H$_2$)(PMe$_3$)$_4$][BAr$^F_4$] in nujol.

ESR Spectra

ESR spectrum of $[Co(PMe_3)_4][BAr^F_4]$

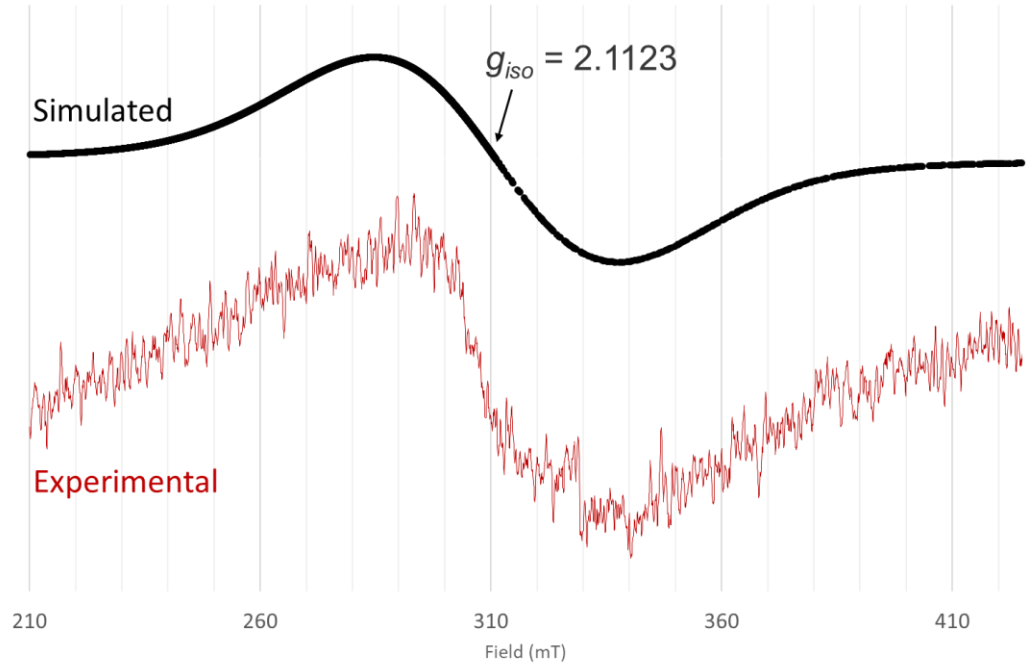

Figure S91 ESR spectrum of $[Co(PMe_3)_4][BAr^F_4]$ in PhF at 295 K.

ESR spectrum of complex 4

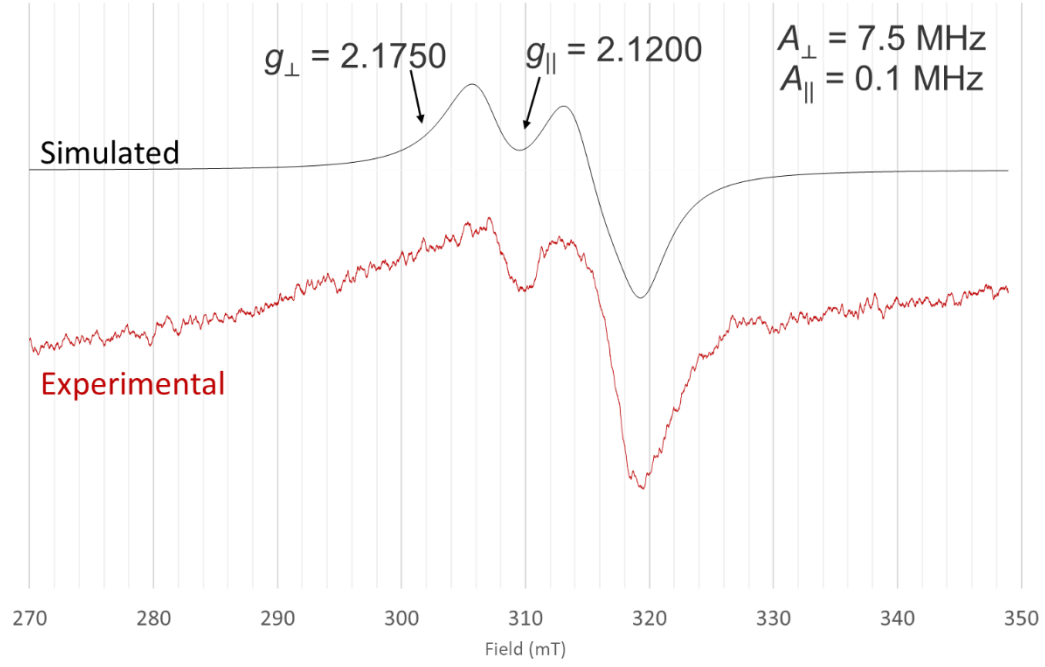

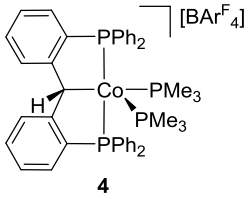

4

Figure S92 ESR spectrum of complex **4** in PhF at 293 K.

ESR spectrum of complex 5

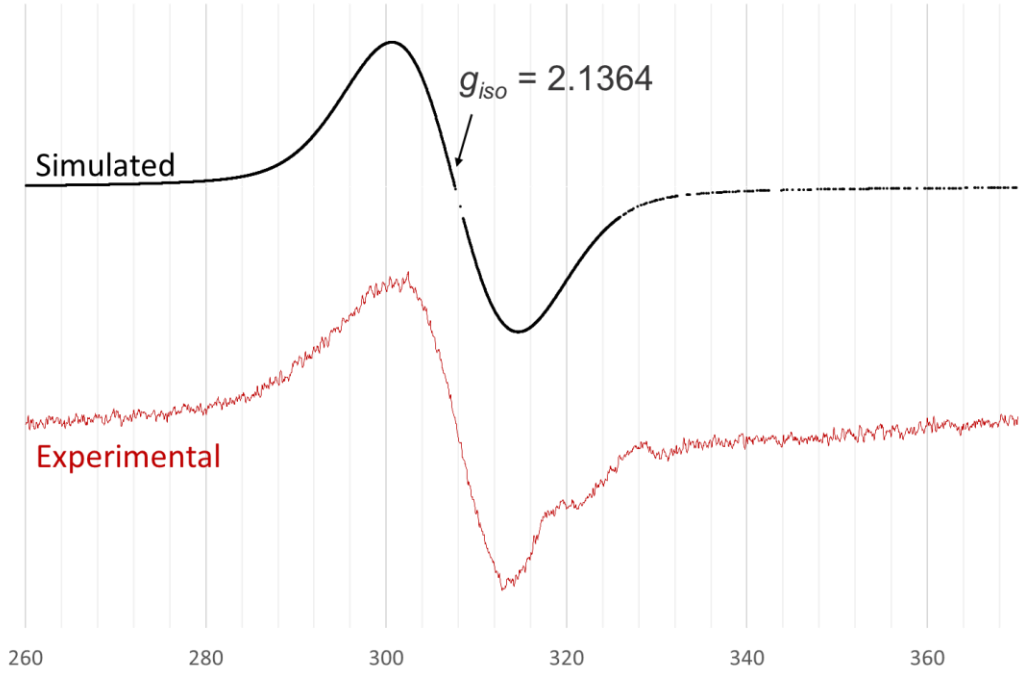

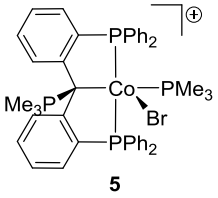

5

Figure S93 ESR spectrum of complex **5** in PhF at 295 K.

ESR spectrum of complex 6

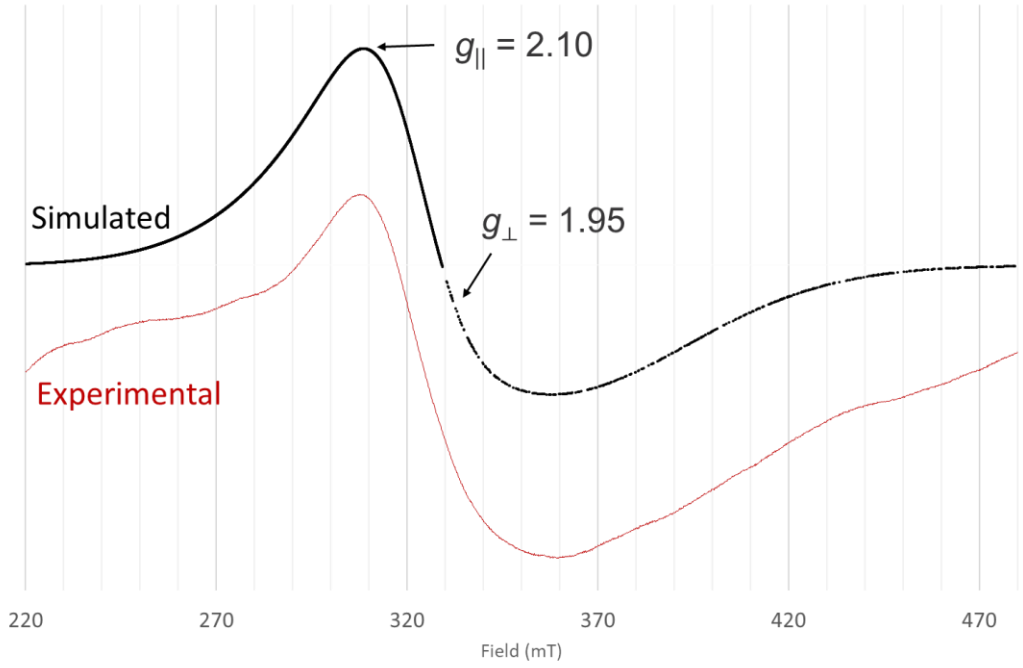

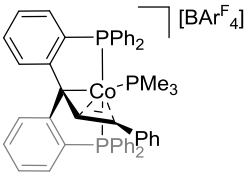

6

Figure S94 ESR spectrum of complex **6** in PhF at 295 K.

ESR spectrum of complex 7

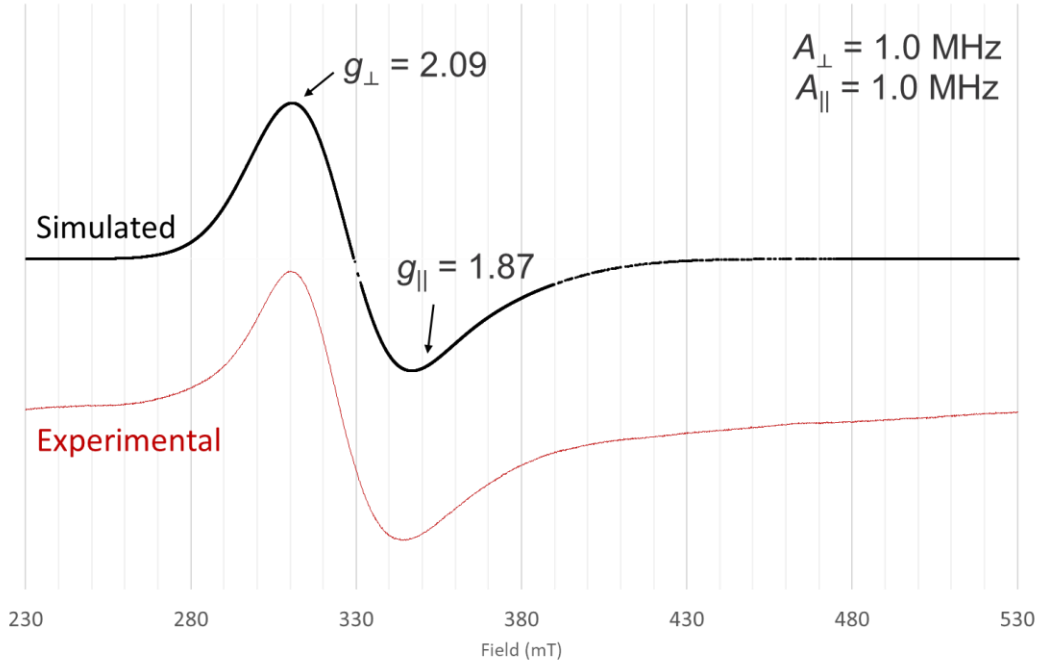

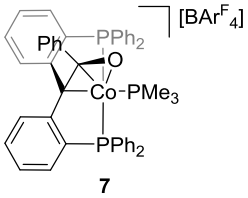

7

Figure S95 ESR spectrum of complex **7** in PhF at 295 K.

ESR spectrum of complex III

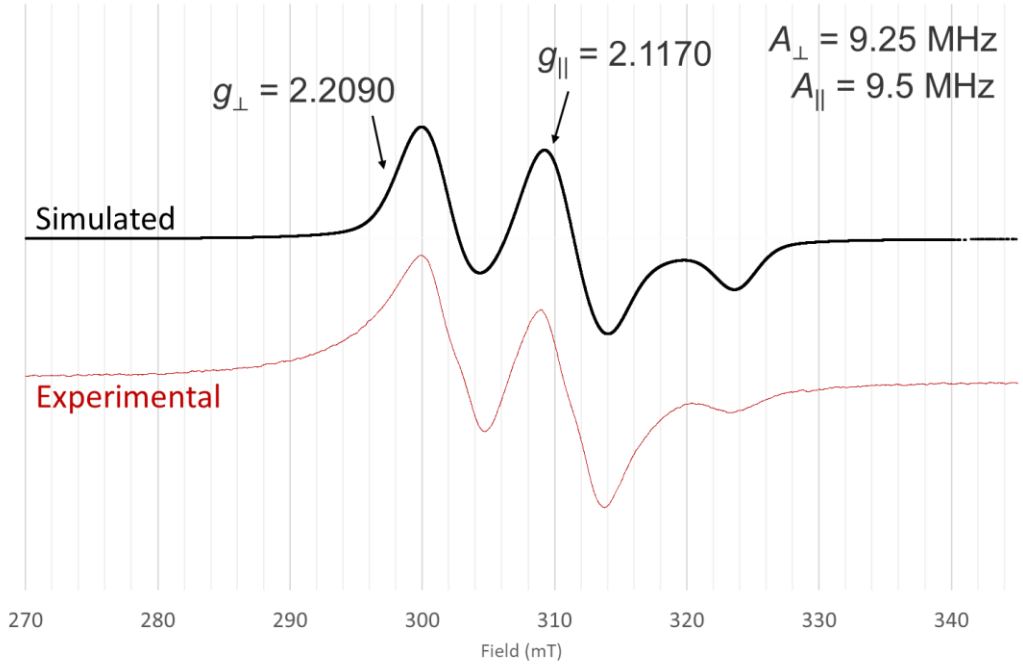

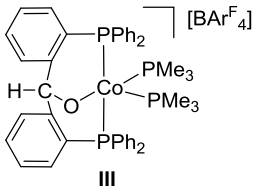

III

Figure S96 ESR spectrum of complex **III** in PhF at 293 K.

X-Ray Crystallography Data Tables

Data	1	3	4	5	6	7
Formula	$C_{84}H_{67}BCoF_{24}P_4$	$C_{80.5}H_{65}BCoF_{24}NP_3$	$C_{75}H_{59}BCoF_{24}P_4$	$C_{75}H_{58}BBrCoF_{24}P_4$	$C_{86}H_{70}BCoF_{24}P_3$	$C_{79}H_{54}BCoF_{24}OP_3$
Formula weight	1726.05	1665.02	1609.88	1688.78	1722.12	1637.87
Colour	Black	Brown	Brown	Black	Brown	Green
Crystal size / mm^3	0.104 x 0.111 x 0.134	0.043 x 0.058 x 0.061	0.634 x 0.753 x 1.170	0.037 x 0.074 x 0.144	0.080 x 0.142 x 0.200	0.144 x 0.051 x 0.043
Temperature / K	100	100	100	100	100	100
Crystal system	Triclinic	Triclinic	Monoclinic	Monoclinic	Triclinic	Monoclinic
Space group	P -1	P -1	$P2_1/c$	$P2_1/c$	P -1	$P2_1/c$
***a* / Å**	13.0252(15)	12.6883(9)	11.8224(6)	13.2806(16)	15.392(4)	14.3130(10)
***b* / Å**	17.6478(19)	18.4229(13)	19.1322(11)	27.575(3)	16.404(4)	28.967(2)
***c* / Å**	18.721(2)	18.5758(12)	33.4483(15)	20.326(2)	17.511(4)	18.3198(12)
α / °	103.179(4)	115.7837(19)	90	90	72.538(8)	90
β / °	108.177(3)	99.469(2)	97.5642(19)	99.632(5)	72.836(8)	104.992(5)
γ / °	99.430(3)	97.331(2)	90	90	86.072(9)	90
***V* / Å^3**	3850.4(4)	3758.4(5)	7499.8(7)	7338.9(15)	4029.0(10)	7336.8(9)
Z	2	2	4	4	2	4
ρ_{calcd} / g cm^{-3}	1.489	1.471	1.426	1.528	1.419	1.483
Radiation used	Mo-Kα	Mo-Kα	Mo-Kα	Mo-Kα	Mo-Kα	Cu-Kα
***μ* / mm^{-1}**	0.410	0.397	0.416	0.970	0.373	3.406
***2θ max* / °**	55.0	54.1	55.1	54.7	51.4	133.184
No. of unique reflns	17558	17374	17149	16572	15244	12715
No. of variables	2095	1012	2076	1477	1036	1030
GoF (S)	0.9753	0.9321	0.9405	1.0304	0.9484	0.943
R factor (I > 2σ)	0.0491 (12305 reflections)	0.0610 (10395 reflections)	0.0525 (15279 reflections)	0.0581 (10116 reflections)	0.0567 (8583 reflections)	0.0789 (5471 reflections)

Table S1 Crystal Data, Data Collection and Refinement Parameters for the structures of **1**, **3** – **7**.

Data	8a	9	10	III	V
Formula	$C_{79}H_{60}BCoF_{24.5}P_4S$	$C_{83}H_{64}BCoF_{24}P_4$	$C_{77.75}H_{61.5}BCoF_{24.12}NP_4$	$C_{81}H_{64}BCoF_{25}OP_4$	$C_{75}H_{58}BCoF_{24}OP_4$
Formula weight	1700.45	1711.01	1661.77	1721.99	1624.88
Colour	Black	Orange	Red	Dark green	Red
Crystal size / mm^3	0.348 x 0.154 x 0.056	0.072 x 0.186 x 0.250	0.342 x 0.142 x 0.136	0.089 x 0.136 x 0.141	0.058 x 0.126 x 0.416
Temperature / K	100	100	100	100	100
Crystal system	Triclinic	Monoclinic	Monoclinic	Triclinic	Triclinic
Space group	P -1	$P2_1/n$	$P2_1/c$	P -1	P -1
***a* / Å**	15.234(3)	16.2021(5)	18.5988(9)	14.7060(6)	13.183(3)
***b* / Å**	17.698(3)	25.6580(9)	21.2082(17)	15.1357(5)	16.540(3)
***c* / Å**	18.812(3)	18.5436(6)	18.9102(12)	19.0310(7)	16.808(3)
α / °	107.508(7)	90	90	71.3492(13)	82.810(6)
β / °	101.067(8)	90.185(2)	90.121(2)	83.8715(14)	83.316(7)
γ / °	114.080(5)	90	90	80.5636(15)	84.810(7)
***V* / Å^3**	4117.5(12)	7708.8(4)	7459.1(8)	3952.6(3)	3600.5(13)
Z	2	4	4	2	2
ρ_{calcd} / g cm^{-3}	1.372	1.474	1.480	1.447	1.499
Radiation used	Mo-Kα	Cu-Kα	Mo-Kα	Mo-Kα	Mo-Kα
μ / mm^{-1}	0.408	3.446	0.421	0.402	0.435
***2θ max* / °**	50.5	133.252	50.5	55.0	53.9
No. of unique reflns	16810	13575	15441	18075	16461
No. of variables	1047	1829	1063	1209	1544
GoF (S)	1.015	0.9381	1.044	1.0241	0.9973
R factor (I > 2σ)	0.0763 (7801 reflections)	0.1126 (5739 reflections)	0.0972 (8354 reflections)	0.0508 (14611 reflections)	0.0786 (10843 reflections)

Table S2 Crystal Data, Data Collection and Refinement Parameters for the structures of **8a** – **10**, **III** and **V**.

DFT Calculations

Computational Methods

All electronic structure calculations employed the Gaussian 09 (Revision E.01) program.[15] Unconstrained geometry optimisations and subsequent frequency calculations of all structures were carried out at the DFT level, using the BP86 GGA functional.[16,17] The Stuttgart-Dresden SDD effective core potential and associate basis sets were chosen to describe Co and P atoms,[18] with polarization functions added to P (ζ_d = 0.387),[19] Ni (ζ_f = 3.130)[20] and Co (ζ_f = 2.780).[20] Pople's 6-31G** basis set was used on all other atoms (C, O, Cl and H).[21,22] The absence of imaginary eigenvalues in the analytical second derivatives of the optimised stationary points confirmed these to be true minima. The electronic structure of the complexes [Co(**A-H$_2$**)(PMe$_3$)$_2$]$^+$, [Ni(**A-H$_2$**)(PPh$_3$)] and [NiCl(**A-H$_2$**)] was interrogated by means of Natural Bond Orbital analysis (NBO6).[23] A Lewis structure consistent with the double-bond character of the keto-group in the ligand **A-H$_2$** was manually selected via the CHOOSE keyword to facilitate comparison between all complexes. Alternative hyperbonded resonance structures are also possible.

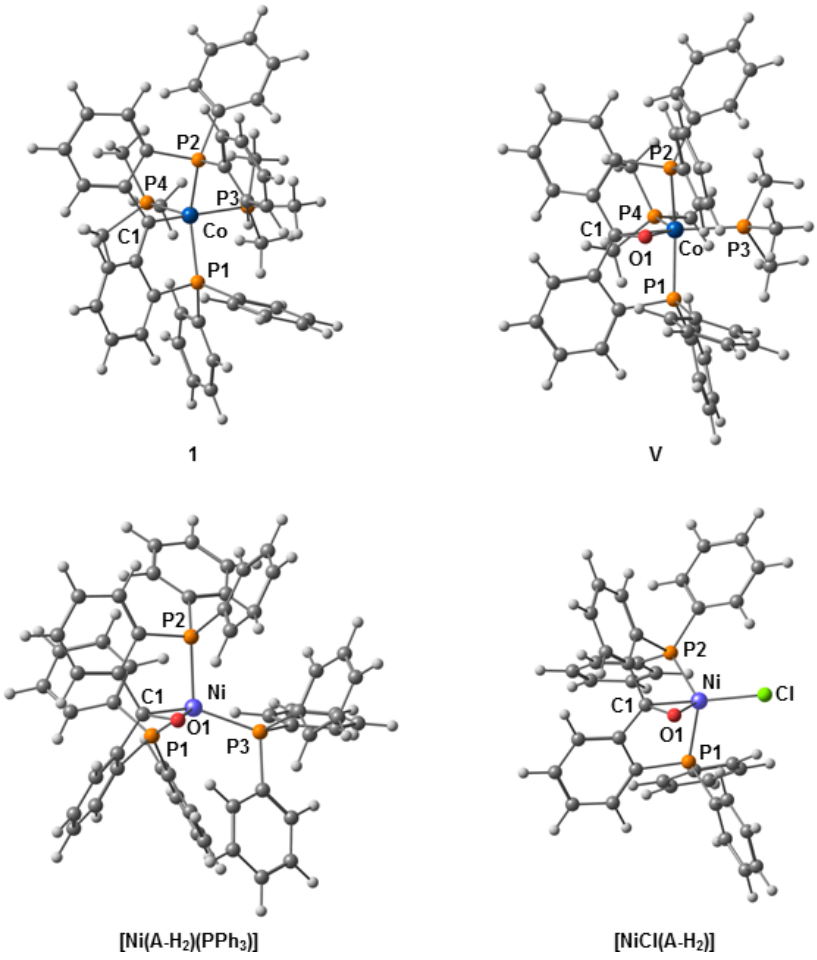

Figure S97 DFT-optimised geometries and numbering scheme of selected complexes (BP86/SDD(Co,Ni,P)/6-31G**).

	DFT	Experimental
1		
Co–P1	2.28	2.233
Co–P2	2.26	2.227
Co–P3	2.30	2.254
Co–P4	2.26	2.224
Co–C1	1.88	1.892
P1–Co–P2	139.1	143.1
C1–Co–P3	169.5	168.1
V		
Co–P1	2.30	2.240
Co–P2	2.33	2.248
Co–P3	2.28	2.236
Co–P4	2.29	2.251
Co–C1	2.12	2.105
Co–O1	1.96	1.948
C1–O1	1.35	1.350
P1–Co–P2	148.1	147.6
C1–Co–P3	162.9	166.4
[Ni(A-H_2)(PPh_3)]		
Ni–P1	2.20	2.158
Ni–P2	2.28	2.240
Ni–P3	2.24	2.205
Ni–C1	2.03	2.001
Ni–O1	2.04	2.009
C1–O1	1.32	1.330
P1–Ni–P2	119.3	120.6
C1–Ni–P3	137.1	139.2
[NiCl(A-H_2)]		
Ni–P1	2.25	2.219
Ni–P2	2.28	2.24
Ni–Cl	2.23	2.232
Ni–C1	2.02	2.005
Ni–O1	2.00	1.979
C1–O1	1.32	1.311
P1–Ni–P2	111.6	105.8
C1–Ni–Cl	147.2	143.4

Table S3 Comparison of key bond parameters (Å, °) for complexes **1**, **V**, **[Ni(A-H_2)(PPh_3)]** and **[NiCl(A-H_2)]**.

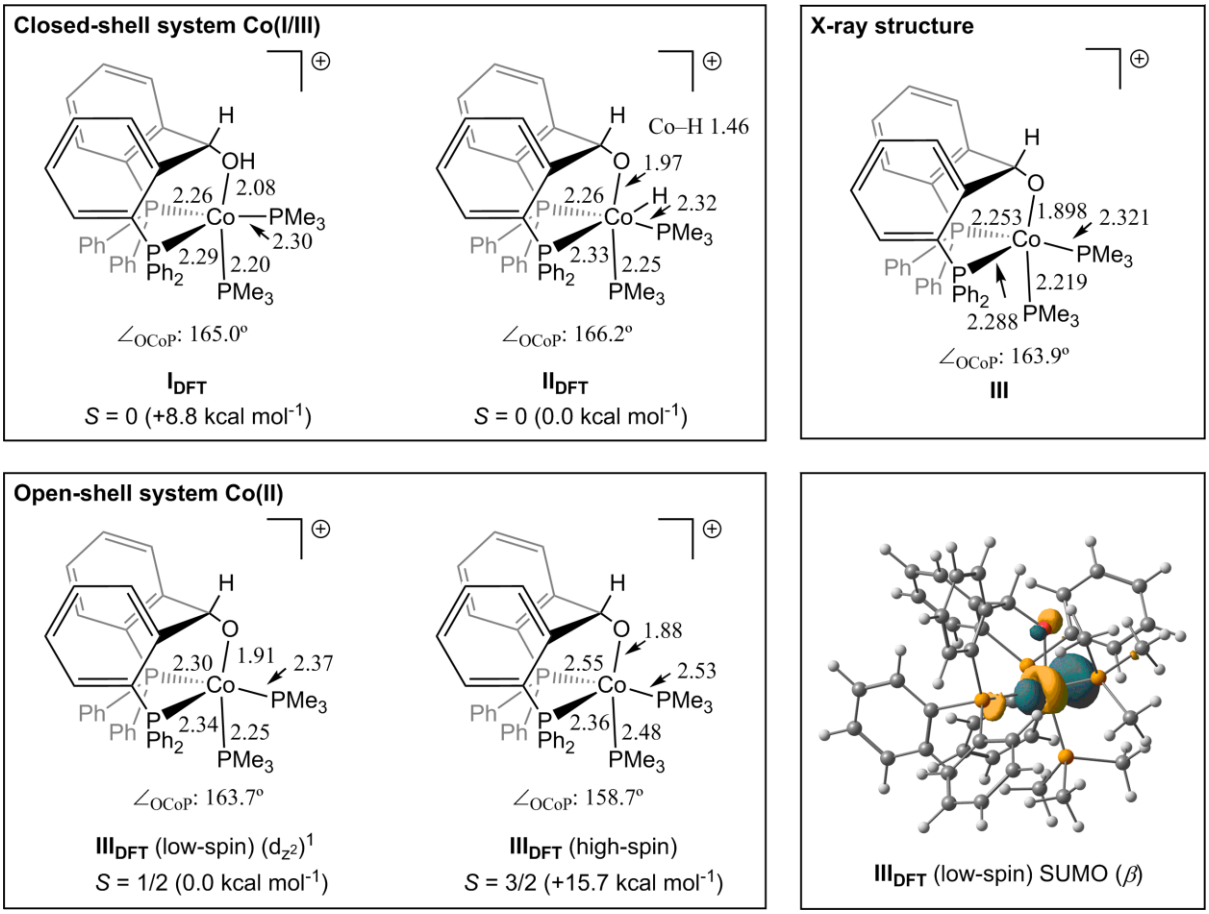

Figure S98 Possible electronic structures for complex **III**, encompassing closed-shell Co(I/III) [complexes **I** and **II** in Scheme 2] and open-shell Co(II) variants (**III** in Scheme 2). Selected bond parameters (Å, °) for optimised geometries are given along with relative energies (kcal mol^{-1}) and total spin *S* for a given set of complexes. The low-spin complex $\mathbf{III}_{\mathbf{DFT}}$ in its doublet spin state ($S = ½$) is fully consistent with the experimental structure and the observed paramagnetism of the complex. The shown molecular orbital represents the vacant minority–spin counterpart of the singly-occupied d_{z^2} orbital.

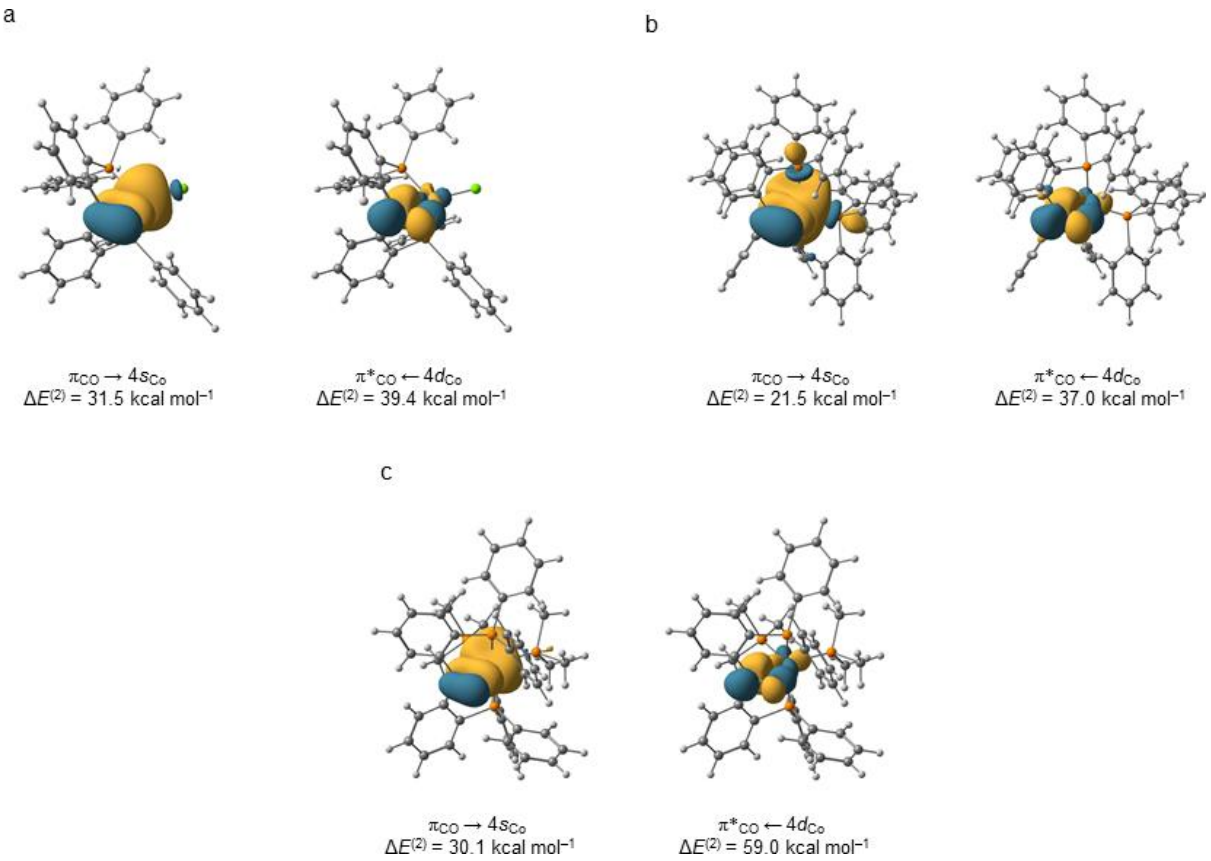

Figure S99 Key donor-acceptor NBOs (contour value = 0.05 a.u.) along with interaction energies from second-order perturbation theory for (**a**) [NiCl(**A-H$_2$**)] (**b**) [Ni(**A-H$_2$**)(PPh$_3$)] and (**c**) [Co(**A-H$_2$**)(PMe$_3$)$_2$]$^+$.

References

1. H. F. Klein, H. H. Karsch, *Inorg. Chem.*, **1975**, *14* (3), 473–477.
2. H. F. Klein, H. H. Karsch, *Chem. Ber.*, **1975**, *108*, 944–955.
3. Y. Nakamura, N. Yoshikai, L. Ilies, E. Nakamura, *Org. Lett.*, **2012**, *14*, 3316–3319.
4. Q. Jing, C. A. Sandoval, Z. Wang, K. Ding, *Eur. J. Org. Chem.* **2006**, *2006*, 3606–3616.
5. N. A. Yakelis, R. G. Bergman, *Organometallics* **2005**, *24*, 3579–3581.
6. J. Le Bras, H. Jiao, W. E. Meyer, F. Hampel, J. A. Gladysz, *J. Organomet. Chem.*, **2000**, *616*, 54–66.
7. A. G. Massey, A. J. Park, *J. Organomet. Chem*., **1964**, *2*, 245.
8. M. Brookhart, B. Grant, A. F. Volpe Jr., *Organometallics*, **1992**, *11*, 3920–3922.
9. G. A. Bain, J. F. Berry, *J. Chem. Educ.*, **2008**, *85*, 532–536.
10. W. Lesueur, E. Solari, C. Floriani, A. Chiesi-Villa, C. Rizzoli, *Inorg. Chem*., **1997**, *36*, 3354–3362.
11. H. Zhao, H. Sun, L. Wang, X. Li, *Acta Chim. Sinica*, **2015**, *73*, 1307–1310.
12. Y. Pérés, M. Dartiguenave, Y. Dartiguenave, J. F. Britten, A. L. Beauchamp, *Organometallics*, **1990**, *9*, 1041-1047.
13. M. Martin, O. Torres, E. Onate, E. Sola, L. A. Oro, *J. Am. Chem. Soc.*, **2005**, *127*, 18074–18084.
14. T. S. Kurtikyan, A. N. Mardyukov, A. Goodwin, *Russ. J. Coord. Chem.*, **2008**, *34*, 606–611.
15. Gaussian 09 (Revision E.01); M. J. Frisch, G. W. Trucks, H. B. Schlegel, G. E. Scuseria, M. A. Robb, J. R. Cheeseman, G. Scalmani, V. Barone, B. Mennucci, G. A. Petersson, H. Nakatsuji, M. Caricato, X. Li, H. P. Hratchian, A. F. Izmaylov, J. Bloino, G. Zheng, J. L. Sonnenberg, M. Hada, M. Ehara, K. Toyota, R. Fukuda, J. Hasegawa, M. Ishida, T. Nakajima, Y. Honda, O. Kitao, H. Nakai, T. Vreven, J. A. J. Montgomery, J. E. Peralta, F. Ogliaro, M. Bearpark, J. J. Heyd, E. Brothers, K. N. Kudin, V. N. Staroverov, R. Kobayashi, J. Normand, K. Raghavachari, A. Rendell, J. C. Burant, S. S. Iyengar, J. Tomasi, M. Cossi, N. Rega, J. M. Millam, M. Klene, J. E. Knox, J. B. Cross, V. Bakken, C. Adamo, J. Jaramillo, R. Gomperts, R. E. Stratmann, O. Yazyev, A. J. Austin, R. Cammi, C. Pomelli, J. W. Ochterski, R. L. Martin, K. Morokuma, V. G. Zakrzewski, G. A. Voth, P. Salvador, J. J. Dannenberg, S. Dapprich, A. D. Daniels, O. Farkas, J. B. Foresman, J. V. Ortiz, J. Cioslowski, D. J. Fox, Gaussian Inc., Wallingford, CT: 2013.
16. A. D. Becke*, Phys. Rev. A*, **1988**, *38*, 3098–3100.
17. J. P. Perdew, *Phys. Rev. B*, **1986**, *33*, 8822–8824.
18. D. Andrae, U. Haussermann, M. Dolg, H. Stoll, H. Preuss, *Theor. Chim. Acta* **1990**, *77*, 123–141.
19. A. Hollwarth, M. Bohme, S. Dapprich, A. W. Ehlers, A. Gobbi, V. Jonas, K. F. Kohler, R. Stegmann, A. Veldkamp, G. Frenking, *Chem. Phys. Lett.*, **1993**, *208*, 237–240.
20. A. W. Ehlers, M. Bohme, S. Dapprich, A. Gobbi, A. Hollwarth, V. Jonas, K. F. Kohler, R. Stegmann, A. Veldkamp, G. Frenking, *Chem. Phys. Lett.*, **1993**, *208*, 111–114.
21. W. J. Hehre, R. Ditchfie, J. A. Pople, *J. Chem. Phys.*, **1972**, *56*, 2257–2261.
22. P. C. Harihara, J. A. Pople, *Theor. Chim. Acta*, **1973**, *28*, 213–222.
23. NBO 6.0. E. D. Glendening, J. K. Badenhoop, A. E. Reed, J. A. Carpenter, J. A. Bohmann, C. M. Morales, C. R. Landis, F. Weinhold, Theoretical Institute, University of Wisconsin, Madison (2013).